# DEVELOPMENT OF DESIGN PARAMETERS FOR H-PILES IN SAND USING STATIC ANALYSIS

A Report

by

RONALD UNGARO

Submitted to the Graduate College of

Texas A&M University

in partial fulfillment of the requirements for the degree of

MASTER OF ENGINEERING

May 1988

Major Subject: Ocean Engineering

DTIC
ELECTE
JUL 27 1988
D

This document has been approved for public release and sale; its distribution is unlimited.

DEVELOPMENT OF DESIGN PARAMETERS FOR H-PILES

IN SAND USING STATIC ANALYSIS

A report

by

RONALD UNGARO

DTIC
COPY
INSPECTED
6

Approved as to style and content by:

| Accession For | |
|---|---|
| NTIS GRA&I | X |
| DTIC TAB | ☐ |
| Unannounced | ☐ |
| Justification per form 50 | |
| By | |
| Distribution/ | |
| Availability Codes | |
| Dist | Avail and/or Special |
| A-1 | |

---
John B. Herbich
(Co-Chairman)

---
Harry M. Coyle
(Co-Chairman)

---
Christopher C. Mathewson
(Member)

## ABSTRACT

Design parameters for H-piles in sand are developed using a static analysis approach from the correlation of full scale field load test data. The design parameters obtained are the ultimate pile capacity and the pile's load-settlement characteristics in compression. In establishing these parameters, the effects of residual driving stresses are included. The results indicate that if the area between the pile flanges is assumed to be one-half plugged by the soil, then the ultimate capacity in compression can be estimated by applying the correlations established by Coyle and Castello for full displacement piles. The results also indicate that the pile's load-settlement characteristics can be approximated by again assuming the flange area to be one-half plugged and modeling the pile-soil system on the axially loaded pile computer program known as APILE. The accuracy of these design parameters are evaluated by comparing the measured ultimate capacity and load-settlement curves of two field tested H-piles to the predicted results.

ACKNOWLEDGEMENT

I would like to acknowledge the efforts of several people without whom this report would not have been possible. I extend my sincere thanks and appreciation to Dr. Harry Coyle for his guidance and insight and for providing me with the data necessary to conduct this study. I also wish to thank Dr. John Herbich and Dr. Christopher Mathewson for their assistance as members of my committee. A special thanks must also go to my family and friends for their patience and support.

TABLE OF CONTENTS


| | Page |
|---|---|
| ABSTRACT | iii |
| ACKNOWLEDGEMENT | iv |
| LIST OF FIGURES | vi |
| LIST OF TABLES | vii |
| I. INTRODUCTION | 1 |
| II. DATA BASE | 6 |
| III. CORRELATION OF COMPRESSION AND TENSION TESTS | 8 |
| Method of Analysis | 9 |
| Results | 18 |
| IV. ULTIMATE PILE CAPACITY | 26 |
| Method of Analysis | 28 |
| Results | 32 |
| V. LOAD-SETTLEMENT CHARACTERISTICS | 42 |
| Method of Analysis | 42 |
| Compute T-Z and TOTLD-$Z_t$ Curves | 44 |
| Predicted Load-settlement Curves Using APILE1 | 54 |
| Results | 55 |
| VI. CONCLUSIONS | 64 |
| VII. RECOMMENDATIONS | 67 |
| APPENDICES | |
| 1. References | 68 |
| 2. Notation | 70 |
| 3. Sample Calculations and Intermediate Results | 73 |

## LIST OF FIGURES


| | | Page |
|---|---|---|
| Figure 1. | Plot of "C" Ratios: Uncorrected for Residual Stress | 19 |
| Figure 2. | Plot of $C^*$ Ratios: Corrected for Residual Stress Using Method 3 | 22 |
| Figure 3. | Plot of $C^*$ Ratios: Corrected for Residual Stress Using the BETA Method | 23 |
| Figure 4. | Effect of Soil Plugging on Pile Areas | 27 |
| Figure 5. | Unit Point Bearing vs. Relative Depth | 36 |
| Figure 6. | Unit Side Friction vs. Relative Depth | 37 |
| Figure 7. | Definition Sketch: Linearly Extrapolated Load Transfer Curves | 47 |
| Figure 8. | Definition Sketch: Typical Segmented Axially Loaded Pile | 51 |
| Figure 9. | Unit Skin Friction Ratio (T) vs. Side Movement (Z) Curves | 56 |
| Figure 10. | Unit Point Bearing Ratio (TOTLD) vs. Tip Movement ($Z_t$) Curves | 57 |
| Figure 11. | Load-Settlement Curves for Kansas City #4 | 61 |
| Figure 12. | Load-Settlement Curves for Kansas City #8 | 62 |

## LIST OF TABLES

Page

Table 1. Test Pile Data Base . . . . . 7

Table 2. Compression-Tension Test Correlations: Uncorrected for Residual Stress . . . . . 19

Table 3. Compression-Tension Test Correlations: Corrected for Residual Stress Using Method 3 . . 22

Table 4. Compression-Tension Test Correlations: Corrected for Residual Stress Using BETA Method . 23

Table 5. Backfigured Unit Resistances, Relative Depths and Friction Angles . . . . . 33

# INTRODUCTION

In the design of deep foundation systems using piles, the ability to accurately predict the ultimate load capacity of each pile is of great importance. In performing a static analysis, the approach used to estimate a pile's load capacity is to compute the maximum resistance developed by the pile tip and side and then sum these values. Using this approach, maximum unit point bearing and unit side friction values are normally estimated from in-situ soil tests and/or boring log data. These maximum unit resistances are multiplied by the corresponding pile point and side areas in contact with the soil to estimate the pile's capacity under loading.

For H-piles in sand, a serious difficulty arises when attempting to predict pile capacity using this static analysis approach. The difficulty occurs in trying to assign a value to the unit bearing capacity of the soil in the vicinity of the pile tip. Specifically, backfigured values of unit point bearing (obtained from field load tests) are usually several times larger than conventionally accepted values. For example, the American Petroleum Institute (11)* recommends a maximum unit bearing capacity of 125 tons per square foot for dense

---

* All citations follow the style of the Journal of Geotechnical Engineering Division, American Society of Civil Engineers.

gravel and very dense sand. However, backfigured values in less dense sands are commonly in the range of 400 to 900 tons per square foot (5). For this reason, using the recommended maximum values for the unit bearing strength of cohesionless soils in a static analysis to predict the ultimate load capacity of H-piles in compression can result in significant error. The need exists to more accurately predict the behavior of H-piles in sand under ultimate loading conditions using the static analysis approach.

The purpose of this study is to develop design parameters which will provide a better estimate of the ultimate load capacity and load-settlement characteristics of H-piles in sand. These parameters will allow foundation engineers to use the static analysis approach to more accurately predict H-pile performance under ultimate loading. This objective is accomplished by correlating the results of ten full scale, field load tested H-piles to the correlations previously developed by Coyle and Castello for full displacement piles (6).

Using the static analysis approach requires that both of the pile's resistance components (i.e. point bearing and side friction) be estimated independently and then summed to predict the pile's ultimate load capacity. Therefore, for each test pile in the data base, measuring or approximating the distribution of the total load between the pile tip and side

represents the first step in developing design parameters which can be used in a static analysis approach. For field load tests in which the pile is fully instrumented, this required load distribution is measured directly through the use of strain gages, strain rods, or both. However, load tests are often conducted on non-fully instrumented test piles. These non-fully instrumented piles are not equipped with strain measuring devices along their embedded length. Therefore, these type of load tests provide no indication of the distribution of the applied load.

Due to the small number of load tests (fully instrumented or otherwise) available from the literature, half of the test piles analyzed in this study are non-fully instrumented. Therefore, to develop correlations and design parameters useful in a static analysis, a method must be devised to approximate the distribution of the applied load for these non-fully instrumented piles. This is done by selecting a data base of piles on which both compression and tension tests have been conducted. By correlating the results of these tests, the load distribution for the non-fully instrumented piles can be approximated.

Once the load distribution between the pile tip and side has been obtained, the desired design parameters can be developed. Parameters for ultimate compression capacity are generated by backfiguring unit point and side resistances and plotting these results on the correlation curves developed by

Coyle and Castello (6). A series of backfigured unit resistances are computed based on assuming the area between the flanges of the pile to be zero, one-third, one-half and fully plugged by the soil. Design parameters for the load-settlement characteristics of H-piles in sand are developed using the axially loaded pile computer program called APILE1. Both the pile elasticity and variation in the unit soil resistances as a function of pile displacement are quantified and used as part of the input for APILE1.

An attempt (hereafter referred to as "class" results) has previously been made to establish design parameters for H-piles in sand using the results of fully instrumented load tests (5). However, the results obtained were based on the analysis of only six piles (5); therefore, this study will help to confirm or modify the results obtained previously by expanding the size of the data base. The design parameters obtained from this study (combined with those from class) will allow designers to utilize static analysis procedures to better predict the ultimate capacity and load-settlement characteristics of H-piles in sand.

As stated earlier, the primary objective of this study is to establish design parameters for H-piles in sand using field compression-tension load test data. In accomplishing this objective three tasks are performed. These tasks are: (1) establish a correlation between the ultimate side load in compression and the ultimate pile capacity in tension; (2) use

the first correlation to predict the ultimate pile capacity in compression; and, (3) use the second correlation to predict the pile load-settlement characteristics. The discussion of these three tasks form the body of this study.

Several different assumptions and methods of analysis are employed in completing each of these tasks. Therefore, to avoid confusion each task is considered separately, and the discussion of each is divided into two parts. First, the method of analysis used to accomplish the task is described in detail. This method of analysis includes both the procedures used in manipulating data and a statement of all assumptions. After the procedures are described, the results obtained for each task are presented.

## DATA BASE

As stated previously, the purpose of this study is to utilize full-scale, field compression-tension pile load test data to develop correlations and design parameters for H-piles in cohesionless soils. Therefore, all of the data which are analyzed in developing these parameters are obtained from pile load tests conducted on H-piles in sand. These piles are shown in Table 1.

All of the piles studied were driven by impact hammer into predominately sandy soils. However, clay lenses, significant amounts of silt, or thin layers of relatively coarse material (i.e. pebbles, cobbles, gravel) are not uncommon soil profile features for some of the test piles. The presence and significance of these features are discussed as necessary in interpreting the results obtained.

The soil strength profiles for each of the test piles are provided by Standard Penetration Test (SPT) data. For the three Lock and Dam 26 piles at site #2, the results of a static cone penetration test are also available.

TABLE 1

Test Pile Data Base

| Test pile | Pile shape | Embedment length, in feet | Compression(CT) or Tension(TT) Test | Reference |
|---|---|---|---|---|
| Arkansas #7* | HP14 73 | 52 | CT and TT | 9 |
| Lock and Dam 26:3IP-IIIS* | " " | 54 | CT and TT | 8 |
| Lock and Dam 26:1-3* | " " | 54 | CT and TT | 2 |
| Lock and Dam 26:2-1* | " " | 55 | TT | 2 |
| Lock and Dam 26:2-4 | " " | 58 | TT | 2 |
| Lock and Dam 26:2-5* | " " | 59 | CT | 2 |
| Lock and Dam 6:K-8 | " " | 39 | CT and TT | 13 |
| Canada 24-4 | HP12 53 | 73 | CT and TT | 10 |
| Canada 24-5 | " " | 50 | CT and TT | 10 |
| Canada 35-1 | HP12 74 | 48 | CT and TT | 10 |

* Fully instrumented pile for which mearured load transfer data is available.

## CORRELATION OF COMPRESSION AND TENSION TESTS

A correlation between ultimate pile loads in compression and tension is desired. This correlation will be defined as the ratio of the ultimate side load in compression ($Q_s$) to the ultimate pile load in tension ($Q_{ut}$). Therefore, this correlation ("C") is given as:

$$C = Q_s/Q_{ut}. \tag{1}$$

An important factor to be considered in establishing this correlation is the effect of residual stress. Therefore, the corrected ratio ($C^*$) is defined as:

$$C^* = Q^*_s/Q_{ut}, \tag{2}$$

where $Q^*_s$ represents the ultimate compressive side load after correcting for residual stress.

Establishing this correlation is an important first step in developing the desired design parameters. A pile subjected to a compressive axial load ($Q_u$) will carry this applied load by side friction developed along the pile's embedded length ($Q_s$) and point bearing resistance at the pile tip ($Q_{pt}$), as shown in the following equation:

$$Q_u = Q_s + Q_{pt}. \tag{3}$$

Knowing the distribution of an applied load between the pile side and tip is required in order to develop design parameters for a static analysis. For fully instrumented piles with load transfer data available, the side and point loads are measured. However, since half of the piles being analyzed in this study are not fully instrumented, a method must be developed to estimate how applied loads are distributed between side friction and point bearing. The "C" ratio (or $C^*$) provides this means by utilizing pile tension tests.

## METHOD OF ANALYSIS

A common problem in the design of piles for deep foundations is how one chooses to define the failure or ultimate load. In this study, the ultimate compression ($Q_u$) and tension ($Q_{ut}$) loads are evaluated at pile movements ($\delta$) of 2.0 and 1.2 inches, respectively. These pile head movements are chosen primarily because the class results indicated that maximum or limiting values of unit point bearing ($q_o$) and unit side friction ($f_s$) are achieved at these respective movements (5). Since no point bearing is developed in a pile tension test, the resistance is due entirely to side friction. If limiting unit side friction is developed at a movement of 1.2 inches, then the maximum pile load in tension should also be developed at a pile head movement of 1.2 inches. Therefore, $Q_{ut}$ is defined at this movement. In a compression test, both side friction and point bearing are developed simultaneously.

Since the class results indicated that maximum unit point bearing was not achieved until a tip movement of 2.0 inches, this movement was selected in defining $Q_u$.

Two different procedures are employed to estimate this "C" ratio. For fully instrumented piles, $Q_s$ is obtained directly from the measured load transfer curves; and, $Q_{ut}$ is obtained from the tension test load-movement curve. An example of this procedure for the Lock and Dam 26:1-3 pile is shown in Appendix 3-A (page 73). The second procedure is applied to those piles for which no measured load transfer data is available. For these piles, $Q_s$ is obtained using both the compression test load-settlement curve and the Coyle-Castello correlations for displacement piles in sand (6). As previously stated, the measured distribution of applied loads between the pile point and side is only available when the pile is fully instrumented and load transfer data is gathered. However, this load distribution can be estimated using the Coyle-Castello correlations. Specifically, these correlations allow the side friction load to be estimated as a percent of the total applied load. This percent (which can be expressed as the ratio $Q_s/Q_u$) is then multiplied by the measured $Q_u$, which is obtained from the load-settlement curve at $\delta$=2.0 inches, to estimate a value for $Q_s$. In both procedures described above, the $Q_{ut}$ value is obtained from the tension test load-settlement curve at $\delta$=1.2 inches. An sample of the second procedure for the Canada 24-4 test pile, as well as a summary

of the results obtained from the other non-fully instrumented test piles, is shown in Appendix 3-B (page 74).

Four important points are noted concerning the two procedures described above.

First, one might question the reason for using the Coyle-Castello correlations on the non-fully instrumented piles in developing this "C" ratio . Since only half of the test piles were fully instrumented, purely empirical ratios could only be obtained from these five piles (since load transfer data was available). By using the Coyle-Castello correlations, semi-empirical values of "C" could be computed for the non-fully instrumented piles. In effect, if "C" were to be computed by purely empirical means, its value would depend on a data base of only five test piles - four of which were located at the same site. Determining semi-empirical values of "C" using the Coyle-Castello correlations for the non-fully instrumented piles allows a larger and more varied data base to be utilized in estimating "C".

The second point concerns the manner in which values for $Q_u$, $Q_s$ and $Q_{ut}$ are obtained from the measured data. As previously stated, $Q_s$ represents the side friction in compression at a pile head settlement of 2.0 inches; and, $Q_{ut}$ is the tension load at a pile head rise of 1.2 inches. However, in some of the load tests, the pile heads were not displaced to these movements. Therefore, some method must be devised to estimate the load carrying capacity these piles

would have been capable of had these movements been reached. Specifically, the movements of Lock and Dam 26:3IP-IIIS, Lock and Dam 26:2-5 and Lock and Dam 6:K-8 are below those desired. One way in which pile loads are estimated at these larger movements is to simply extend the terminal portion of the measured load-movement curve linearly. This "straight-line" extrapolation of the measured curve is used to estimate the $Q_s$ and $Q_{ut}$ values for all three of the aforementioned test piles. Hereafter, this procedure will be referred to as "Method 1". An sample of this procedure for Lock and Dam 6:K-8 is shown in Appendix 3-C (page 78). For Lock and Dam 26:2-5 and Lock and Dam 6:K-8, the application of Method 1 probably yields reasonably accurate results, since the measured movements obtained in the load tests for these piles are close to the required movements and the load-movement curves are either plunging or close to plunging (2,13). A plunging load-movement curve is defined as a curve in which the pile head movements become large (i.e. asmyptotic) at small additional applied loads. However, the Lock and Dam 26:3IP-IIIS test pile was loaded in compression to a pile head settlement of only about 0.48 inches - at which movement the load-settlement curve is non-plunging (8). Therefore, Method 1 applied to this pile probably yields questionable results, since the estimated values of $Q_u$ and $Q_s$ are likely to be significantly overestimated by the Method 1 assumption that the load-settlement curve continues to increase linearly with applied

load (i.e. not plung) prior to a head settlement of 2.0 inches. For this reason a second procedure is developed to estimate $Q_u$ and $Q_s$ for this pile. This second procedure (hereafter referred to as "Method 2") involves applying the results of an analysis of the shapes of nine different load-settlement curves to allow the curve from Lock and Dam 26:3IP-IIIS to be extended asmyptotically to a settlement of 2.0 inches. The details of this procedure and the resulting load-settlement curve are shown in Appendix 3-D (page 80). Both Methods 1 and 2 are applied separately to Lock and Dam 26:3IP-IIIS yielding two different values of "C". Also, to be consistent an asmyptotic value for $Q_{ut}$ is obtained from reference 8 and used when computing "C" by Method 2.

The third comment concerning the procedures used to estimate the value of "C" regards the method employed to extrapolate the measured load transfer data for one of the fully instrumented piles. As explained above, $Q_s$ is determined by one of two procedures, namely: (1) empirically from the measured load transfer data - for the fully instrumented piles; or, (2) semi-empirically using both the Coyle-Castello correlations and the measured compression load-settlement curves - for the non-fully instrumented piles. For the fully instrumented Lock and Dam 26:3IP-IIIS test pile, the maximum load applied during the compression test is significantly smaller than the $Q_u$ values estimated from Methods 1 and 2. Therefore, since a $Q_s$ value corresponding to the estimated

value of $Q_u$ cannot be obtained directly from the measured test data, either the Coyle-Castello correlations or extrapolation of the measured load transfer data is required to estimate $Q_s$. Extrapolation of the measured data is chosen in this case. Three measured load transfer curves (corresponding to applied loads well below the estimated value of $Q_u$) are available for the Lock and Dam 26:3IP-IIIS test pile (8). From these three measured load transfer curves, the side friction load - expressed as a percent of total applied load - can be computed. This percent (i.e. $Q_s/Q_u$) is then multiplied by the estimated $Q_u$ to determine $Q_s$.

The final comment explains why data from three test piles (i.e. Lock and Dam 26:2-1, Lock and Dam 26:2-4 and Lock and Dam 26:2-5) is used to compute only two different "C" values. From Table 1, piles 2-1 and 2-4 were load tested in tension only, while 2-5 was tested in compression only. All three piles were driven by impact hammer at the same site to approximately the same depth. Therefore, if an extraction test were performed on pile 2-5, then the ultimate load to be expected (i.e. $Q_{ut}$) is assumed to be close to the measured $Q_{ut}$ loads obtained from piles 2-1 and 2-4. If this assumption is reasonable, then computing two "C" values by relating the tension test results of each of 2-1 and 2-4 to the compression test results of 2-5 should correlate well with the values of "C" computed from the other test piles. Two "C" values are therefore computed: the first by relating $Q_{ut}$ (from 2-1) to $Q_s$

(from 2-5), and the second by relating $Q_{ut}$ (from 2-4) to the same $Q_s$ value. Two corrections are made to the measured $Q_{ut}$ load from pile 2-1 prior to computing "C". First, the $Q_{ut}$ load (obtained from the load-movement curve for pile 2-1 at $\delta$=1.2 inches) is increased by seven percent, since its embedded length is about seven percent less than the embedded length of pile 2-5 (2). This result is then decreased by 22 percent, since pile 2-1 was subjected to a quick test in tension (2). A quick test is one in which loads are applied to a pile at a higher than normal rate during load testing. Compared to the capacity of a pile loaded at a normal rate, a quick test usually results in a greater pile capacity in both tension and compression. Since test pile 2-1 is the only pile in the data base subjected to a quick test, its measured $Q_{ut}$ load was reduced. The specific reduction of 22 percent was determined after comparing the quick and normal compression load test results conducted on other test piles not in the data base (10).

After the above analysis is accomplished and the "C" values are computed for each test pile, the effect of residual stresses are taken into account resulting in a corrected ultimate side friction ($Q^*_s$) and a corrected ratio (i.e. $C^*$) for "C". For comparison purposes, two methods of correcting for residual stress are applied to each test pile in the data base. These two methods are described in the following paragraphs.

The first method used will be referred to as "Method 3: No Unloading Reading Method" (3). Simply stated, Method 3 assumes that the pile tip load remaining after ultimate failure in tension is equal to the residual stress. The significant consideration in using this method is that only the residual stress ($Q_{res}$) due to driving stresses are corrected for, and the residual stresses contributed by load testing are not included (3). If unloading data (i.e. stress in the pile measured after load testing) were available for the test piles used in this study, then residual stresses due to both driving and compression testing could be corrected for by using the Hunter-Davisson method (7). In applying Method 3, the unit stress remaining at the pile tip after the tension test is defined as the unit residual stress ($q_{res}$) due to driving. With load transfer data available, values of $q_{res}$ were calculated for the five fully instrumented test piles. These results are then plotted versus pile embedded length (D). Each test pile's embedded length is then used in the D versus $q_{res}$ plot to estimate values for $q_{res}$ for the non-fully instrumented piles. In developing and using this D versus $q_{res}$ plot, the pile tip is assumed to be one-half plugged by the soil - as indicated by the class results (5). At least two major factors - other than embedded length - effect the magnitude of residual stresses, namely, the pile-soil stiffness ratio and the unloading stiffness ratio (3). Therefore, one might question the reason for correlating $q_{res}$

to D only. This correlation is established since it is believed by the author that for the piles in this study, $q_{res}$ changes most significantly with D. This assumption is made since all of the test piles under study are H-piles driven into sandy soils. Therefore, the pile-soil and unloading stiffness ratios should be similar for all piles which would cause D to effect $q_{res}$ most significantly. The graph of D versus $q_{res}$ is shown in Appendix 3-E (page 84). The total residual stress ($Q_{res}$) is computed for each test pile compression test by multiplying $q_{res}$ - obtained from Appendix 3-E - by the cross sectional area of the pile in the half plugged condition. Then, $Q_{res}$ is subtracted from $Q_s$ to obtain $Q^*_s$ - which is then used to compute the corrected ratio $C^*$ (see equation 2).

The second method used to correct for residual stress is based on correlations for full displacement piles as developed by Briaud, et al (3). This method will be referred to as the BETA method. The usefulness of this method is that it does not require data from fully instrumented load tests to predict $q_{res}$. Instead, $q_{res}$ is estimated from the characteristics of the soil and pile. In using this method, a significant assumption must be made concerning the degree to which the pile is plugged by the soil along its embedded length. Since the BETA method was developed based on the correlation of data from full displacement piles, the region between the flanges of the pile is assumed to be fully plugged by the soil when

calculating $Q_{res}$. Interestingly, the assumption of a fully plugged pile yielded the most reasonable estimates of $Q_{res}$. A sample calculation using the BETA method for Arkansas #7 is presented in Appendix 3-F (page 85).

Finally, in these methods used to determine the corrected ($C^*$) and uncorrected (C) ratios, three important assumptions are made concerning the linear extrapolation of measured data. These assumptions are: (1) $Q_{ut}$ will increase linearly with D in a tension test - applied to Lock and Dam 26:2-1; (2) load transfer curves can be extrapolated linearly with the side load to point load ratio (i.e. $Q_s/Q_{pt}$) remaining the same - applied to Lock and Dam 26:3IP-IIIS; and, (3) residual stresses increase linearly with pile embedment depth - used in Method 3.

## RESULTS

The results obtained without correcting for the effects of residual stress are shown in Table 2. These results are plotted in Figure 1 to provide a clearer indication of the amount of scatter in the computed values of "C". The average "C" value is 2.16; and, although the scatter is significant, all of the computed values lie close to or within $\pm 25$ percent of the average. Considering the different methods of analysis and assumptions used in determining these "C" ratios, the amount of scatter is less than what might be expected.

TABLE 2

Compression-Tension Test Correlations:
Uncorrected for Residual Stress
(All loads in tons)

| Test pile | Loads at Ultimate Failure: Compression test Total $Q_u$ | Compression test Point $Q_{pt}$ | Compression test Side $Q_s$ | Tension test $Q_{ut}$ | Uncorrected Ratio C |
|---|---|---|---|---|---|
| Fully instrumented: | | | | | |
| Arkansas #7 | 250.0 | 62.5 | 187.5 | 65.0 | 2.88 |
| L+D 26:3IP-IIIS(Meth.1) | 367.0 | 118.5 | 248.5 | 96.6 | 2.57 |
| L+D 26:3IP-IIIS(Meth.2) | 216.0 | 69.8 | 146.0 | 87.0 | 1.68 |
| L+D 26:1-3 | 322.0 | 160.0 | 165.0 | 64.4 | 2.56 |
| L+D 26:2-1 and 2-5 | 236.5 | 63.9 | 172.6 | 108.4(a) | 1.59 |
| L+D 26:2-4 and 2-5 | 236.5 | 63.9 | 172.6 | 96.0 | 1.80 |
| Non-fully instrumented:(b) | | | | | |
| L+D 6:K-8 | 387.5 | 155.5 | 232.0 | 145.8 | 1.59 |
| Canada 24-4 | 168.6 | 34.6 | 134.0 | 47.8 | 2.80 |
| Canada 24-5 | 88.8 | 19.3 | 69.5 | 33.7 | 2.06 |
| Canada 35-1 | 198.0 | 69.3 | 128.7 | 61.9 | 2.08 |
| | | | | Average "C" = | 2:16 |

(a) Value adjusted due to shorter embedment length and quick test of Lock and Dam 26:2-1 test pile.
(b) $Q_s$ and $Q_{pt}$ loads estimated using Coyle-Castello correlations (See Appendix 3-3, page 74).

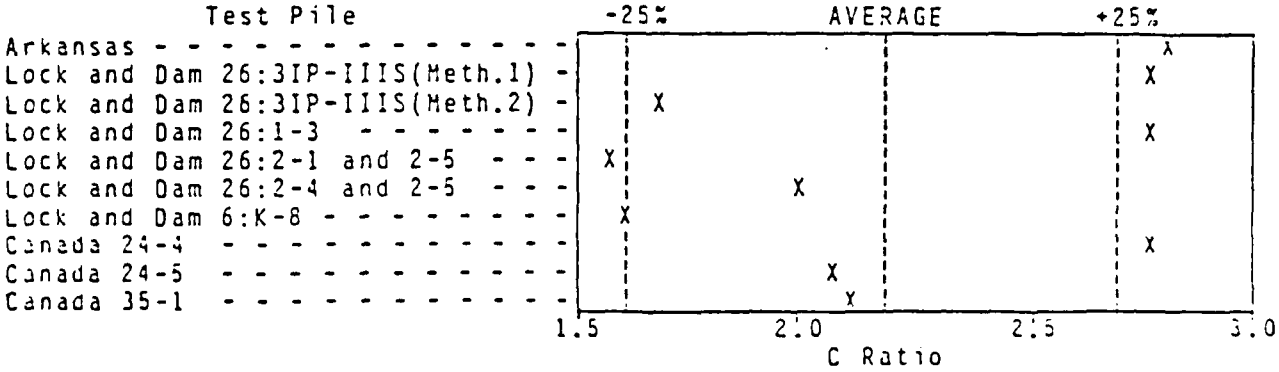


FIGURE 1. - Plot of C Ratios: Uncorrected for Residual Stress

As previously stated, the Coyle-Castello correlations were used to compute semi-empirical "C" values for the non-fully instrumented test piles. In two cases, the application of these correlations may seem inappropriate. The reason for this is that the ultimate capacity ($Q_u$), which is predicted by the Coyle-Castello correlations is not close to the measured $Q_u$ for two of the test piles (see Appendix 3-B, page 77). Specifically, the $Q_u$ values predicted for Lock and Dam 6:K-8 and Canada 24-5 grossly underpredict and overpredict, respectively, the measured loads. This inaccuracy does not necessarily result in an erroneous computation of "C", since only the predicted ratio of $Q_s/Q_u$ is used to estimate a value for $Q_s$. This estimated $Q_s$ value is obtained by multiplying the aforementioned predicted ratio by the corresponding measured $Q_u$ load. Referring to the table in Appendix 3-B (page 77), $Q_s$ shown under the measured loads column is the product of the corresponding measured $Q_u$ and computed $Q_s/Q_u$ ratio. Therefore, even if the predicted $Q_u$ load is grossly inaccurate, the computed $Q_s$ is not necessarily inaccurate, since the relative magnitudes of the $Q_u$ and $Q_s$ loads may still yield a predicted $Q_s/Q_u$ ratio which is reasonably accurate. To test this assertion, the Coyle-Castello correlations were used to determine this predicted ratio of side to total load for the fully instrumented Lock and Dam 26:2-5 test pile. The predicted and measured $Q_s/Q_u$ ratios varied by only seven

percent - even though the predicted $Q_u$ was 33 percent larger than the measured value.

The results obtained after correcting for the effects of residual stress using Method 3 are shown in Table 3. Figure 2 shows the computed $C^*$ values plotted for each test pile.

The most notable change which occurs after correcting for residual stress using this method is a reduction of 19 percent in the average "C" value (from 2.16 to 1.76). Since pile side friction ($Q_s$) is always reduced after correcting for residual stress, the fact that the average value of $C^*$ is less than the average value of "C" was to be expected. Since residual stress causes an increase in pile point bearing ($Q_{pt}$) and an equivalent decrease in side friction ($Q_s$), the ultimate pile capacity ($Q_u$) - which is the sum of $Q_{pt}$ and $Q_s$ - will remain the same before and after correcting for residual stress. Also, after correcting for residual stress by this method the amount of scatter in the data was reduced by about 14 percent. This reduction in scatter can be seen by comparing Figures 1 and 2. This reduction is not due to the effects of reduced scale, since the scatter in both cases is indicated by counting the number of data points lying within $\pm 25$ percent of each average.

Correcting for residual stress using the BETA method also resulted in a reduced value of "C" and a reduction in scatter compared to the uncorrected case. The results obtained using this method are tabulated in Table 4, and plotted in Figure 3.

TABLE 3

Compression-Tension Test Correlations:
Corrected for Residual Stress Using Method 3
(All loads in tons)

| Test pile | Loads at Ultimate Failure: Uncorrected Side $Q_s$ (a) | Residual $Q_{res}$ (b) | Corrected Side $Q^*_s$ (c) | Tension Test $Q_{ut}$ (a) | Corrected Ratio $C^*$ |
|---|---|---|---|---|---|
| Arkansas #7 | 187.5 | 25.0 | 162.5 | 65.0 | 2.50 |
| L+D 26:3IP-IIIS (Meth.1) | 248.5 | 39.6(d) | 208.9 | 96.6 | 2.16 |
| L+D 26:3IP-IIIS (Meth.2) | 146.0 | 35.7 | 110.3 | 87.0 | 1.27 |
| L+D 26:1-3 | 165.0 | 35.0 | 130.0 | 64.4 | 2.02 |
| L+D 26:2-1 and 2-5 | 172.6 | 32.7 | 139.9 | 108.4 | 1.29 |
| L+D 26:2-4 and 2-5 | 172.6 | 32.7 | 139.9 | 96.0 | 1.46 |
| L+D 6:K-8 | 232.0 | 21.8 | 210.2 | 145.8 | 1.44 |
| Canada 24-4 | 134.0 | 29.0 | 105.0 | 47.8 | 2.20 |
| Canada 24-5 | 69.5 | 20.0 | 49.5 | 33.7 | 1.47 |
| Canada 35-1 | 128.7 | 20.6 | 108.1 | 61.9 | 1.75 |

Average $C^* = 1.76$

(a) From Table 2.
(b) Estimated load from Appendix 3-E (page 84).
(c) $Q^*_s = Q_s - Q_{res}$.
(d) From linear extrapolation of load transfer curves.

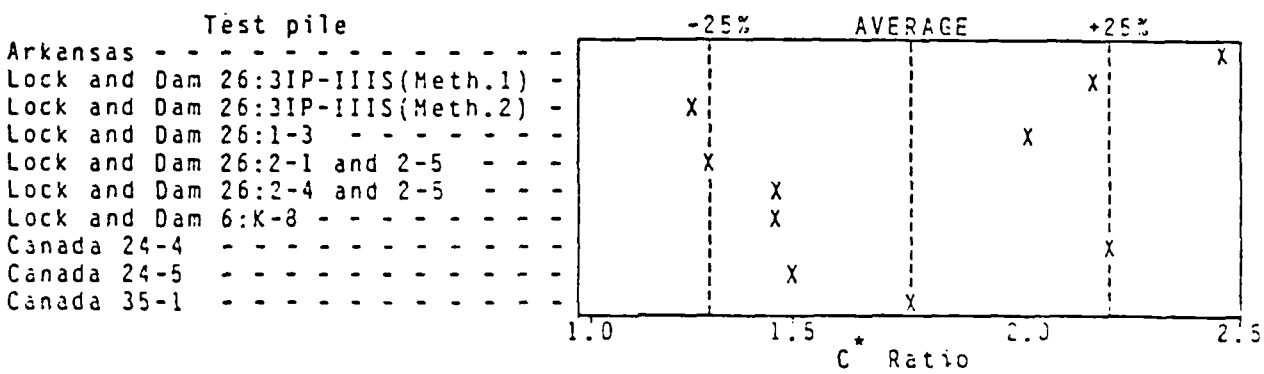


FIGURE 2. - Plot of $C^*$ Ratios: Corrected for Residual Stress Using Method 3

TABLE 4

Compression-Tension Test Correlations:
Corrected for Residual Stress Using the BETA Method
(All loads in tons)

| Test pile | Loads at Ultimate Failure: Uncorrected Side $Q_s$ (a) | Residual $Q_{res}$ (b) | Corrected Side $Q^*_s$ (c) | Tension Test $Q_{ut}$ (a) | Corrected Ratio $C^*$ |
|---|---|---|---|---|---|
| Arkansas #7 | 187.5 | 16.3 | 171.2 | 65.0 | 2.63 |
| L+D 26:3IP-IIIS (Meth.1) | 248.5 | 17.9 | 230.6 | 96.6 | 2.48 |
| L+D 26:3IP-IIIS (Meth.2) | 146.0 | 17.9 | 128.1 | 87.0 | 1.47 |
| L+D 26:1-3 | 165.0 | 17.3 | 147.7 | 64.4 | 2.29 |
| L+D 26:2-1 and 2-5 | 172.6 | 18.2 | 154.4 | 108.4 | 1.42 |
| L+D 26:2-4 and 2-5 | 172.6 | 18.2 | 154.4 | 96.0 | 1.61 |
| L+D 6:K-8 | 232.0 | 12.0 | 220.0 | 145.8 | 1.51 |
| Canada 24-4 | 134.0 | 19.9 | 114.1 | 47.8 | 2.39 |
| Canada 24-5 | 69.5 | 13.9 | 55.6 | 33.7 | 1.65 |
| Canada 35-1 | 128.7 | 11.5 | 117.2 | 61.9 | 1.89 |

Average $C^* = 1.93$

(a) From Table 2.
(b) Estimated from BETA Method - assuming area between pile flanges fully plugged by soil.
(c) $Q^*_s = Q_s - Q_{res}$.

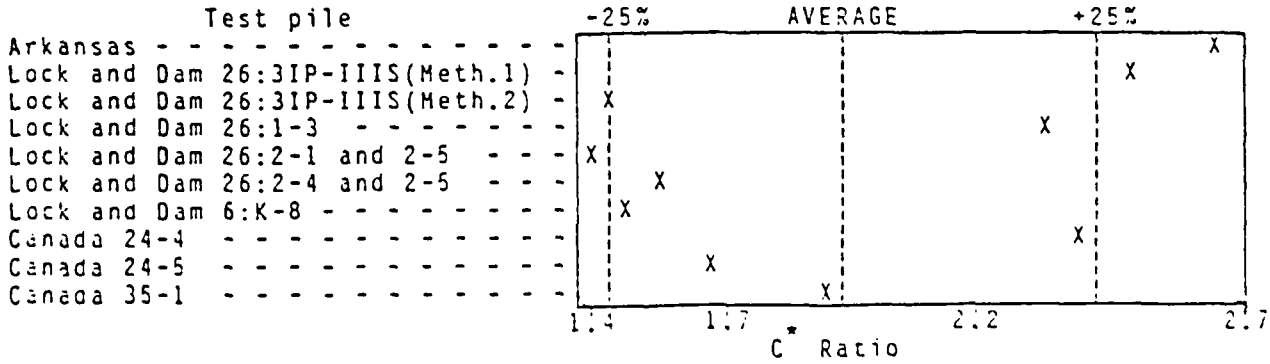


FIGURE 3. - Plot of $C^*$ Ratios: Corrected for Residual Stress Using the BETA Method

Again, the most significant changes from the uncorrected case are: an 11 percent reduction in the average "C" value - from 2.16 to 1.93; and, a reduction in the scatter by approximately 13 percent. Since the residual stresses estimated by the BETA method are somewhat smaller than the corresponding stresses estimated by Method 3 (see Tables 3 and 4), the latter correction method results in a lower average $C^*$ value. However, the amount of scatter in the computed values of $C^*$ resulting from these two methods is about the same.

From the results described above, a corrected $C^*$ equal to 1.8 will be used to develop the design parameters below. The specific value of 1.8 is chosen for two reasons. These reasons are: (1) based on field measured residual stress data (5), Method 3 seems to only slightly overestimate $Q_{res}$, while the BETA method underestimates $Q_{res}$; and, (2) Method 3 resulted in the least scatter in the data. Therefore, a value of $C^*$ was chosen which was close to the Method 3 average of 1.76 - but still between this average and the average $C^*$ value of 1.93 obtained from the BETA method.

The physical meaning of this ratio ($C^*$) is stated as follows. If the ultimate tension capacity of an H-pile in sand is measured at a movement of 1.2 inches and then multiplied by 1.8, the resulting load is approximately equal to the side friction load which would be developed in a compression test on the same pile measured at a settlement of 2.0 inches. This approximation includes a correction for residual driving

stresses. The ultimate tension capacity ($Q_{ut}$) is assumed to result solely from the development of side friction along the pile, since the pile point bearing is assumed to be zero during a tension test. This is due to the fact that the pile tip will either remain stationary or be displaced upward during extraction.

As previously stated, the importance of the ratio represented by $C^*$ is that by using this ratio in conjuction with the results of a tension test, a field measured ultimate compression load ($Q_u$) can be separated into its corrected side friction ($Q^*_s$) and point bearing ($Q^*_{pt}$) load components. This capability is useful in that: by separating a total compression load into its component parts, it allows one to utilize the results of non-fully instrumented pile tests in establishing design parameters. The development of these parameters is the subject of the remainder of this study.

## ULTIMATE PILE CAPACITY

In this section, design parameters for the ultimate pile capacity in compression for an H-pile in sand are determined. As discussed previously, the ultimate compression capacity is defined as the load corresponding to a pile head settlement of 2.0 inches. To determine this capacity, a $C^*$ value equal to 1.8 and the Coyle-Castello correlations are applied to the test piles in Table 1.

To predict the ultimate capacity of an H-pile - as well as other types of deep foundation systems - some information or assumption concerning the size and shape of the failure surface is usually required. For an H-pile in sand, this requirement translates into making an assumption concerning the degree to which the soil "acts as a plug" between the pile flanges during load testing. A "soil plug" means that some or all of the soil located between the flanges of the H-pile moves with the pile as the pile reaches its ultimate axial load capacity in tension or compression. This movement of soil with the pile changes the effective pile displacement, thereby changing the size and shape of the failure surface. Figure 4 shows an unplugged and fully plugged H-pile. Therefore, predicting the ultimate compression capacity is largely a problem of determining to what extent the soil is plugged between the flanges during failure. For this reason, a primary

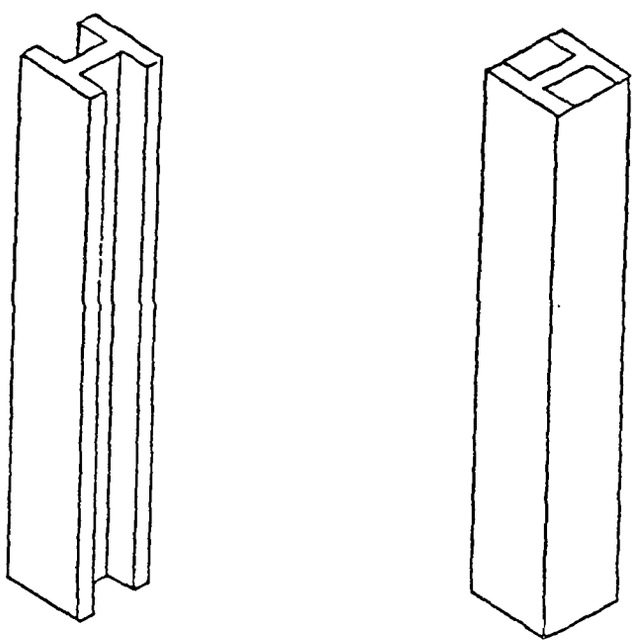

(a) Unplugged Perimeter (b) Fully Plugged Perimeter

(a) Unplugged Cross Section (b) Fully Plugged Cross Section

FIGURE 4. - Effect of Soil Plugging on Pile Areas (from ref.2):
(a) Unplugged Pile
(b) Fully Plugged Pile

objective of this section is to establish the degree to which this plugging occurs.

Although discussions and an analysis are presented concerning the percent of soil plugging that takes place, it should be noted that any percentage obtained represents only an average over the entire embedded length of the pile. For example, if the results indicate the pile to be one-half plugged in compression, this may mean that the bottom half of the embedded length is fully plugged while the upper half is unplugged (or vice versa). In fact, an infinite number of different plugging situations may occur along the pile's length which all result in the same degree of plugging averaged over the entire length.

## METHOD OF ANALYSIS

The previously established ratio of $C^* = 1.8$ and the Coyle-Castello correlations are utilized to determine the extent to which this plugging occurs during ultimate failure in compression. In general, the procedure used to analyze the test pile data can be divided into four parts. These parts are: (1) determine the corrected side ($Q^*_s$) and point ($Q^*_{pt}$) loads; (2) compute unit point bearing ($q^*_o$) and side friction ($f^*_s$); (3) compute the relative depths for the pile tip and side; and, (4) plot the backfigured data from (2) and (3) on the Coyle-Castello curves and compare the predicted point and side friction angles ($\phi_{pt,p}$ and $\phi_{s,p}$, respectively) with the

corresponding in-situ friction angles ( $\phi_{pt}$ and $\phi_s$) to determine the closest correlations. The detailed procedures used to accomplish each of these steps are described in the following paragraphs.

First, to determine $Q^*_{pt}$ and $Q^*_s$ the ratio of $C^* = 1.8$ is applied to each test pile. This ratio is multiplied by the measured $Q_{ut}$ (as listed in Table 2) to estimate values for $Q^*_s$ as shown in the following equation:

$$Q^*_s = C^* * Q_{ut}. \tag{4}$$

This computed $Q^*_s$ load is then subtracted from the measured $Q_u$ (as listed in Table 2) to determine $Q^*_{pt}$ as follows:

$$Q^*_{pt} = Q_u - Q^*_s. \tag{5}$$

For the fully instrumented piles, load transfer data could have been utilized to obtain measured values for $Q^*_{pt}$ and $Q^*_s$. However, to avoid an inconsistency by using one method for the fully instrumented piles and a different method for the non-fully instrumented piles, the method described above is used to estimate $Q^*_{pt}$ and $Q^*_s$ for all test piles.

Once these corrected point and side loads are computed, they are divided by the total point ($A_{pt}$) and side ($A_s$) areas, respectively, to obtain corrected values for unit point bearing ($q^*_o$) and unit side friction ($f^*_s$) as follows:

$$q^*_o = Q^*_{pt}/A_{pt}, \tag{6}$$

and,

$$f^*_s = Q^*_s/A_s. \tag{7}$$

In computing these unit resistances, four cases are considered. These cases are: (1) an unplugged; (2) a one-third plugged; (3) a one-half plugged; and, (4) a fully plugged H-pile. In each case, the total areas of the pile point ($A_{pt}$) and side ($A_s$) surfaces are computed. These areas are then used in equations (6) and (7) to determine the unit resistances $q^*_o$ and $f^*_s$.

The third step requires the calculation of the relative depths for the pile point $(D/B)_{pt}$ and side $(D/B)_s$. In each of the four plugging conditions mentioned above, the equivalent circular pile diameter (B) is computed from the pile cross sectional area ($A_{pt}$) as shown below:

$$B = \sqrt{4 * A_{pt}/\pi}. \tag{8}$$

Since the unit side friction ($f^*_s$) and soil friction angles for the pile side ($\phi_s$) represent averages over the embedded length of the pile, $(D/B)_s$ is computed based on a D value equal to one-half of the piles embedment depth. However, since the D value used in calculating $(D/B)_{pt}$ represents the depth of the pile tip, D in this case is equal to the total embedded

depth of the pile. Therefore, $(D/B)_{pt}$ and $(D/B)_s$ are related by:

$$(D/B)_{pt} = (D/B)_s * 2.0 \ . \tag{9}$$

The last step involves plotting $q^*_o$ and $f^*_s$ versus the corresponding relative depths - $(D/B)_{pt}$ and $(D/B)_s$ - for each case and comparing the predicted point and side soil friction angles ( $\phi_{pt,p}$ and $\phi_{s,p}$) against the corresponding in-situ angles ($\phi_{pt}$ and $\phi_s$). The least amount of deviation between the predicted and in-situ friction angles is used as the criteria for establishing the closest correlation and determining to what degree the pile is plugged by the soil. The in-situ friction angles are determined from SPT blow count (N) data using a relationship between $\phi$ and N obtained from reference 2. To allow the results to be analyzed in greater detail, minimum and maximum $\phi$ values are estimated based on the adjusted ($N_{ad}$) and unadjusted (N) blow counts, respectively. From reference 1, the relation between the adjusted and unadjusted blow count is:

$$N_{ad} = 15 + (N-15)/2. \tag{10}$$

Also by reference 1, this adjustment is usually applied to N values greater than 15 in fine silty sands below the water table. However, for the purpose of analyzing the results in this section, this adjustment is applied regardless of the

soil profile. A sample calculation of the above procedures for Arkansas #7 are presented in Appendix 3-G (page 87).

The most significant assumptions made in the above method of analysis concerns whether or not channel iron was welded to the web of some of the fully instrumented test piles. To protect the strain gages or strain rods located along the web of a fully instrumented pile, channel iron is usually welded along the pile web and capped at the bottom to provide a protective covering during driving and testing. If channel iron is welded to the web, then $A_s$ and $A_{pt}$ will both increase significantly in the zero soil plug case. The data available did not indicate whether or not this channel was attached to the fully instrumented Lock and Dam 26:3IP-IIIS and Lock and Dam 26:2-5 test piles; therefore, the assumption is made that channel iron is welded to the web and the tip and side areas are computed accordingly. Similarly, the data did not indicate whether or not channel iron was attached to any of the non-fully instrumented piles. For these piles, the assumption is made that channel iron is not attached, since strain devices were not installed along the pile's embedded length.

## RESULTS

The data resulting from the above analysis is presented in Table 5. After reviewing the data in this table, three significant features are noted. First, as the percent of plugging in the pile increases from zero to 100 percent, the

TABLE 5

Backfigured Unit Resistances, Relative Depths and Friction Angles

| Test pile | Unit Resistances - in tsf: Point bearing ($q^*_o$) Percent plug 0 | 33 | 50 | 100 | Side friction ($f^*_s$) Percent plug 0 | 33 | 50 | 100 | Relative Depths: Point - $(D/B)_{pt}$ Percent Plug 0 | 33 | 50 | 100 | Side - $(D/B)_s$ Percent plug 0 | 33 | 50 | 100 |
|---|---|---|---|---|---|---|---|---|---|---|---|---|---|---|---|---|
| Arkansas #7 | 475 | 238 | 174 | 108 | .30 | .37 | .39 | .50 | 88 | 62 | 52 | 42 | 44 | 31 | 26 | 21 |
| L+D 26:3IP-IIIS (Meth.1) | 689 | 345 | 252 | 157 | .43 | .53 | .56 | .71 | 90 | 64 | 54 | 44 | 45 | 32 | 27 | 22 |
| L+D 26:3IP-IIIS (Meth.2) | 211 | 106 | 77 | 48 | .39 | .48 | .50 | .64 | 90 | 64 | 54 | 44 | 45 | 32 | 27 | 22 |
| L+D 26:1-3 | 857 | 374 | 273 | 170 | .29 | .35 | .37 | .47 | 96 | 64 | 54 | 44 | 48 | 32 | 27 | 22 |
| L+D 26:2-1 and 2-5 | 169 | 74 | 54 | 33 | .44 | .54 | .57 | .73 | 98 | 65 | 56 | 44 | 49 | 33 | 28 | 22 |
| L+D 26:2-4 and 2-5 | 261 | 114 | 83 | 52 | .39 | .48 | .50 | .65 | 98 | 65 | 56 | 44 | 49 | 33 | 28 | 22 |
| L+D 6:K-8 | 840 | 224 | 125 | 102 | .97 | 1.10 | 1.15 | 1.47 | 90 | 47 | 40 | 31 | 45 | 23 | 20 | 16 |
| Canada 24-4 | 765 | 206 | 151 | 84 | .21 | .23 | .25 | .31 | 196 | 102 | 88 | 64 | 98 | 51 | 44 | 32 |
| Canada 24-5 | 260 | 70 | 51 | 28 | .21 | .24 | .25 | .32 | 135 | 70 | 60 | 45 | 67 | 35 | 30 | 22 |
| Canada 35-1 | 574 | 295 | 147 | 84 | .40 | .45 | .48 | .60 | 110 | 64 | 56 | 42 | 55 | 32 | 28 | 21 |

| Test pile | In-Situ Soil Friction Angle[a] - in degrees: Point - pt[b] MIN | MAX | Side - s[c] MIN | MAX |
|---|---|---|---|---|
| Arkansas #7 | 36.0 | 40.0 | 33.0 | 35.0 |
| L+D 26:3IP-IIIS (Meth.1) | 38.5 | 43.5 | 35.5 | 38.5 |
| L+D 26:3IP-IIIS (Meth.2) | 38.5 | 43.5 | 35.5 | 38.5 |
| L+D 26:1-3 | 37.0 | 41.0 | 34.0 | 36.0 |
| L+D 26:2-1 and 2-5 | 35.5 | 39.5 | 33.0 | 34.5 |
| L+D 26:2-4 and 2-5 | 35.5 | 39.5 | 33.0 | 34.5 |
| L+D 6:K-8 | 34.5 | 37.0 | 32.5 | 33.0 |
| Canada 24-4 | 32.0 | 32.0 | 32.5 | 34.0 |
| Canada 24-5 | 33.5 | 35.5 | 33.0 | 35.0 |
| Canada 35-1 | 36.0 | 40.0 | 32.5 | 33.0 |

(a) Minimum friction angles from adjusted SPT blow count (i.e. $N_{ad}$). Maximum friction angles from unadjusted blow count (i.e. N).

(b) Point friction angle from average blow count ±3 pile diameters from tip.

(c) Side friction angles from weighted average blow count along embedded length of pile.

unit point bearing ($q^*_o$) decreases and the unit side friction ($f^*_s$) increases. This pattern is explained by the changes which occur in the computed tip ($A_{pt}$) and side ($A_s$) areas as the extent of the soil plug changes. Specifically, as the percentage of plugging between the pile flanges increases, then $A_{pt}$ and $A_s$ increase and decrease, respectively. In equations (6) and (7), $Q^*_{pt}$ and $Q^*_s$ are constant for a given ultimate load ($Q_u$); therefore, $q^*_o$ and $f^*_s$ are inversely proportional to $A_{pt}$ and $A_s$, respectively. A second observation concerning the data in Table 5 is the fact that the $q^*_o$ and $f^*_s$ values for Lock and Dam 26:3IP-IIIS (Method 1) and Lock and Dam 6:K-8 are much larger than the corresponding values computed for the other test piles. This is probably due to the fact that both of the measured load-settlement curves for the aforementioned piles do not extend to a movement of 2.0 inches (8,12). Therefore, as previously described, the curves for these piles were extended linearly to $\delta$=2.0 inches by Method 1. This linear extension probably overestimated their $Q_u$ values, since load-settlement curves in general become asmyptotic (or at least undergo a change in slope) before a settlement of 2.0 inches. A non-linear curve would then result in a smaller $Q_u$ load. If $Q_u$ is overestimated, then one or both of the $Q^*_s$ and $Q^*_{pt}$ loads would also be overestimated. Therefore, by equations (6) and (7), $q^*_o$ and $f^*_s$ would be too large. The final observation concerns the unit resistances computed for the Lock and Dam 26:1-3 test pile. While this

pile shows the largest computed values for $q^*_o$, the values for $f^*_s$ are the third smallest of the ten piles analyzed. These results indicate that $q^*_o$ - relative to $f^*_s$ - is larger than what would normally be expected. This can perhaps be explained by the location of the tip of this pile in - or slightly above - a thin layer of gravel/cobbles (2). The presence of this coarse material may have caused a sharp increase in the effective soil friction angle at the tip; consequently, the unit point bearing capacity would probably be significantly larger relative to the unit side friction.

As discussed earlier, to predict the ultimate compression capacity of an H-pile, a correlation must be established concerning the degree to which the soil becomes plugged between the flanges of the pile. To develop this correlation, the data from Table 5 is plotted on the Coyle-Castello curves for full displacement piles in sand (6). These plotted data are shown in Figures 5 and 6. These figures relate unit resistance to relative depth for different soil friction angles. Referring to these figures, the solid soil friction angle curves indicate those portions of the curves obtained from reference 6. The dashed curves represent the portion of the curves extended by the author to allow for a more accurate analysis of the plotted data.

For the purpose of analyzing the results, deviation friction angles are established. These deviation angles are simply the difference between the predicted friction angles (

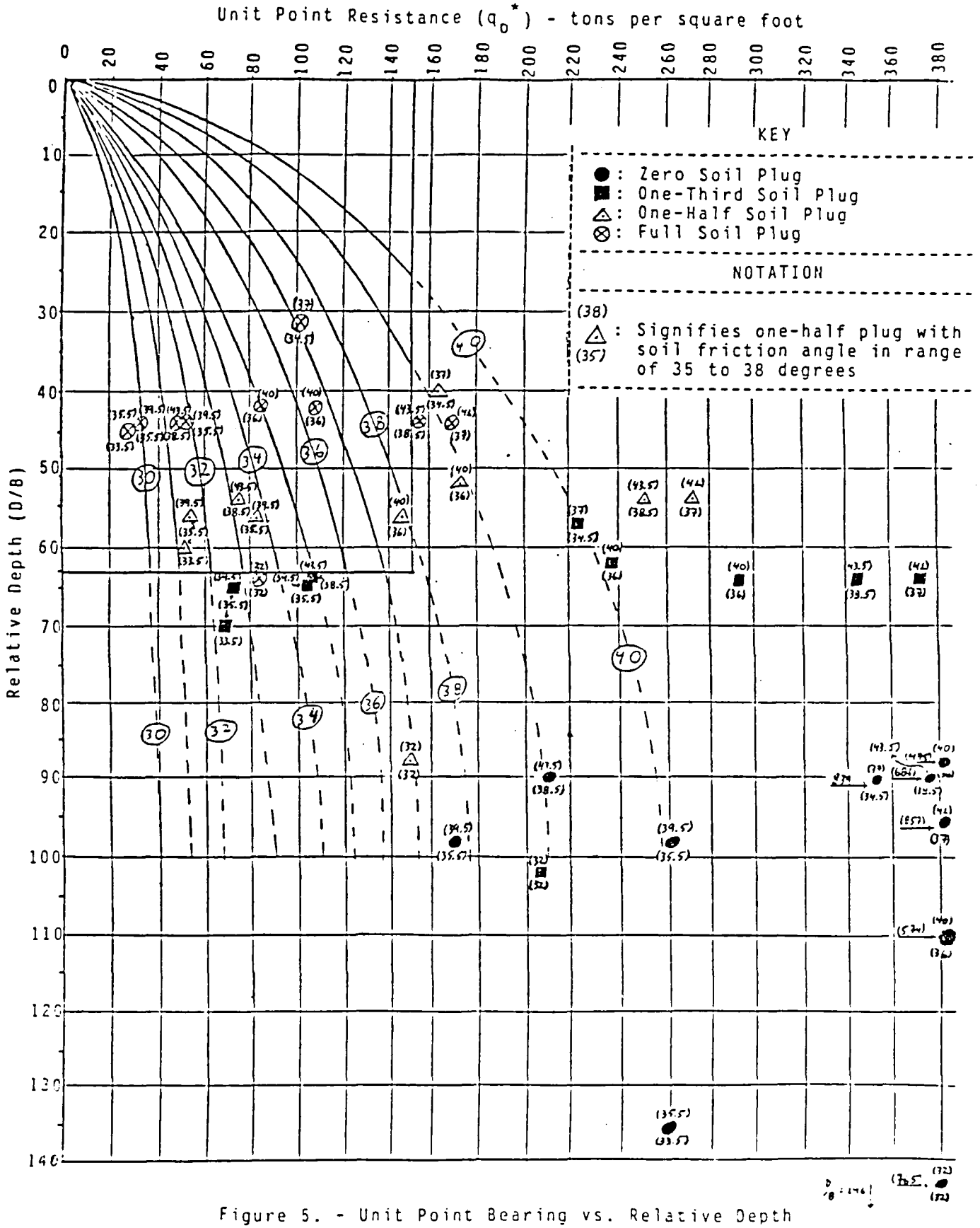


Figure 5. - Unit Point Bearing vs. Relative Depth

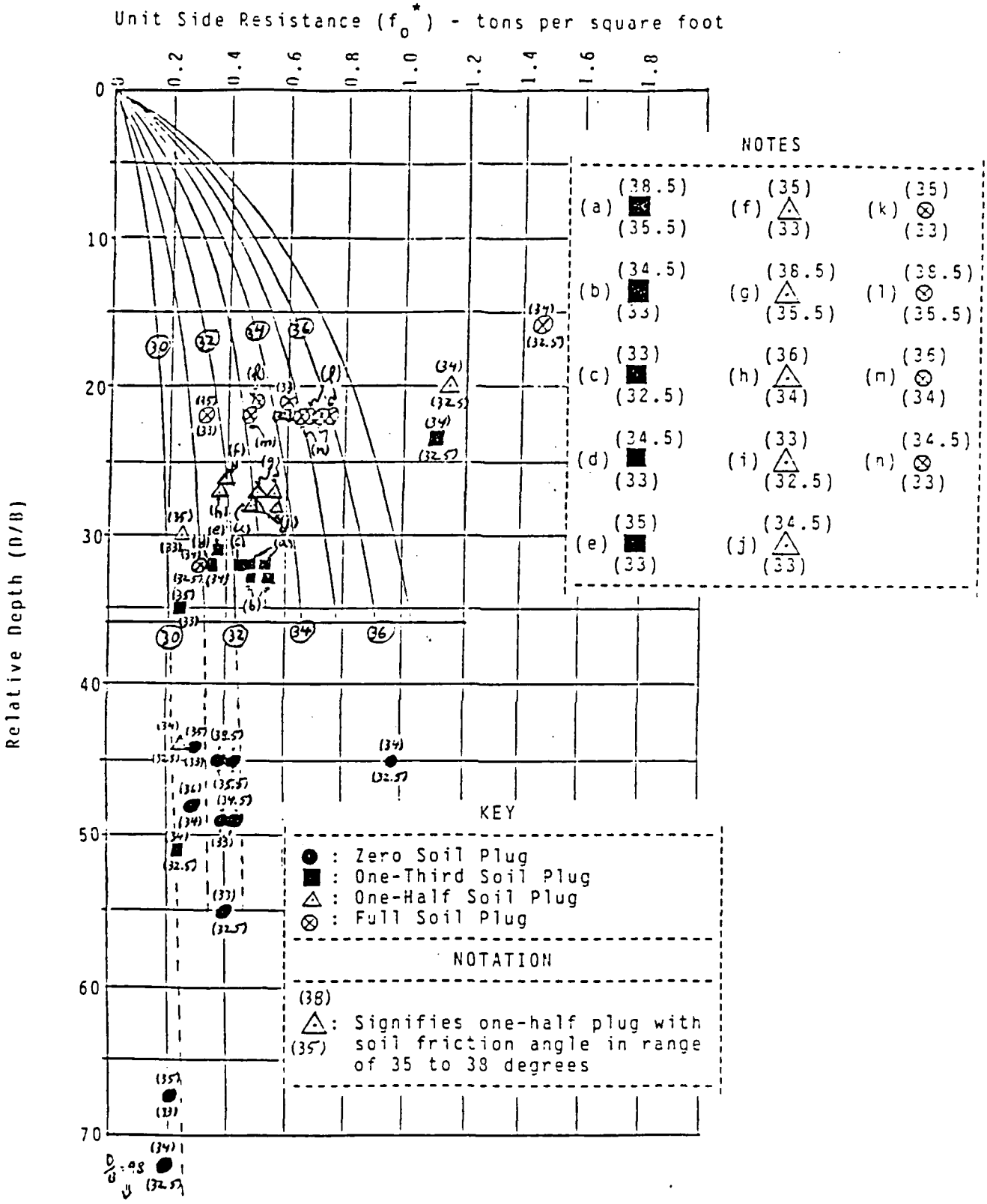


Figure 6. - Unit Side Friction vs. Relative Depth

$\phi_{pt,p}$ and $\phi_{s,p}$) - obtained from the position of each data point in Figures 5 and 6 with respect to the $\phi$ curves - and the corresponding in-situ friction angles ($\phi_{pt}$ and $\phi_s$) which each data point represents. For point bearing this deviation angle is defined as:

$$\phi_{pt,dev} = ( \phi_{pt} - \phi_{pt,p}), \tag{11}$$

and for side friction;

$$\phi_{s,dev} = ( \phi_s - \phi_{s,p}). \tag{12}$$

The usefulness of these deviation angles is that the closest correlation between the plotted data and the Coyle-Castello curves is determined by the smallest deviation angle.

To determine the closest correlation three different methods are used to estimate the in-situ soil friction angle. Therefore, for each plugging assumption three different deviation angles are computed. The three in-situ soil friction angles which are estimated for each pile are based on: (1) the unadjusted blow count (N); (2) the adjusted blow count ($N_{ad}$); and, (3) the average of N and $N_{ad}$ ($N_{avg}$). All calculated deviation angles are presented in Appendix 3-H (page 90).

Two factors are considered to establish the best correlation from the results shown in Appendix 3-H. These considerations are: (1) the smallest average deviation angle; and, (2) the smallest amount of scatter in the plotted data. Using these two criteria, the best correlation between the

computed data and the Coyle-Castello curves were found as follows. For point bearing, the best correlation occurs when the H-pile is assumed to be one-half plugged and the in-situ friction angle at the tip is determined using an adjusted blow count ($N_{ad}$) value. For side friction, the best correlation occurs when the H-pile is assumed to be fully plugged and the in-situ friction angle along the side is estimated using an average of the adjusted and unadjusted blow counts ($N_{avg}$). The Lock and Dam 6:K-8 test pile was disregarded in establishing these correlations, since the $q^*_o$ and $f^*_s$ values shown in Table 5 for this pile seem to be grossly overestimated by linearly extending the load-settlement curve to a 2.0 inch movement. Interestingly, the results obtained above for unit point bearing agree with the results obtained in class (5). Namely, both determined that the best correlation occurs when the pile tip is assumed to be one-half plugged and the in-situ soil friction angle ( $\phi_{pt}$) is estimated using an adjusted blow count ($N_{ad}$) value. For unit side friction, the class results differed from the best correlation obtained in this study. Specifically, the class results determined that the best correlation occurs if: (1) the pile is assumed to be one-half plugged by the soil - instead of fully plugged; and, (2) an unadjusted N value is used to estimate $\phi_s$ - instead of $N_{avg}$ (5).

An attempt was made to correlate the large unit point resistances ($q^*_o$) calculated for the zero plug condition to

the soil strength as determined by the static Cone Penetrometer Test (CPT). This attempt was undertaken since these $q^*_o$ values were found to correlate poorly with the Coyle-Castello curves (see Figure 5). The desired correlation - designated as X - between $q^*_o$ and the CPT results is defined as the ratio:

$$X = q^*_o / q_c, \tag{13}$$

where $q_c$ is the bearing strength of the soil as determined by the CPT. Initially, the following procedure was used to compute X. A data base of six test piles (five of which were driven at the same site) were analyzed. For each pile, $q^*_o$ was estimated using the ratio of $C^* = 1.8$. For each of the soil profiles at the two different sites, $q_c$ was computed using: the Cone Method; the deRuiter and Beringen Method; the Bustamante and Gianeselli Method; and, the L.P.C. Method (4). With the values for $q^*_o$ and $q_c$ computed in this way, no correlation was evident due to the large amount of scatter in the calculated values of X. A second procedure was then tried using: (1) a smaller data base of two test piles - at different sites; (2) $q^*_o$ obtained from measured load transfer data; and, (3) $q_c$ values obtained from the Cone Method only. Four test piles were not considered in this second attempt since either: (1) the CPT was conducted at a significant distance from the test pile; or, (2) the test pile was driven through layers of coarse material. This second attempt yielded

an X value of about 2.74 for both piles with almost no scatter. The calculation of X for these two piles is shown in Appendix 3-I (page 92). Unfortunately, no conclusions can be drawn from these results, since the data base consisted of only two test piles. The analysis of additional data are required before a correlation or trend can be established with any degree of confidence.

## LOAD - SETTLEMENT CHARACTERISTICS

The objective of this section is to predict the load-settlement characteristics of H-piles in cohesionless soil. After this objective is achieved, the accuracy of the prediction model is tested by its ability to predict the measured load-settlement curves of two full-scale, field load tested H-piles, which are not part of the data base. The procedures required to accomplish these goals are described in the following paragraphs.

### METHOD OF ANALYSIS

Heretofore, pile movements resulting from applied loads have only been considered for the purpose of establishing ultimate compression ($Q_u$) and tension ($Q_{ut}$) loads. To accomplish the above objective, the utilization of pile movements will be expanded. Specifically, the relationship between these measured pile movements must be investigated as they relate to: (1) pile elasticity; and, (2) the development of unit point bearing ($q^*_o$) and unit side friction ($f^*_s$) - expressed as a percentage of their maximum values. These important relationships - as well as other factors - are incorporated into the modified axially loaded pile computer program known as APILE1 (5). By using the proper input data, APILE1 can accurately predict the measured load-settlement

curve of an axially loaded pile. The input data required for this program can be divided into two types: (1) that which can be easily obtained from the given pile-soil characteristics; and, (2) computed data obtained from an analysis of several pile load tests. Therefore, the method of analysis described below is devoted primarily to explaining how the latter computed input data are obtained.

This computed data consists of the T-Z and TOTLD-$Z_t$ curves. Here, Z is defined as the relative movement between the pile and the surrounding soil at some point along the pile side, and it is obtained after correcting the measured pile movement for elastic load deformations. The value $Z_t$ is the movement of the pile tip relative to the surrounding soil, and it is similarly obtained after correcting the measured tip movement for elastic deformation along the pile's length. The variables T and TOTLD are defined respectively as the percent of maximum unit side friction and unit point bearing developed as the pile side and tip move under some applied load. These variables are defined as follows:

$$T = f^*_s / f_{s,max}, \tag{14}$$

and,

$$TOTLD = q^*_o / q_{o,max}. \tag{15}$$

Therefore, the T-Z and TOTLD-$Z_t$ curves can be physically interpreted as the percent of the maximum unit resistances

which are developed as the pile side and tip move relative to the surrounding soil. The test pile data base listed in Table 1 and the previously computed ratio of $C^* = 1.8$ are both utilized to calculate these curves. The method of analysis described in the following paragraphs is divided into two parts. First, the procedures and assumptions employed to compute the T-Z and TOTLD-$Z_t$ curves are fully described. The second part explains how these computed curves are used with APILE1 to predict the measured load-settlement curves of two H-piles in cohesionless soil.

## Compute T-Z and TOTLD-$Z_t$ Curves

Three steps are required to compute these curves. These steps are: (1) the extrapolation of load transfer curves for each test pile in the data base; (2) the development of T-Z and TOTLD-$Z_t$ curves for each pile - from the load transfer curves extrapolated above; and, (3) the combination of the curves developed in (2) to obtain one T-Z and one TOTLD-$Z_t$ curve, which are representative of the entire data base. The two curves obtained from step (3) will then be used as part of the input data for APILE1. Each of these steps are described in detail below.

The usefulness of the load transfer curves extrapolated in step (1) is that for each pile, each load transfer curve will eventually result in a single data point on each of the T-Z and TOTLD-$Z_t$ plots for that pile. Therefore, if several

load transfer curves for each test pile can be extrapolated, then several data points can eventually be plotted on the T-Z and TOTLD-$Z_t$ plots for that pile - allowing curves to be drawn to fit the data.

To extrapolate these load transfer curves, two pieces of information are required. First, for each test pile the shape and location of the load transfer curve representing an applied load ($Q_{app}$) equal to the ultimate load ($Q_u$) is needed. Once this load transfer curve is plotted, a knowledge of how the shape and location of load transfer curves for H-piles in sand change as $Q_{app}$ decreases is required to extrapolate additional curves at smaller applied loads. To simplify the problem, the shape of all extrapolated load transfer curves are assumed to be linear with depth. Therefore, once the load transfer curve corresponding to $Q_{app} = Q_u$ is plotted, then to plot additional load transfer curves at smaller applied loads the problem reduces to one of determining how the slopes of the linear load transfer curves change with respect to one another as $Q_{app}$ is reduced. Consequently, the analysis below is sub-divided as follows: (1) the load transfer curve corresponding to an applied load equal to $Q_u$ is plotted for each test pile in the data base; and, (2) from an analysis of measured load transfer curves of H-piles in sand, a correlation is established between the relative changes in the slopes of these curves with respect to one another. This information on relative changes in slope will allow additional

load transfer curves to be extrapolated for each pile at applied loads below $Q_u$. Figure 7a shows the general shape of extrapolated load transfer curves if their slopes are assumed not to change with respect to one another. Conversely, Figure 7b shows extrapolated curves if their slopes are assumed to change with respect to one another. The solid line in Figures 7a and 7b represent the load transfer curve corresponding to an applied load of $Q_u$, while the dashed lines represent the extrapolated curves resulting from an analysis of measured load transfer curve slope relationships.

As stated earlier, the first part of the analysis requires plotting the load transfer curves corresponding to an applied load of $Q_u$ for each test pile. To plot these load transfer curves the ratio of $C^* = 1.8$ is used. Since $Q_{ut}$ is known for each test pile (see Table 2), $Q^*_s$ is easily computed using this ratio. Therefore, since $Q_u$ is also known from Table 2, $Q^*_{pt}$ can be calculated as shown below:

$$Q^*_{pt} = Q_u - Q^*_s. \tag{16}$$

Once $Q^*_s$ and $Q^*_{pt}$ are obtained, the load transfer curve corresponding to an applied load of $Q_u$ can be plotted - as shown by the solid lines in Figure 7. Three points are noted concerning this procedure. First, the load transfer curves plotted in this way are clearly estimated from the ratio of $C^* = 1.8$. Secondly, these curves are already corrected for residual stress, since 1.8 represents a corrected value for

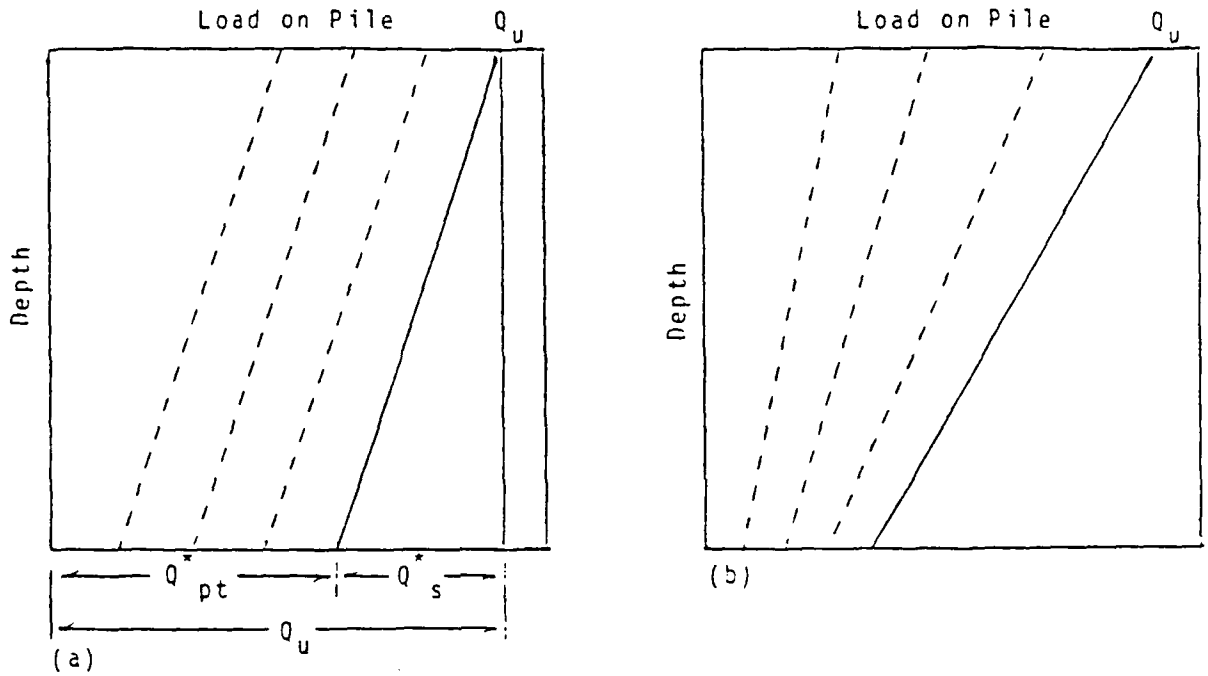


FIGURE 7. - Sketch of Linear Extrapolated Load Transfer Curves Assuming:
(a) Constant relative slope between curves; and,
(b) Varying relative slope between curves.

$C^*$. Finally, one may question the reason for estimating these load transfer curves for the fully instrumented test piles, since measured load transfer data is available for these piles. The reasons for this are: (1) to maintain a consistent method of analysis between the fully and non-fully instrumented test piles; and, (2) to test the accuracy and usefulness of the computed $C^*$ value of 1.8 in developing desired design parameters.

The next step in the analysis requires the extrapolation of load transfer curves at applied loads less than $Q_u$ for each pile. To accomplish this extrapolation a data base of six fully instrumented, field load tested H-piles in sand are used to determine how the slopes of the load transfer curves vary with respect to one another. This group of six test piles will hereafter be referred to as Group 1. The names of the piles in Group 1 are given in Appendix 3-J (page 93). For the purpose of analyzing the measured load transfer data provided by the piles in Group 1, the following ratios are established:

$$R_1 = Q_{app}/Q_u, \tag{17}$$

and,

$$R_2 = Q^*_s/Q^*_{pt}. \tag{18}$$

The ratio $R_2$ is corrected for residual stress by assuming that the computed residual stress, which exists at $Q_u$, decreases proportional to $Q_{app}$ (refer to Appendix 3-E on page 84 for the

residual stress at $Q_{app}$). The above ratios are then computed for each measured load transfer curve for the piles in Group 1. These computed ratios are then tabulated and graphed against one another. This tabulated and plotted data is presented in Appendix 3-J (page 95), as well as the complete set of calculations for the Arkansas #6 test pile. The physical significance of graphing corresponding values of $R_1$ versus $R_2$ is that the resulting straight lines which are formed for each pile in the group indicate how applied loads are distributed between $Q^*_s$ and $Q^*_{pt}$ as $Q_{app}$ changes. Once these six straight lines were graphed and compared with one another, the line corresponding to the Lock and Dam 26:1-3 test pile was found to have an unusually flat slope compared to the lines obtained from the other five piles (see Appendix 3-J, page 95). The measured load transfer data from this pile probably yielded a flatter slope due to the fact that its tip rests in or near a layer of cobbles or gravel (2). This situation may have caused the smaller relative change noticed between $Q^*_s$ and $Q^*_{pt}$, as $Q_{app}$ was increased. Therefore, this pile was disregarded and the slopes of the remaining five lines were averaged. This average slope is useful since it provides a means of estimating how pile loads are distributed between the point and side as the applied load is varied. Knowing this, load transfer curves can be extrapolated for each of the test piles in the data base.

Therefore, using the ratio of $C^* = 1.8$ and the analysis of measured load transfer data from the fully instrumented piles in Group 1, four load transfer curves for each pile in the data base are extrapolated at applied loads equal to $Q_u$, $.85Q_u$, $.70Q_u$ and $.55Q_u$. The tabulated and graphical results are presented in Appendix 3-K (page 96).

As mentioned above, the second step required to establish these T-Z and TOTLD-$Z_t$ curves is the development of individual curves for each data base test pile. This was done as follows. For each load transfer curve extrapolated above, two data points can be plotted - one on the T-Z plot and one on the TOTLD-$Z_t$ plot. Therefore, four load transfer curves per pile will yield four points on each of these plots. These four points allow rough curves to be drawn to fit the plotted data. After normalization, these rough curves form the T-Z and TOTLD-$Z_t$ curves for each test pile.

For each load transfer curve, two computations are required. Namely, determining the elastic pile deformations ($Y_m$ and $Y_t$) and the unit resistances ($q^*_o$ and $f^*_s$). Figure 8 shows a typical pile and its linear load transfer curve corresponding to some applied load $Q_{app}$.

Referring to Figure 8, the pile movements $Z_m$ and $Z_t$ are first computed by taking into account the elastic load deformation which occurs along the pile. The load-settlement curve provides the value of the pile head movement ($\delta$) corresponding to $Q_{app}$. Then referring to Figure 8a, $Z_m$ is

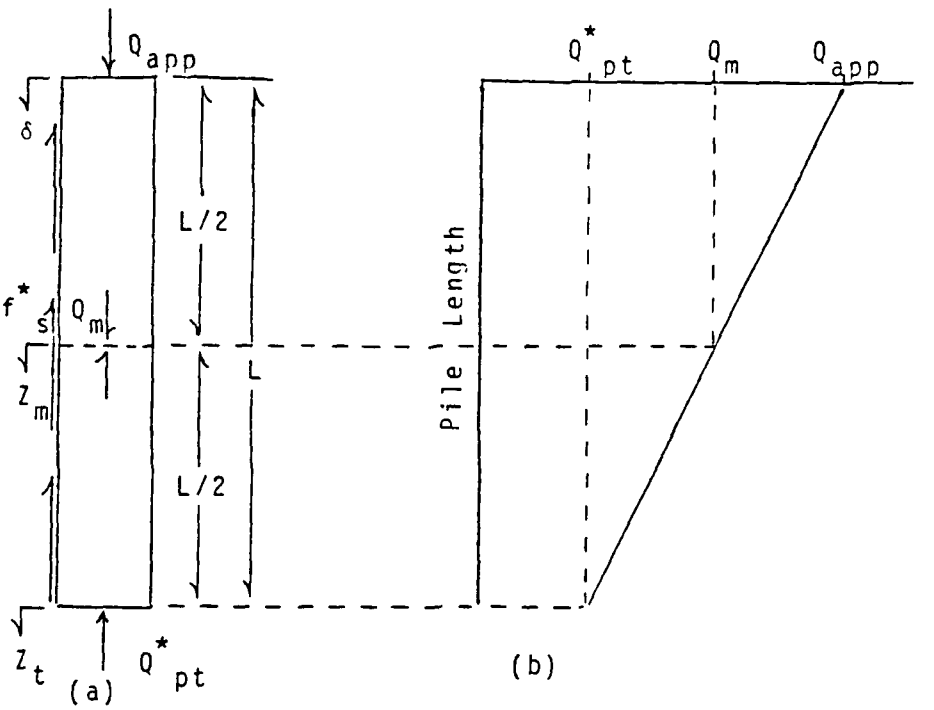


FIGURE 8. - Typical Segmented Axially Loaded Pile Showing:
(a) Loads and displacements; and,
(b) Linear load distribution in pile.

equal to $\delta$ minus the elastic deformation in the upper half of the pile - which is represented by $Y_m$. Similarly, $Z_t$ is equal to $Z_m$ minus the elastic deformation in the lower half - represented by $Y_t$. These relationships are shown as follows:

$$Z_m = \delta - Y_m, \tag{19}$$

and,

$$Z_t = Z_m - Y_t. \tag{20}$$

The elastic deformations are computed using the following formula:

$$Y_m \ , \ Y_t = (P_{avg}*L)/(2*A_{st}*E_{st}) \tag{21}$$

where $P_{avg}$ is the average load in the pile segment, (L/2) is the length of the segment, $A_{st}$ is the cross-sectional area of the steel (including any channel iron), and $E_{st}$ is Youngs Modulus for steel. In computing $Y_m$ and $Y_t$, the only variables in equation (21) are $P_{avg}$ and L. Since all load transfer curves are assumed to be linear with depth, $P_{avg}$ is computed as the average of either: (1) $Q_{app}$ and $Q_m$; or, (2) $Q_m$ and $Q^*_{pt}$ - depending on whether the upper or lower pile segment is being considered, respectively.

After these movements are computed, the unit resistances $q^*_o$ and $f^*_s$ are calculated. As shown in Figure 7a, $Q^*_{pt}$ and $Q^*_s$ can be determined from each extrapolated load transfer curve. Therefore, by dividing $Q^*_{pt}$ and $Q^*_s$ by the point and

side areas, respectively, the unit resistances $q^*_o$ and $f^*_s$ are computed. Again, since the extrapolated load transfer curves are linear, the value of $f^*_s$ can be averaged over the embedded length of the pile. For these calculations point and side areas are assumed to be those of an unplugged pile. However, since the curves obtained from these data are eventually normalized, the plugging assumption is not important. Sample calculations showing how $Z_m$, $Z_t$, $q^*_o$ and $f^*_s$ are determined for the Arkansas #7 test pile are provided in Appendix 3-L (page 108). The computed data from all the test piles are tabulated on the last page of Appendix 3-L (page 111).

After these data are computed, $Z_m$ is plotted against corresponding values of $f^*_s$. Similarly, $Z_t$ is plotted against corresponding values of $q^*_o$. Therefore, two graphs are developed for each pile in the data base. Curves are then drawn on these plots to form a best fit of the data. However, since only four data points are available on each plot, the construction of these "best fit" curves is rather subjective. After these curves are drawn on both plots, the ordinate (i.e. $q^*_o$ or $f^*_s$ axis) of each plot is normalized by dividing by the limiting unit resistance indicated by the rough curves drawn to fit the data. These limiting or maximum unit resistances are designated as $q_{o,max}$ and $f_{s,max}$ for the point and side, respectively. The curves obtained after this normalization are the T-Z and TOTLD-$Z_t$ curves for each test pile. The plotted

data and normalized curves obtained for each pile are shown in Appendix 3-M (page 112).

The final step requires that the T-Z and TOTLD-$Z_t$ curves for each pile be combined to form one T-Z and one TOTLD-$Z_t$ curve. These two curves, which are representative of all of the piles in the data base, can then be used as input data for the APILE1 program. These two curves are shown in Appendix 3-N (page 122). Two different TOTLD-$Z_t$ curves are presented in Appendix 3-N instead of one. One TOTLD-$Z_t$ curve is obtained using data from the Lock and Dam 26:3IP-IIIS (Method 1) test pile and the second curve is computed without including these data. The data points from this test pile - using Method 1 - did not correlate with the data from the other nine piles (see Appendix 3-N, page 123). Specifically, the $Q_u$ load estimated by Method 1 is probably significantly overestimated. This overestimation may have resulted in a TOTLD-$Z_t$ curve for this pile which does not reach a limiting unit resistance of $q_{o,max}$ (see Appendix 3-M, page 113). Therefore, the TOTLD-$Z_t$ curve computed by disregarding these data is used as part of the input for APILE1.

Predicted Load-Settlement Curves Using APILE1

To provide an indication of the overall accuracy of the design parameters determined thus far and allow for the prediction of load-settlement curves, the computer program APILE1 is used. The accuracy of the following design

parameters will be tested: the ratio of $C^* = 1.8$; the correlations of a one-half plugged pile point and a fully plugged side; and, the computed T-Z and TOTLD-$Z_t$ curves. To test the accuracy of these parameters, the load-settlement curves of two full-scale field load tested H-piles in sand will be predicted by APILE1. The predicted results are then compared to the measured load-settlement curves. The two test piles utilized in this procedure are called Kansas City #4 and Kansas City #8 (12). These piles are chosen from outside of the test pile data base which was used to develop the design parameters. To compute the input data for these two piles, the pile-soil characteristics and the aforementioned parameters are used. A sample of the specific calculations as well as the input and output data for Kansas City #4 are presented in Appendix 3-0 (page 124).

After the predicted load-settlement curves for these two piles are obtained, the same procedure is repeated using the design parameters obtained from class (5).

## RESULTS

The computed T-Z and TOTLD-$Z_t$ curves are presented in Figures 9 and 10, respectively. In these figures, the curves computed in this study are represented as solid lines, the curves from class are shown as long dashed lines, and the curves recommended for full displacement piles are the short dashed lines. Both figures clearly show that at the same

FIGURE 9. – SKIN FRICTION RATIO (T) VS. MOVEMENT (Z)

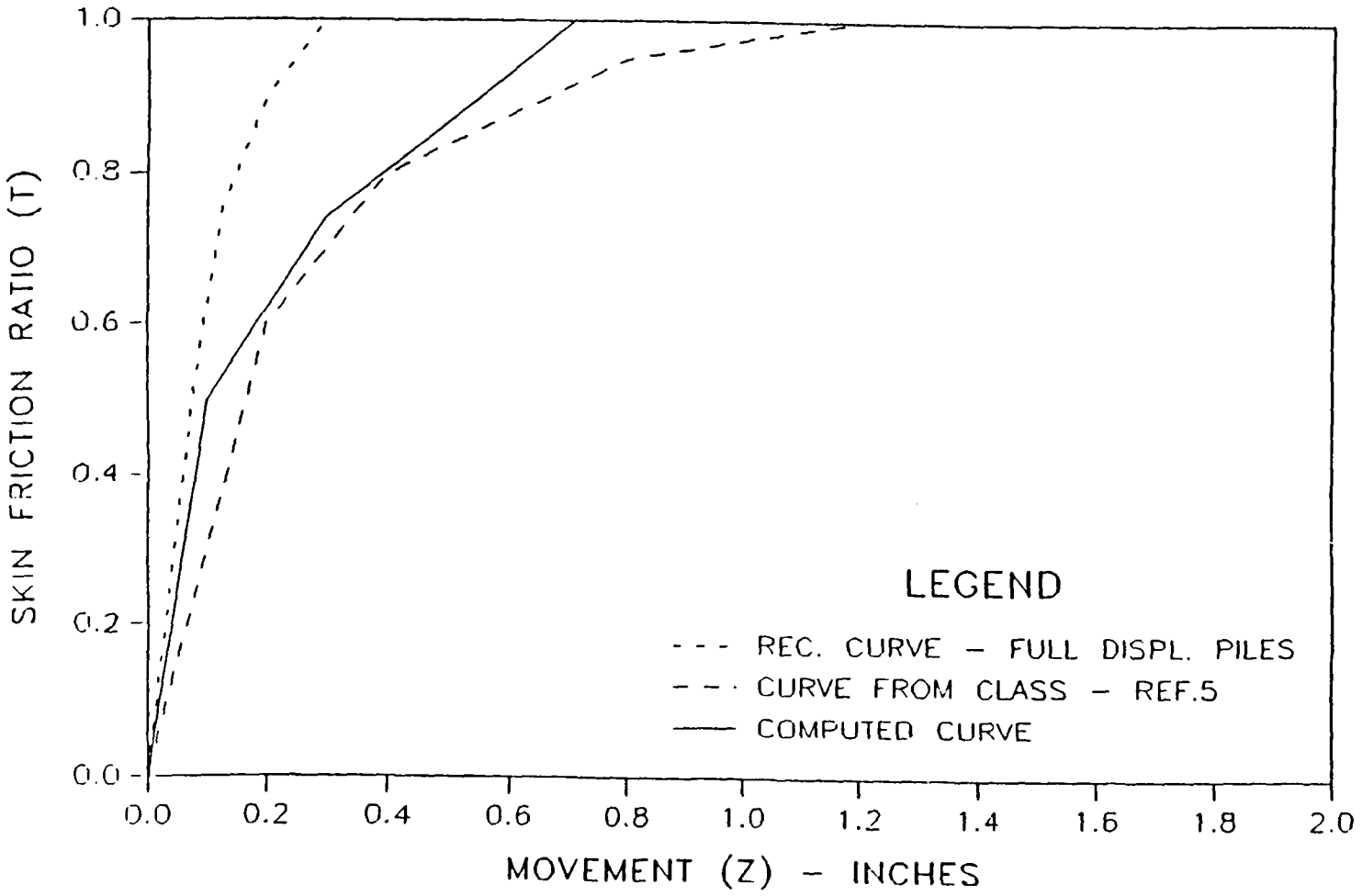

FIG.10 – UNIT PT. BRNG RATIO(TOTLD) VS. TIP MOVEMENT($Z_t$)

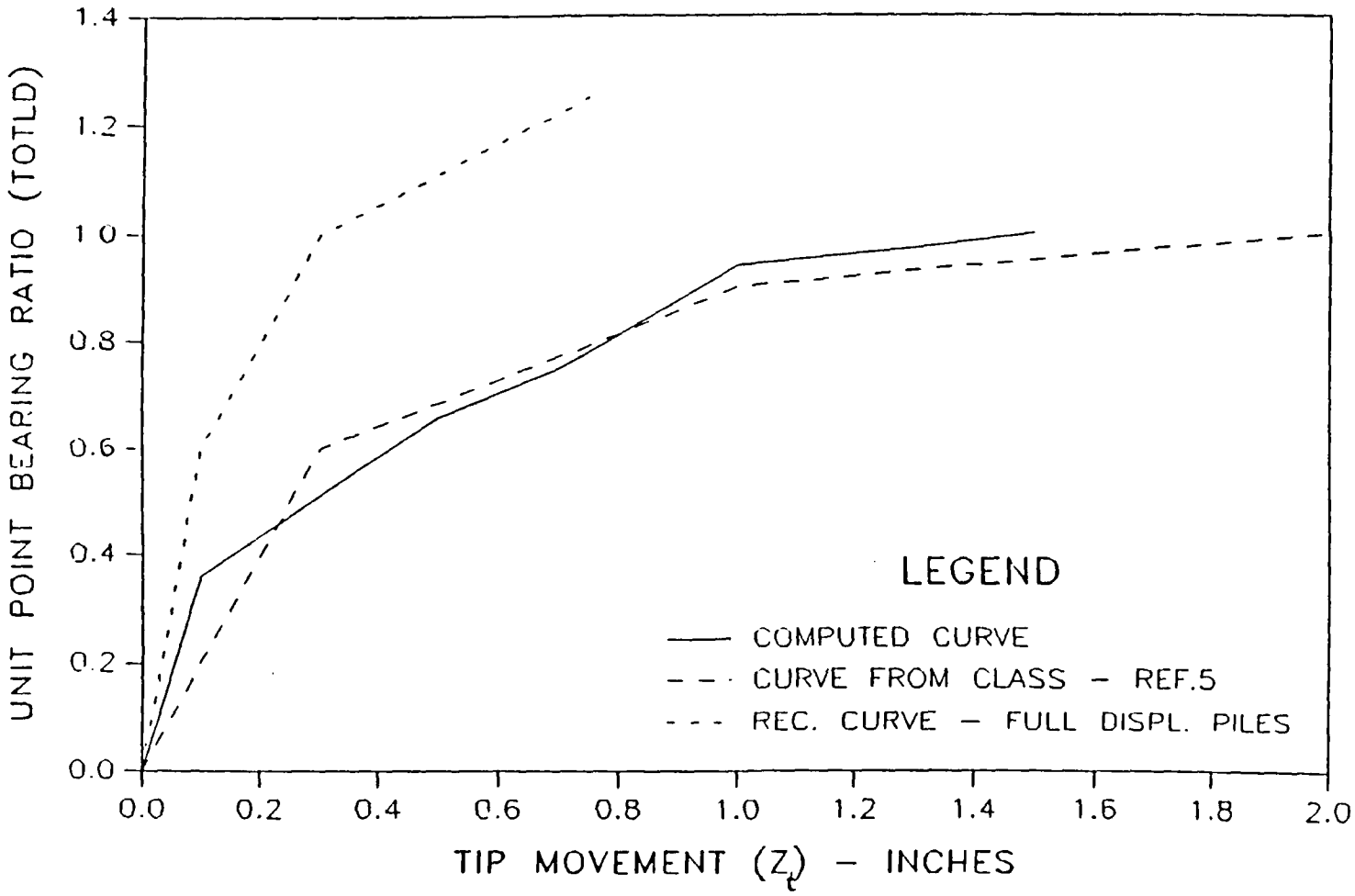

movement, the percent of maximum unit resistance (i.e. T or TOTLD) which is developed by H-piles in sand is significantly less than the corresponding resistances developed by full displacement piles. The T-Z and TOTLD-$Z_t$ curves obtained in this study are very similar to the corresponding curves obtained previously in class. However, one significant difference between the computed and class curves is that the curves obtained in this study indicate that the unit resistances ($f^*_s$ and $q^*_o$) will reach their limiting values at smaller pile movements. Specifically, the computed T-Z curve predicts $f^*_s$ to reach its limiting value at a movement of only 0.71 inches, while the T-Z curve obtained in class does not predict this limiting resistance to be achieved until a pile movement of 1.2 inches (see Figure 9). This represents a difference of 42 percent in the pile movement required to reach a maximum unit side friction value. Similarly, the computed TOTLD-$Z_t$ curve indicates that $q^*_o$ will reach a limiting value at a pile tip movement of 1.50 inches, while the TOTLD-$Z_t$ curve from class does not predict this limiting resistance to be achieved until a tip movement of 2.0 inches (see Figure 10). This represents a difference of 25 percent in the tip movement required to reach a maximum unit point bearing value.

In attempting to establish T-Z and TOTLD-$Z_t$ design curves for H-piles in cohesionless soils, the close similarity between the computed and class curves is significant. This

similarity becomes even more meaningful when one considers the fact that eight of the ten piles analyzed in this study were not utilized to develop the class results. Specifically, only Arkansas #7 and Lock and Dam 26:1-3 were used in developing both the curves computed in this study and the class curves. However, this close similarity between the computed and class curves may be at least partially due to the fact that four of the six test piles from Group 1 - which represents the data base used to correlate $R_1$ and $R_2$ for extrapolating the load transfer curves - were test piles which were also used to determine the T-Z and TOTLD-$Z_t$ curves in class. Recalling the method of analysis discussed previously, the extrapolation procedure developed from the piles of Group 1 was only applied to the three load transfer curves per pile which corresponded to the three applied loads less than $Q_u$. At an applied load equal to $Q_u$, the ratio of $C^* = 1.8$ was utilized to compute the fourth load transfer curve for each pile. The significance of this is: a relationship exists between the slopes of the extrapolated load transfer curves (relative to one another) which are used in this study, and the relative slopes of the measured load transfer curves used to determine the class T-Z and TOTLD-$Z_t$ curves. Again this relationship does not exist for those extrapolated load transfer curves computed using $C^*$. In explaining the similarity between the T-Z and TOTLD-$Z_t$ curves obtained in this study and in class, the importance of this relationship is difficult to determine. However, since

the six piles in Group 1 were selected from three different sites and yielded measured load transfer curves which are typical of other instrumented H-piles in sand, the author contends that avoiding this relationship by selecting test piles in Group 1 from outside of the data base used in class would probably not significantly alter the T-Z and TOTLD-$Z_t$ curves computed in this study.

The load-settlement curves predicted by APILE1 and the corresponding measured curves for the Kansas City #4 and #8 test piles are shown in Figures 11 and 12, respectively. In each of these figures: the highest dashed curve is the field curve; the lowest dashed curve represents the settlement curve predicted using the design parameters obtained in this study; the dashed curve just below the solid line is the predicted curve using the results from class; and, the solid curve is that predicted from the combined results of this study and class. Using the design parameters determined in this study, APILE1 underpredicted the measured ultimate compression capacity of both Kansas City #4 and #8 by about 36 and 30 percent, respectively. Using the design parameters obtained from class, APILE1 again underpredicted the measured capacity of these piles by about 22 and 14 percent, respectively (see Figures 11 and 12). Therefore, the results obtained in class predicted the load-settlement characteristics of these two piles more accurately than did the design parameters computed in this study.

FIGURE 11. – LOAD – SETTLEMENT CURVES FOR KANSAS CITY #4

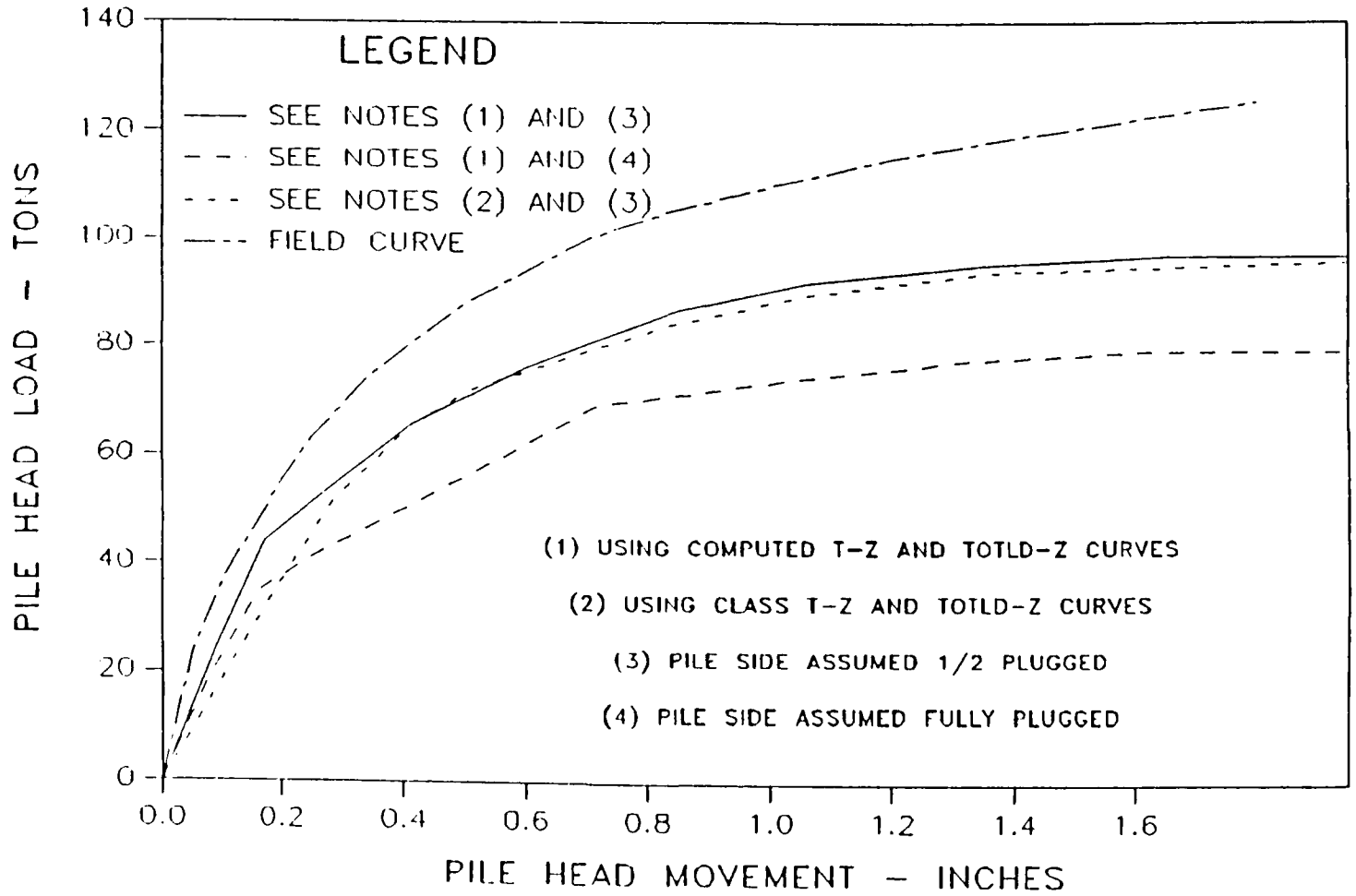

FIGURE 12. - LOAD - SETTLEMENT CURVES FOR KANSAS CITY #8

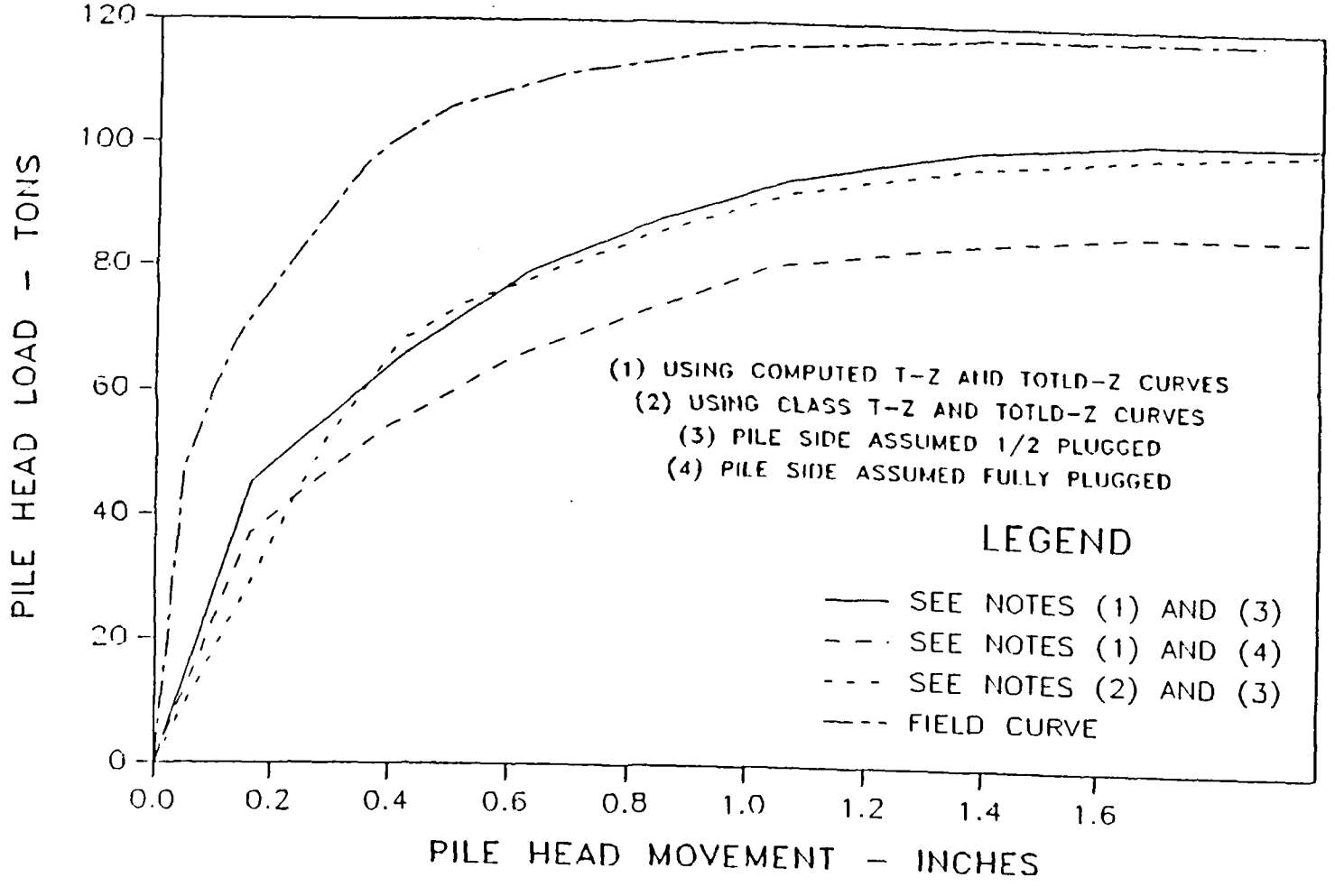

The reason why the class results yielded a more accurate prediction of the measured load-settlement curves is due to the different assumptions made concerning the degree of soil plugging which occurs between the flanges of the pile. Specifically, the most significant difference between the design parameters determined in this study and those obtained in class is the degree of soil plugging which occurs along the side of the pile at ultimate failure. In this study, to compute side load the best correlation occurs when the area between the flanges is assumed to be fully plugged; whereas, the best correlation in class was obtained by assuming the pile to be one-half plugged by the soil (5). The importance of this difference is shown by predicting the load-settlement curves of the Kansas City piles using APILE1 with the design parameters obtained in this study - but assuming the pile side to be one-half instead of fully plugged. The load-settlement curves predicted in this way are shown as solid lines in Figures 11 and 12 and closely match the predicted curves obtained by using the class design parameters exclusively. The small difference between these two predicted load-settlement curves for each Kansas City pile is due to the slight differences that exist between the T-Z and TOTLD-$Z_t$ curves computed in this study and in class.

## CONCLUSIONS

Based on a static analysis approach, the following conclusions are made concerning the performance of H-piles in cohesionless soils.

For piles subjected to both a compression and tension load test, a definite trend exists to indicate that the ultimate side load in compression - corrected for residual driving stresses - may be estimated by multiplying the ultimate load in tension by a factor of 1.8. For this calculation, the ultimate compression and tension loads are defined at movements of 2.0 and 1.2 inches, respectively. From Figures 2 and 3, the ultimate side load in compression predicted using this multiplier factor of 1.8 yielded results which were accurate to within about $\pm 25$ percent.

As mentioned previously, static analysis procedures require the prediction of both point and side loads to estimate total pile capacity. The results of this study indicate that the ultimate point bearing capacity can be estimated using the correlations developed by Coyle and Castello for full displacement piles (6) by: (1) assuming that the area between the flanges of the H-pile are one-half plugged by the surrounding soil; and, (2) using an adjusted Standard Penetration Test (SPT) blow count ($N_{ad}$) to estimate the average in-situ soil friction angle over a depth of $\pm 3$

pile diameters from the pile tip. These results agree with those obtained in class (5).

In predicting the ultimate side friction developed by the pile, a discrepancy exists between the design parameters obtained in this study and the parameters developed in class. Specifically, when using the Coyle-Castello correlations, the results of this study indicated that the ultimate side load could be most accurately predicted by assuming the pile side to be fully plugged by the soil, while the class results indicated that more accurate load estimates would be obtained by assuming a one-half plugged condition (5). Based on a comparison of the predicted and measured load-settlement curves for the Kansas City #4 and #8 piles (see Figures 11 and 12), the fully plugged assumption underpredicted the ultimate capacity by 30 and 36 percent. However, the one-half plugged assumption underpredicted by only 14 and 22 percent. Despite the fact that both of these plugging conditions are based on the analysis of relatively small data bases and that the one-half and fully plugged cases were tested for accuracy against only two field curves, the author believes that in predicting side friction load the one-half plugged condition will yield more accurate estimates in most cases. Therefore, using the Coyle-Castello correlations, the ultimate side friction capacity can be estimated by: (1) assuming the pile to be one-half plugged by the soil; and, (2) using an unadjusted SPT

blow count (N) to estimate the average in-situ soil friction angle along the pile's embedded length.

Finally, the results of this study indicate that the load-settlement curves of H-piles in sand may be predicted with reasonable accuracy by the computer program APILE1, if the conclusions presented in the preceeding paragraphs and the T-Z and TOTLD-$Z_t$ curves obtained in this study are utilized to develop the input data for APILE1. Referring to Figures 11 and 12, the close similarity between the solid curve and the dashed curve just below it signify that no significant shift in the load-settlement curve resulted when the T-Z and TOTLD-$Z_t$ curves from class were used as the input for APILE1.

## RECOMMENDATIONS

The design parameters obtained in this study were based on an analysis of only ten different field load tests. Therefore, due to the limited size of the data base, additional research work is required to confirm the results of this study. Also, in designing H-piles in cohesionless soils, it is recommended that at least one full scale field load test accompany any pile foundation design determined exclusively from the results presented in this study.

Finally, the possible existance of a correlation between the results of a cone penetrometer test and unit point bearing capacity of an H-pile should be investigated further.

## APPENDIX 1: REFERENCES


1. Bowles, J.E., Foundation Analysis and Design, 3rd ed., New York, McGraw-Hill Book Company, 1982.

2. Briaud, J.-L., Huff, L.G., Tucker, L.M., Coyle, H.M., "Evaluation of In-Situ Design Methods for Vertically Loaded H-Piles at Lock and Dam No. 26 Replacement Site," Research Report RF 4690-1, Texas A&M University, College Station, TX., July, 1984.

3. Briaud, J.-L., Tucker, L.M., Lytton, R.L., Coyle, H.M., "The Behavior of Piles and Pile Groups in Cohesionless Soils," Report No. FHWA-RD-83-38, Texas A&M University, College Station, TX., Sept., 1983.

4. Briaud, J.-L., Tucker, L.M., "Pressuremeter, Cone Penetrometer and Foundation Design," Texas A&M University, College Station, TX., Aug., 1984.

5. Coyle, H.M., Marine Foundation Engineering, Unpublished class notes, Texas A&M University, Spring, 1987.

6. Coyle, H.M., and Castello, R.R., "New Design Correlations for Piles in Sand," Journal of Geotechnical Engineering Division, ASCE, Vol. 107, No. GT7, Proc. paper, July, 1981, pp. 965-986.

7. Hunter, A.H. and Davisson, M.T., "Measurements of Pile Load Transfer," Performance of Deep Foundations, ASTM STP 444, American Society for Testing and Materials, 1969, pp. 106-117.

8. "Overwater Steel H-Pile Driving and Testing Program: Locks and Dam No. 26 (Replacement) Upper Mississippi River Basin Near Alton, Illinois," Fruco and Associates, Inc., St. Louis, MS., Sept., 1973.

9. "Pile Driving and Loading Tests: Locks and Dam No. 4, Arkansas River and Tributaries, Arkansas and Oklahoma," Fruco and Associates, Inc., St. Louis, MS., Sept., 1964.

10. "Pile Load and Extraction Tests 1954-1980," Report EM-48, Ministry of Transportation and Communications, Engineering Materials Office, Ontario, Canada, June, 1981.

11. Planning, Designing and Constructing Fixed Offshore Platforms, American Petroleum Institute, API-RP-2A, Washington D.C., April 1987.

12. Smith, J.B., "Intercity Viaduct Test Pile Program," Foundation Facts, No. 1, Vol. II, 1966, pp. 6-8.

13. Winter, C., "Soils and Construction Foundations Report, Locks and Dam No. 6, Arkansas River Project, Report No. 1," U.S. Army Engineer District, Little Rock, Ark., Dec., 1965. (Unpublished report).

## APPENDIX 2: NOTATION

$A_{pt}$ = tip area of pile - in square feet;

$A_s$ = total embedded side area of pile - in square feet;

$A_{st}$ = cross sectional area of steel pile (including channel iron) - in square feet;

B = equivalent circular pile diameter - in feet;

C = the ratio between the ultimate pile side load in compression and ultimate load in tension, defined as $(Q_s/Q_{ut})$;

$C^*$ = the ratio between the ultimate pile side load in compression, corrected for residual stress, and the ultimate load in tension, defined as $(Q^*_s/Q_{ut})$;

D = embedded length of pile - in feet;

$E_{st}$ = Youngs Modulus for steel - in tons per square foot;

$f^*_s$ = unit side friction corrected for residual stress - in tons per square foot;

$f_{s,max}$ = maximum or limiting value of unit side friction - in tons per square foot;

L = total test pile length, from point of load application to the pile tip - in feet;

N = unadjusted Standard Penetration Test blow count - in blows per foot of penetration;

$N_{ad}$ = adjusted Standard Penetration Test blow count for silty sand below the water table - in blows per foot of penetration;

$N_{avg}$ = average of the adjusted and unadjusted blow counts - in blows per foot of penetration;

$P_{avg}$ = average load in a segment of embedded pile - in tons;

$q_c$ = soil strength as determined by the cone penetrometer test - in tons per square foot;

$Q_m$ = load on the pile at the midpoint of its total length - in tons;

$Q_{pt}$ = pile tip load in compression at ultimate failure - in tons;

$Q^*_{pt}$ = pile tip load in compression at ultimate failure, corrected for residual stress - in tons;

$Q_{res}$ = residual stress load at the pile tip - in tons;

$q_{res}$ = unit residual stress at the pile tip - in tons per square foot;

$Q_s$ = side friction load along the pile in compression at ultimate failure - in tons;

$Q^*_s$ = side friction load along the pile in compression at ultimate failure, corrected for residual stress - in tons;

$Q_u$ = total pile load in compression at ultimate failure - in tons;

$Q_{ut}$ = total pile load in tension at ultimate failure - in tons;

$q^*_o$ = unit pile tip bearing resistance, corrected for residual stress - in tons per square foot;

$q_{o,max}$ = maximum or limiting value of unit tip bearing resistance - in tons per square foot;

$R_1$ = ratio of applied to ultimate compression loads, defined as $(Q_{app}/Q_u)$;

$R_2$ = ratio of pile side to point load in compression corrected for residual stress, defined as $(Q^*_s/Q^*_{pt})$;

T = amount of unit side friction developed expressed as a percentage of its maximum value, defined as $(f^*_s/f_{s,max})$ - in percent;

TOTLD = amount of unit point bearing developed expressed as a percentage of its maximum value, defined as $(q^*_o/q_{o,max})$ - in percent;

TOTLD = amount of unit point bearing developed expressed as a percentage of its maximum value, defined as $(q^*_o/q_{o,max})$ - in percent;

X = correlation between unit tip resistance in the zero plug condition and the soil strength as determined from the cone penetrometer test, defined as the ratio $(q^*_o/q_c)$;

$Y_m$ = elastic deformation in the upper half of the pile - in inches;

$Y_t$ = elastic deformation in the lower half of the pile - in inches;

Z = relative movement between the pile and surrounding soil along the side of the pile, obtained after correcting for elastic load deformation - in inches;

$Z_m$ = movement at the midpoint of the pile's embedded length relative to the surrounding soil, obtained after correcting for elastic load deformation - in inches;

$Z_t$ = movement of the pile tip relative to the surrounding soil, obtained after correcting for elastic load deformation - in inches;

$\delta$ = movement of the pile head in either compression or tension - in inches;

$\phi_{pt,dev}$ = deviation angle for unit point bearing, defined as $(\phi_{pt,p} - \phi_{pt})$ - in degrees;

$\phi_{s,dev}$ = deviation angle for unit side friction, defined as $(\phi_{s,p} - \phi_s)$ - in degrees;

$\phi_{pt,p}$ = friction angle of the soil, predicted by the Coyle-Castello correlations, at the pile tip - in degrees;

$\phi_{s,p}$ = average friction angle of the soil, predicted by the Coyle-Castello correlations, along the pile side - in degrees;

$\phi_{pt}$ = average in-situ soil friction angle at the pile tip - in degrees;

$\phi_s$ = average in-situ soil friction angle along the pile side - in degrees.

# APPENDIX 3-A: [COMPUTE C - FULLY INSTRUMENTED] (3-A-1)

## LOCK AND DAM #26: 1-3

* TENSION TEST RESULTS.

AT A PILEHEAD MOVEMENT OF $\delta = 1.2''$, THEN $Q_{UT} = 64.4$ TONS (REF 2 (FROM TENSION TEST LOAD-SETTLEMENT CURVE)

* COMPRESSION TEST RESULTS:

FROM THE COMPRESSION TEST LOAD-SETTLEMENT CURVES, AT $\delta = 2.0''$, THE $Q_u = 322$ TONS (REF 2)

FROM THE MEASURED LOAD TRANSFER CURVES IN COMPRESSION, AT $Q_U \doteq 325$ TONS, THEN $Q_{PT} \doteq 160$ TONS; THEREFORE, USING

$$Q_U = Q_{PT} + Q_s$$

$$Q_s = Q_u - Q_p$$

$$= (325 - 160) \text{ TONS}$$

AND $Q_s \doteq 165$ TONS

* DETERMINE RATIO C:

$$C = \frac{Q_s}{Q_{UT}} = \frac{165}{64.4} \quad ; \quad \boxed{C = 2.56}$$

# APPENDIX 3-B:
## [COMPUTE C FOR NON-FULLY INSTRUMENTED PILE]

## CANADA 24-4:

- USE COYLE - CASTELLO CORRELATIONS TO ESTIMATE $Q_s/Q_u$

- $D/B$ RATIOS:

FROM REF 10, ASSUMING THE PILE TO BE ½ PLUGGED, THEN:

$D = 72.8$ FT (DEPTH) AND $A_{PT.\frac{1}{2}} = 0.548\ FT^2$ (HP 12 x 53) (TIP AREA, ½ PLUGGED)

TO COMPUTE THE EQUIVALENT DIAMETER, $B$:

$$\frac{\pi B^2}{4} = A_{PT,\frac{1}{2}}, \text{ OR } B = \sqrt{(A_{PT,\frac{1}{2}})(4)/\pi}$$

$$= \sqrt{(0.548\ FT^2)(4)/\pi}, \quad \underline{B = 0.835\ FT}$$

THEREFORE, $D/B = 72.8/.835$ : $\underline{D/B = 87.2}$ (FOR PILE TIP)

- DETERMINE $\phi_s$ AND $\phi_{PT}$:

FOR $\phi_{SIDE}$:

FROM THE SPT BLOW COUNT DATA IN REF 10,

$N = 22.2$, $N_{AD} = 18.5$ $\therefore N_{AVG} = \frac{1}{2}(22.2 + 18.5)$ : $N_{AVG} = 20$

THEREFORE, FROM REF 2, AT $N = 20$, THEN $\underline{\phi_s = 32^\circ}$

FOR $\phi_{PTIP}$:

FROM THE SPT BLOW COUNT DATA IN REF 10,

$N = 16$, $N_{AD} = 16$ ; $N_{AVG} = 6$. $\therefore$ FROM REF 2 AT $N_{AVG} = 16$, $\underline{\phi_{PT} = 32^\circ}$

# APPENDIX 3-B:

- DETERMINE $q_o$ AND $f_s$:

FOR $f_s$

THE AVERAGE UNIT SIDE FRICTION IS TAKEN AT THE MIDPOINT OF THE PILES EMBEDDED LENGTH; THEREFORE,

$$\left(D/B\right)_{SIDE} = \frac{1}{2}\left(D/B\right)_{PT} = \frac{1}{2}(87.2), \quad \therefore \quad \left(D/B\right)_s \doteq 44$$

FROM REF 6, AT $\phi_s = 33°$ AND $(D/B)_s \doteq 44$, THEN: $f_s = 0.43\ \text{TON/FT}^2$

FOR $q_o$

FROM REF 6, AT $\phi_{PT} = 32°$ AND $(D/B)_{PT} = 87$, THEN: $q_o = 70\ \text{TONS/FT}^2$

- DETERMINE $Q_s$ AND $Q_{PT}$

FOR $Q_s$:

FROM THE PILE SIZE, SHAPE AND EMBEDDED LENGTH AS SHOWN IN REF 10, $A_s = 349\ \text{FT}^2$ (ASSUMING ½ PLUGGED); THEREFORE:

$$Q_s = f_s \times A_s = (0.43\ \text{TON/FT}^2)(349\ \text{FT}^2); \quad Q_s = 150\ \text{TONS}$$

FOR $Q_{PT}$:

FOR THE PILE SIZE, SHAPE AND EMBEDDED LENGTH AS SHOWN IN REF 10, $A_{PT} = 0.548\ \text{FT}^2$ (ASSUMING ½ PLUGGED); THEREFORE:

$$Q_{PT} = q_o \times A_{PT} = (70\ \text{TONS/FT}^2)(0.548\ \text{FT}^2); \quad Q_{PT} = 38.4\ \text{TONS}$$

SINCE $Q_u = Q_s + Q_{PT}$, THEN:

$$Q_u = (150 + 38.4)\ \text{TONS}$$

$$Q_u = 188.4\ \text{TONS}$$

FROM THE COMPRESSION TEST LOAD-SETTLEMENT CURVE (REF 10) AT $\delta = 2.0$ $Q_u = 168.6$ TONS; THEREFORE, THE COYLE-CASTELLO CORRELATIONS SLIGHTLY OVERPREDICT THE ULTIMATE BEARING CAPACITY OF THIS PILE.

# APPENDIX 3-B

- ESTIMATED $Q_s/Q_u$ - FROM COYLE - CASTELLO

$Q_s/Q_u$, THEREFORE, USING THE VALUES PREVIOUSLY OBTAINED FROM THE COYLE - CASTELLO CORRELATIONS:

$$Q_s/Q_u = 150/153.4 = 79.6\%$$

OR, 79.6% OF THE TOTAL LOAD IS CARRIED BY SIDE FRICTION AND 20.4% IS CARRIED BY THE PILE POINT.

* USE COYLE - CASTELLO RESULTS TO PREDICT C

FROM THE LOAD - SETTLEMENT CURVE (REF 10) AT $\delta = 2.0''$; THEN:

$$Q_u = 168.4 \text{ TONS}$$

USING THE COYLE - CASTELLO RESULT OF $Q_s/Q_u = .796$, THEN:

$$Q_s \doteq (.796)\,Q_u = (.796)(168.4 \text{ TONS})$$

$$\underline{Q_s \doteq 134 \text{ TONS}}$$

FROM THE TENSION TEST LOAD SETTLEMENT CURVE (REF 10) AT $\delta = 1.2$ THE $\underline{Q_{ut} = 47.8 \text{ TONS}}$; THEREFORE,

$$C = Q_s/Q_{ut} = 134/47.8 : \boxed{C = 2.80}$$

# APPENDIX 3-B

## * SUMMARY OF COYLE - CASTELLO CORRELATION RESULTS FOR THE NON - FULLY INSTRUMENTED PILES

| PILE | COYLE - CASTELLO RESULTS | | | | | | | MEASURED LOADS | | | C-RATIO |
|---|---|---|---|---|---|---|---|---|---|---|---|
| | RELATIVE DEPTH (P/B) (a) | FRICTION ANGLES - DEG | | ESTIMATE LOADS - TONS | | | | | | | |
| | | $\phi_s$ (b) | $\phi_{PT}$ (b),(c) | $Q_U$ | $Q_{PT}$ | $Q_s$ | $Q_s/Q_U$ | $Q_U$ | $Q_{UT}$ | $Q_s$ (d) | |
| LOCK AND DAM # 6 : K-8 | 20 | 32.0 | 34.5 | 167.5 | 67.2 | 100.3 | .598 | 387.5 | 145.8 | 232.0 | 1.59 |
| CANADA 24-4 | 44 | 33.0 | 32.0 | 188.4 | 38.4 | 150.0 | .796 | 168.6 | 47.8 | 134.0 | 2.80 |
| CANADA 24-5 | 30 | 34.5 | 33.5 | 206.7 | 44.9 | 161.8 | .783 | 88.8 | 33.7 | 69.5 | 2.06 |
| CANADA 35-1 | 28 | 32.7 | 36.0 | 194.7 | 68.0 | 126.7 | .651 | 198.0 | 61.9 | 128.7 | 2.08 |

NOTES: (a) EQUIVALENT DIAMETER (B) COMPUTED ASSUMING PILE IS ½ PLUGGED.

(b) FROM AVERAGE OF UNADJUSTED (N) AND ADJUSTED ($N_{an}$) SPT BLOW COUNT OVER EMBEDDED LENGTH.

(c) N VALUE AVERAGED OVER ±3 PILE DIAMETERS (B) FROM TIP.

(d) COMPUTED FROM $Q_s = (Q_s/Q_U) \times Q_U$: $Q_U$ = MEASURED VALUE, $(Q_s/Q_U)$ = FROM COYLE - CASTELLO CORRELATION.

# APPENDIX 3-C

(3-C-1)

## [LINEAR EXTRAPOLATION OF LOAD-SETTLEMENT CURVES]

### LOCK AND DAM 6: K-8

COMPRESSION TEST LOAD-SETTLEMENT CURVE

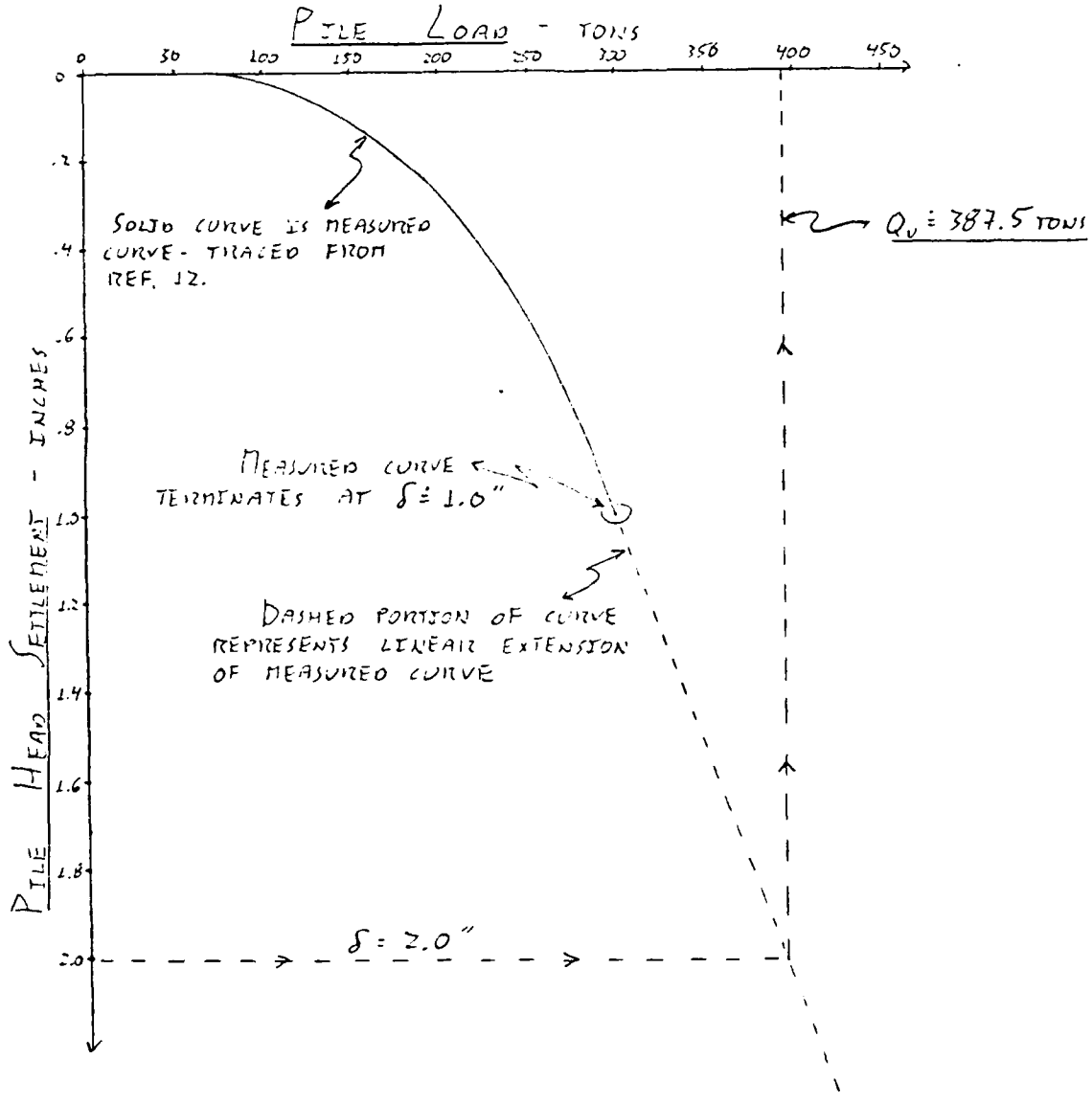


THEREFORE, AT $\delta = 2.0''$, $Q_u \doteq 387.5$ TONS

# Appendix 3-C

## Lock and Dam 6: K-8

### Tension Test Load-Settlement Curve

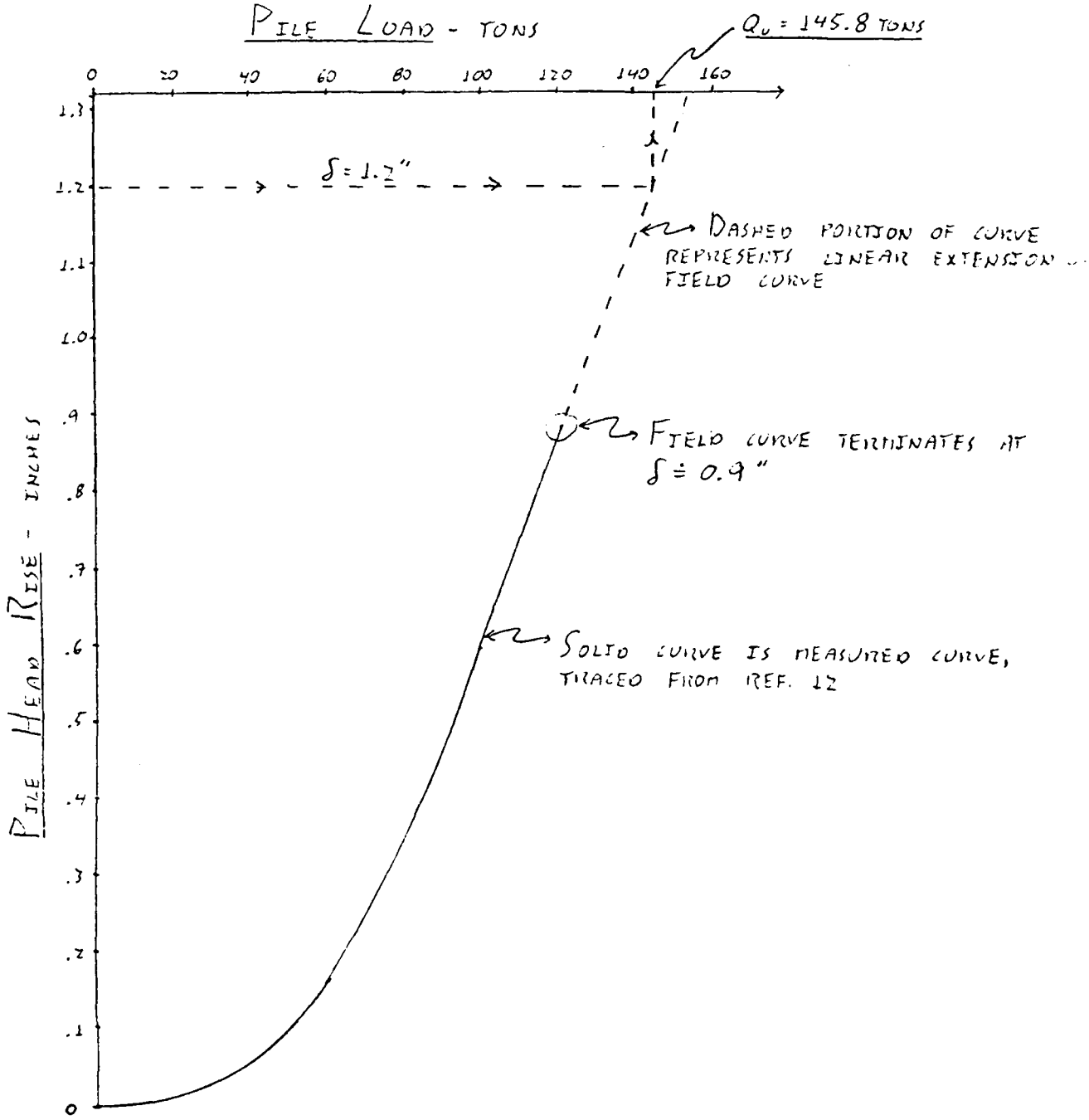

Copy available to DTIC does not permit fully legible reproduction

# APPENDIX 3-D



## [ASYMPTOTIC EXTRAPOLATION OF LOAD-SETTLEMENT CURVE]

### LOCK AND DAM 26:3IP-III S

- STEP 1: BETWEEN $0.2'' < \delta < 0.43''$, THE LOAD-SETTLEMENT CURVE FOR LOCK AND DAM 26:3IP-III S IS A STRAIGHT LINE WITH A SLOPE OF $m_o = .007$ IN/TON.

- STEP 2: THIS COMPUTED $m_o$ WAS THEN APPLIED TO THE PLUNGING LOAD-SETTLEMENT CURVES OF: ARKANSAS #6, #7 AND #9; L+D26:1-3, L+D26:2-5, CANADA 24-5 AND CANADA 35-1 AS DESCRIBED BELOW.

- A LINE WITH A SLOPE OF $m_o$ IS SUPERIMPOSED ON THE LOAD-SETTLEMENT CURVES OF EACH OF THE AFOREMENTIONED TEST PILE TO FIND A POINT OF TANGENCY $(Q_o, \delta_o)$

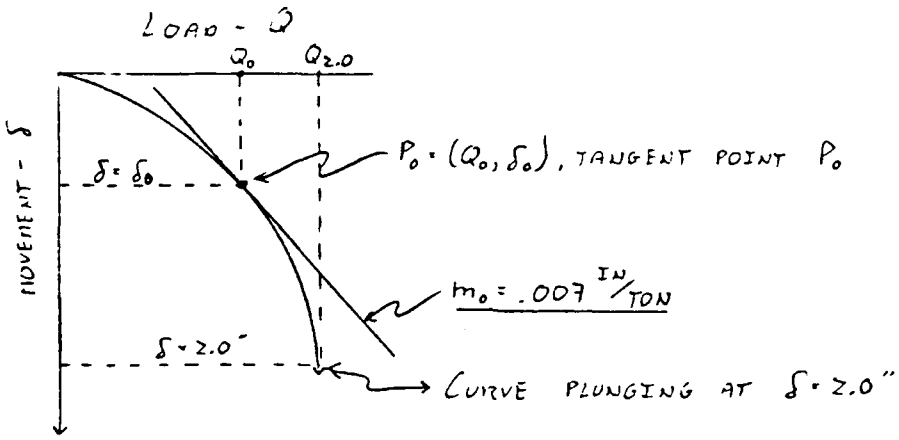


- FOR EACH PILE, $Q_u$ WAS DETERMINED AT $\delta = 2.0''$. THIS LOAD IS SHOWN ABOVE AS $Q_{2.0}$

- THE DIFFERENCE $(Q_{2.0} - Q_o)$ IS COMPUTED. THIS DIFFERENCE $(\Delta Q)$ REPRESENTS THE ADDITIONAL LOAD THAT EACH PILE WAS ABLE TO CARRY-PAST THE POINT WHERE THE SLOPE OF ITS LOAD SETTLEMENT CURVE WAS EQUAL TO $m_o$ - PRIOR TO REACHING ULTIMATE FAILURE (i.e. $\delta = 2.0''$).

$$\Delta Q = Q_{2.0} - Q_o$$

• THE PERCENT OF THE LOAD THAT THE PILES WERE ABLE TO CARRY PAST $Q_0$ WAS THEN CALCULATED AS:

$$P(\%) = \frac{(Q_{f.o} - Q_0)}{Q_0} \times 100$$

$$= \frac{\Delta Q}{Q_0} \times 100$$

THIS PERCENT IS DETERMINED FOR EACH OF THE PILES MENTIONED ABOVE. A SUMMARY OF THE RESULTS OBTAINED IS SHOWN BELOW

| PILE | CAN. 24-5 | CAN. 35-1 | ARK #6 | ARK #7 | ARK #9 | L-D26:1-3 | L-D26 |
|---|---|---|---|---|---|---|---|
| P(%) | 93 | 53 | 51 | 17 | 11 | 42 | 31 |
| $\delta_0$ (in) | .16 | .30 | .35 | .60 | .55 | .47 | .31 |
| D(FT) | 50 | 48 | 40 | 52 | 53 | 54 | 59 |

* STEP 3: THE ABOVE RESULTS WERE THEN APPLIED BACK TO L-D26:3IP-III S UNDER THE ASSUMPTION THAT THE COMPRESSION TESTS ON DIFFERENT H-PILES IN SAND WILL EXHIBIT LOAD-SETTLEMENT CURVES WITH SIMILAR SHAPES IF: (1) EACH CURVE HAS A POINT WHICH IS TANGENT TO A LINE HAVING A SLOPE $m_0$; AND, (2) THIS POINT OF TANGENCY OCCURS CLOSE TO SOME CONSTANT MOVEMENT $\delta_0$.

* STEP 4: FROM THE TABLE ABOVE, A RELATIONSHIP WAS NOTED BETWEEN $\delta_0$ AND P IN THAT IF $\delta_0$ IS RELATIVELY SMALL, P WAS RELATIVELY LARGE; CONVERSELY IF $\delta_0$ IS LARGE, P IS SMALL. PHYSICALLY, THIS INDICATES THAT IF A CURVE SLOPE OF $m_0 = .007$ IN/TON IS REACHED AT AN EARLY POINT IN THE CURVE (i.e. SMALL $\delta$), THEN THE PILE IS CAPABLE OF CARRYING SIGNIFICANTLY GREATER ADDITIONAL LOADS PRIOR TO PLUNGING. CONVERSELY, IF $\delta_0$ IS LARGE, THEN THE PILE IS ONLY CAPABLE OF CARRYING A RELATIVELY SMALL ADDITIONAL LOAD PRIOR TO PLUNGING.

WITH THIS IN MIND, A VALUE FOR P TO USE IN EXTRAPOLATING THE L-D26:3IP-III S CURVE WAS ESTIMATED FROM THE ABOVE TABLE

Copy available to DTIC does not permit fully legible reproduction



FROM THOSE PILES WITH $\delta_0$ VALUES CLOSE TO THE $\delta_0$ VALUE OF .45 OBTAINED FROM L+DZ6:3IP-IIIS.

THEREFORE, FROM THE ABOVE TABLE AND CONSIDERING ONLY THOSE PILES WITH $.30 < \delta_0 < .50$, THEN P IS ESTIMATED AT 44%. WITH P=.44, THEN

$$P = \frac{Q_{2.0} - Q_0}{Q_0} \; ; \quad Q_{2.0} = P \times Q_0 + Q_0 \text{, or, } Q_{2.0} = Q_0 (P + 1)$$

FROM REF 8, AT $m_0 = .007$ IN/TON, THEN $Q_0 = 150$ TONS FOR L+DZ6:3IP-IIIS, AND:

$$Q_{2.0} = 150 \text{ TONS } (.44 + 1.00)$$
$$= 150 (1.44) \text{ TONS}$$
$$\underline{Q_{2.0} = 216 \text{ TONS}}$$

THEREFORE, FROM AN ANALYSIS OF THE SHAPES OF THE LOAD-SETTLEMENT CURVES OF THE TEST PILES IN THE ABOVE TABLE; THE ULTIMATE CAPACITY FOR THE L+DZ6:3IP-IIIS PILE IN COMPRESSION SHOULD BE ABOUT 216 TONS. THIS REPRESENTS AN INCREASE IN LOAD CARRYING CAPACITY OF 44% BEYOND THE POINT AT WHICH THE CURVE SLOPE IS EQUAL TO .007 IN/TON.

THE ASMYPTOTICALLY EXTENDED CURVE IS SHOWN ON THE NEXT PAGE.

L+D26:3IP-IIIS: LOAD - SETTLEMENT CURVE

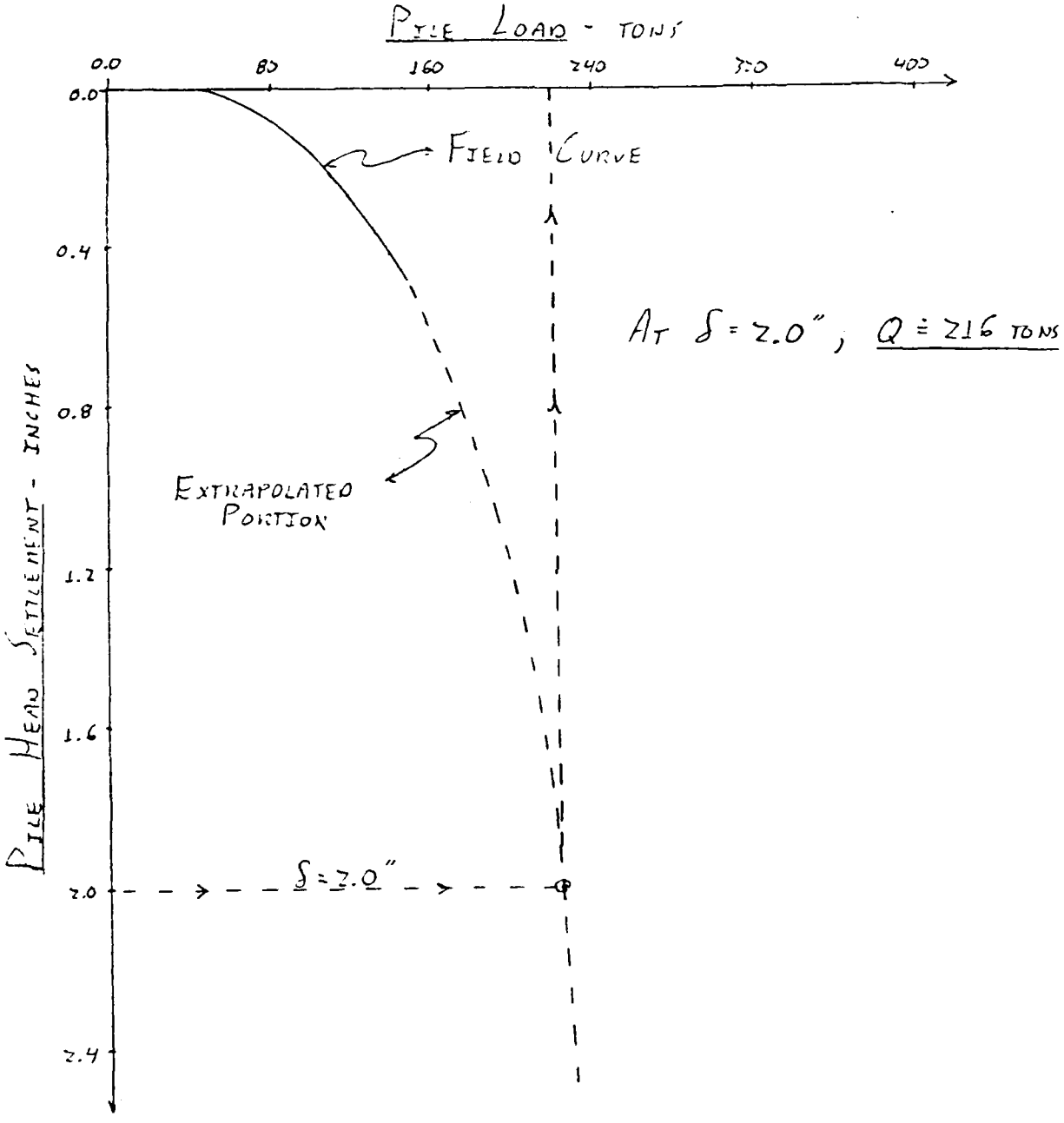

# APPENDIX 3-E

## [GRAPH OF RESIDUAL STRESS VS. EMBEDMENT LENGTH]

(METHOD 3)

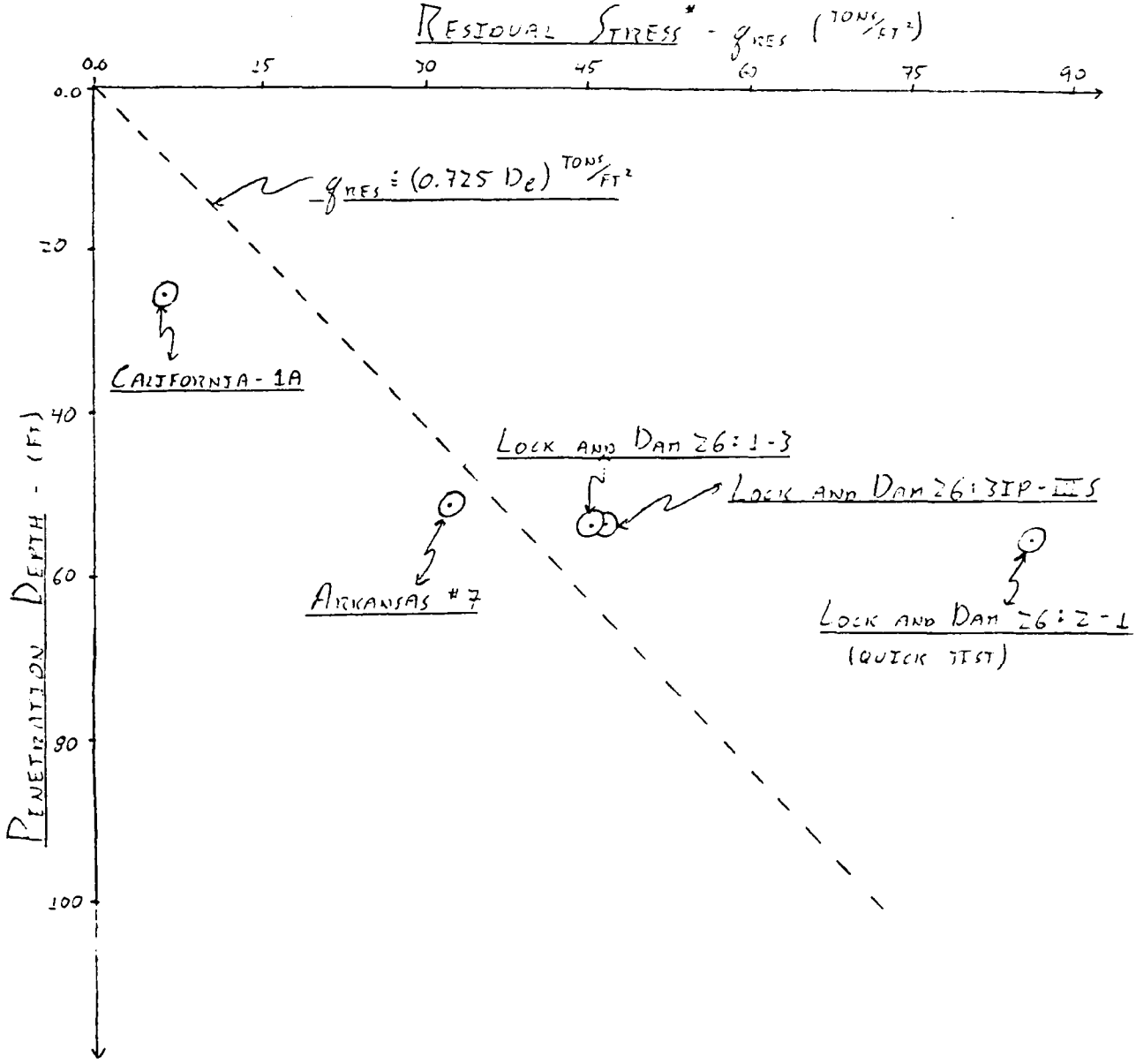


* DATA POINTS OBTAINED FROM MEASURED LOAD TRANSFER CURVES AT AN APPLIED LOAD CORRESPONDING TO $\delta = 1.2''$

* UNIT STRESSES COMPUTED ASSUMING PILE IS ½ PLUGGED; THEREFORE, $A_{PT}$ IS EQUAL TO ITS ½ PLUGGED VALUE: $q_{RES} = Q_{RES}/A_{PT}$

# APPENDIX 3-F
## [COMPUTING RESIDUAL STRESS USING BETA METHOD]

### ARKANSAS #7

THREE PRINCIPLE EQUATIONS ARE USED IN COMPUTING $Q_{RES}$ BY THE BETA METHOD. THESE ARE (REF 3)

(1) $K_3 = 5.01\,(N_{SIDE})^{.27}$ TONS/FT²-IN

(2) $\beta = \sqrt{K_3 P / A E_p}$ (FT⁻¹)

(3) $q_{RES} = 5.57\,L\beta$ (TONS/FT²)

$K_3$ ≡ INITIAL TANGENT MODULUS FOR SIDE FRICTION VS MOVEMENT CURVE (TSF/IN)
$N_{SIDE}$ ≡ AVERAGE SPT BLOW COUNT VALUE ALONG PILE SIDE.
$P$ ≡ PILE PERIMETER
$A$ ≡ CROSS SECTIONAL AREA OF STEEL IN PILE
$E_p$ ≡ YOUNG'S MODULUS OF STEEL.
$L$ ≡ PILE EMBEDDED LENGTH

### FOR ARKANSAS #7:

FROM THE SOIL BORING DATA IN REF 9, $N_{SIDE} \doteq 26.7$; THEREFORE,

$K_3 = 5.01(26.7)^{.27}$ : $\underline{K_3 = 12.2 \text{ TSF/IN}}$

FOR THE HP14×73 PILE SHAPE, $A = .149$ FT². ALSO, $E = 2.088 \times 10^6$ TON/FT² AND $P = 4.44$ FT (FOR A FULLY PLUGGED PILE); THEREFORE;

$$\beta = \sqrt{K_3 P / A E_p} = \sqrt{\frac{(12.2 \text{ TSF/IN})(4.44 \text{ FT})(12 \text{ IN/FT})}{(.149 \text{ FT}^2)(2.088 \times 10^6 \text{ TON/FT}^2)}}$$

$\underline{\beta = .0457 \text{ FT}^{-1}}$

Copy available to DTIC does not permit fully legible reproduction



THEREFORE,

$$q_{RES} = 5.57\,L\,B \text{ , WITH } L = 52\text{ FT (FROM REF 3)}$$

$$= 5.57(52\text{FT})(.0457\text{ FT})$$

$$q_{RES} = 13.2\ \text{TONS/FT}^2$$

ASSUMING A FULLY PLUGGED PILE POINT, THE $A_{PT} = 1.233\ \text{FT}^2$, AND

$$Q_{RES} = q_{RES} \times A_{PT}$$

$$= (13.2\ \text{TON/FT}^2)(1.233\ \text{FT}^2)$$

$$Q_{RES} = 16.3\ \text{TONS}$$

# APPENDIX 3-G
## [PERCENT SOIL PLUGGING IN PILE USING COYLE-CASTELLO CORRELATIONS]

### ARKANSAS #7

* ESTIMATE VALUES FOR $Q_{PT}^*$ AND $Q_s^*$

FROM THE RESULTS OF THE TENSION TEST AT $\delta = 1.2''$, THEN $Q_{UT} \doteq 65$ TONS AND FROM THE COMPRESSION TEST RESULTS AT $\delta = 2.0''$, $Q_U = 250$ TONS (REF 3)

THEREFORE, USING THE FOLLOWING RELATIONSHIP:

$$C^* = Q_s^* / Q_{UT}, \quad Q_s^* = C^*(Q_{UT}), \quad \text{WHERE } C^* = 1.8, \text{ THEREFORE,}$$

$$Q_s^* = (1.8)(65 \text{ TONS}) \quad : \quad Q_s^* = 117 \text{ TONS}$$

SINCE,

$$Q_U = Q_{PT}^* + Q_s^*, \quad \text{OR,} \quad Q_{PT}^* = Q_U - Q_s^*, \quad \text{THEREFORE,}$$

$$Q_{PT}^* = (250 - 117) \text{ TONS}, \quad Q_{PT}^* = 133 \text{ TONS}$$

* DETERMINE UNIT POINT ($q_o^*$) AND SIDE FRICTION ($f_s^*$) CAPACITIES

ASSUMING ZERO SOIL PLUG: THEN $A_{PT} = .28 \text{ FT}^2$ AND $A_s = 390 \text{ FT}^2$ (REF ; THEREFORE:

$$q_o^* = Q_{PT}^* / A_{PT} = 133 \text{ TONS} / .28 \text{ FT}^2 \quad : \quad q_o^* = 475 \text{ TSF}$$

$$f_s^* = Q_s^* / A_s = 117 \text{ TONS} / 390 \text{ FT}^2 \quad : \quad f_s^* = .30 \text{ TSF}$$

ASSUMING ONE-THIRD PLUG: THEN $A_{PT} = .56 \text{ FT}^2$ AND $A_s = 316 \text{ FT}^2$ (REF 3) ; THEREFORE:

$$q_o^* = Q_{PT}^* / A_{PT} = 133 \text{ TONS} / .56 \text{ FT}^2 \quad : \quad q_o^* = 238 \text{ TSF}$$

$$f_s^* = Q_s^* / A_s = 117 \text{ TONS} / 316 \text{ FT}^2 \quad : \quad f_s^* = .37 \text{ TSF}$$

ASSUMING ONE-HALF PLUG: THEN $A_{PT} = .765\ FT^2$ AND $A_s = 302\ FT^2$ (REF

; THEREFORE:

$$q_o^* = Q_{PT}^*/A_{PT} = 133\ TONS/.765\ FT^2 : \quad q_o^* = 174\ TSF$$

$$f_s^* = Q_s^*/A_s = 117\ TONS/302\ FT^2 : \quad f_s^* = .39\ TSF$$

ASSUMING FULLY PLUGGED: THEN $A_{PT} = 1.233\ FT^2$ AND $A_s = 235.6\ FT^2$ (REF 3)

; THEREFORE:

$$q_o^* = Q_{PT}^*/A_{PT} = 133\ TONS/1.233\ FT^2 : \quad q_o^* = 108\ TSF$$

$$f_s^* = Q_s^*/A_s = 117\ TONS/235.6\ FT^2 : \quad f_s^* = .50\ TSF$$

* ESTIMATE THE IN-SITU FRICTION ANGLES $\phi_s$ AND $\phi_{PT}$

FOR $\phi_s$:

FROM THE SOIL BORING DATA (REF 3), $N \doteq 26.7$ ; THEREFORE:

$$N_{AD} = \tfrac{1}{2}(N-15) + 15 = \tfrac{1}{2}(26.7-15) + 15 : \quad N_{AD} = 21$$

FROM REF 2, AT: $N = 26.7 \Rightarrow \phi_s \doteq 35°$
$N_{AD} = 21 \Rightarrow \phi_s \doteq 33°$ } THEREFORE: $33° < \phi_s < 35°$

FOR $\phi_{PT}$:

FROM THE SOIL BORING DATA (REF 3), THE AVERAGE N VALUE ±3 PILE DIAMETERS FROM THE PILE TIP IS: $N \doteq 45$ ; THEREFORE:

$$N_{AD} = 15 + \tfrac{1}{2}(N-15) = \tfrac{1}{2}(45-15) + 15 : \quad N_{AD} = 30$$

FROM REF 2, AT $N = 45 \Rightarrow \phi_{PT} \doteq 40°$
$N_{AD} = 30 \Rightarrow \phi_{PT} \doteq 36°$ } THEREFORE: $36° < \phi_{PT} < 40°$

* DETERMINE THE RELATIVE DEPTHS $(D/B)$

ASSUMING ZERO SOIL PLUG: SINCE $A_{PT} = .28\ FT^2$, THEN:

$B = \sqrt{\frac{4(A_{PT})}{\pi}} = \sqrt{\frac{4(.28\ FT^2)}{\pi}}$ ; $B = .597\ FT$ ; THEREFORE:

$(D/B)_{PT} = (52/.597)$ : $\underline{(D/B)_{PT} = 88}$ (AT $D = 52\ FT$, REF 3)

SINCE $(D/B)_S = \frac{1}{2}(D/B)_{PT}$, THEN $\underline{(D/B)_{SIDE} = 44}$

ASSUMING ONE-THIRD PLUG: SINCE $A_{PT} = .56\ FT^2$, THEN:

$B = \sqrt{\frac{4(A_{PT})}{\pi}} = 2\sqrt{(.56)FT^2/\pi}$ : $B = .844\ FT$ ; THEREFORE:

$(D/B)_{PT} = (52/.844)$ : $\underline{(D/B)_{PT} = 62}$

SINCE $(D/B)_S = \frac{1}{2}(D/B)_{PT}$, THEN $\underline{(D/B)_{SIDE} = 31}$

ASSUMING ONE-HALF PLUG: SINCE $A_{PT} = .765\ FT^2$, THEN:

$B = 2\sqrt{A_{PT}/\pi} = 2\sqrt{\frac{(.765\ FT^2)}{\pi}}$ : $B = .987\ FT$ ; THEREFORE:

$(D/B)_{PT} = (52/.987)$ : $\underline{(D/B)_{PT} = 52}$

SINCE $(D/B)_S = \frac{1}{2}(D/B)_{PT}$, THEN $\underline{(D/B)_{SIDE} = 26}$

ASSUMING FULLY PLUGGED: SINCE $A_{PT} = 1.233\ FT^2$; THEN,

$B = 2\sqrt{A_{PT}/\pi} = 2\sqrt{(1.233\ FT^2)/\pi}$ : $B = 1.253\ FT$ ; THEREFORE,

$(D/B)_{PT} = (52/1.253)$ : $\underline{(D/B)_{PT} = 42}$

SINCE $(D/B)_S = \frac{1}{2}(D/B)_{PT}$, THEN $\underline{(D/B)_{SIDE} = 21}$

# APPENDIX 3-H
## [TABULATION OF DEVIATION ANGLES: $\phi_{PT,DEV}$ AND $\phi_{S,DEV}$]

* UNIT POINT BEARING CAPACITY ($q_o^*$) CASE:

$\phi_{PT,DEV} = (\phi_{PT} - \phi_{PT,P})$

$\phi_{PT,DEV}$ ≡ DEVIATION ANGLE REPRESENTING THE DIFFERENCE BETWEEN THE IN-SITU AND PREDICTED FRICTION ANGLES.

$\phi_{PT}$ ≡ IN-SITU FRICTION ANGLE AT PILE TIP.

$\phi_{PT,P}$ ≡ PREDICTED FRICTION ANGLE AT PILE TIP - OBTAINED FROM LOCATION OF DATA POINT ON COYLE-CASTELLO CURVES.

### DEVIATION ANGLES - WITH $\phi_{PT}$ ESTIMATED FROM N AND $N_{AD}$*

| PILE | 1/3 PLUG | | 1/2 PLUG | | FULLY PLUGGED | |
|---|---|---|---|---|---|---|
| | N | $N_{AD}$ | N | $N_{AD}$ | N | $N_{AD}$ |
| ARK. #7 | -1.0° | -5.0° | +1.0° | -3.0° | +3.5° | -0.5° |
| L+D26: 3IP-IIIS (METH. 2) | +1.5° | -3.5° | +2.5° | -2.5° | +5.0° | 0.0° |
| L+D26: 3IP-IIIS (METH. 3) | +8.5° | +3.5° | +10.5° | +5.5° | +12.0° | +7.0° |
| L+D26: 1-3 | -1.5° | -5.5° | 0.0° | -4.0° | +2.0° | -2.0° |
| CAN. 24-4 | -7.0° | -7.0° | -5.0° | -5.0° | -1.5° | -1.5° |
| CAN. 24-5 | +3.0° | +1.0° | +4.5° | +2.5° | +6.5° | +4.5° |
| CAN. 35-1 | 0.0° | -4.0° | +2.0° | -2.0° | +5.0° | +1.0° |
| L+D26: 2-1 AND 2-5 | +7.0° | +3.0° | +8.0° | +4.0° | +9.5° | +5.5° |
| L+D26: 2-4 AND 2-5 | +4.5° | +0.5° | +5.5° | +1.5° | +7.5° | +3.5° |
| L+D6: K-8 | -3.0 | -5.5 | -2.0 | -4.5 | 0.0 | -2.5 |
| AVERAGE - PER PILE | +1.20 | -2.25 | +2.70 | -0.75 | +4.95 | +1.50 |
| SCATTER - PER PILE | 3.70 | 3.85 | 4.10 | 3.45 | 5.25 | 2.80 |

* TABLE ENTRIES ARE DEVIATION ANGLES ($\phi_{PT,DEV}$) ASSUMING $\phi_{PT}$ IS ESTIMATED USING EITHER N OR $N_{AD}$.

## * UNIT SIDE FRICTION ($f_s^*$) CASE

$\phi_{s,DEV} = (\phi_s - \phi_{s,p})$

$\phi_{s,DEV}$ ≡ DEVIATION ANGLE FOR SIDE FRICTION CASE.

$\phi_s$ ≡ IN-SITU SOIL FRICTION ANGLE - ESTIMATED USING N, $N_{AD}$ AND $N_{AVG}$.

$\phi_{s,p}$ ≡ PREDICTED FRICTION ANGLE ALONG PILE SIDE - OBTAINED FROM LOCATION OF DATA POINT ON COYLE-CASTELLO CURVES.

### DEVIATION ANGLES - WITH $\phi_p$ ESTIMATED FROM N, $N_{AD}$ AND $N_{AVG}$*

| | ⅓ PLUGGED | | | ½ PLUGGED | | | FULLY PLUGGED | | |
|---|---|---|---|---|---|---|---|---|---|
| PILE | N | $N_{AD}$ | $N_{AVG}$ | N | $N_{AD}$ | $N_{AVG}$ | N | $N_{AD}$ | $N_{AVG}$ |
| ARK. #7 | +3.5 | +1.5 | +2.5 | +3.0 | +1.0 | +2.0 | +1.5 | -0.5 | +0.5 |
| L+D26:3IP-IIIS (METH. 2) | +5.5 | +2.5 | +4.0 | +4.9 | +1.9 | +3.4 | +2.5 | -0.5 | +1.0 |
| L+D26:3IP-IIIS (METH. 3) | +6.0 | +3.0 | +4.5 | +5.3 | +2.3 | +3.8 | +3.3 | +0.3 | +1.8 |
| L+D26:1-3 | +4.7 | +2.7 | +3.7 | +4.3 | +2.3 | +3.3 | +2.7 | +0.7 | +1.7 |
| CAN. 24-4 | +4.0 | +2.4 | +3.2 | +3.8 | +2.2 | +3.0 | +3.0 | +1.4 | +2.2 |
| CAN. 24-5 | +4.7 | +2.7 | +3.7 | +4.5 | +2.5 | +3.5 | +3.5 | +1.5 | +2.5 |
| CAN. 35-1 | +0.8 | +0.2 | +0.5 | +0.2 | -0.4 | -0.1 | -1.6 | -2.2 | -1.9 |
| L+D26:2-1 AND 2-5 | +1.4 | 0.0 | +0.7 | +0.9 | -0.5 | +0.2 | -1.5 | -2.9 | -2.2 |
| L+D26:2-4 AND 2-5 | +2.0 | +0.6 | +1.3 | +1.5 | +0.1 | +0.8 | -0.7 | -2.1 | -1.4 |
| L+D6:K-8** | - | - | - | - | - | - | - | - | - |
| AVERAGE - PER PILE | +3.6 | +1.7 | +2.7 | +3.2 | +1.3 | +2.2 | +1.4 | -0.5 | +0.5 |
| SCATTER - PER PILE | 3.6 | 1.7 | 2.7 | 3.2 | 1.4 | 2.2 | 1.8 | 1.2 | 1.1 |

* TABLE ENTRIES ARE DEVIATION ANGLES ($\phi_{s,DEV}$) ASSUMING $\phi_s$ IS ESTIMATED USING EITHER N, $N_{AD}$ OR $N_{AVG}$.

** VALUES FOR L+D6:K-8 NOT SHOWN SINCE ALL DEVIATION ANGLES ARE EXCESSIVELY LARGE DUE TO LINEAR EXTRAPOLATION OF LOAD-SETTLEMENT CURVES. THEREFORE, THIS TEST PILE IS IGNORED IN DETERMINING CLOSEST CORRELATION FOR SIDE FRICTION CASE.

# Appendix 3-I

## [Correlation Between the Zero Plug $q_o^*$ Value and CPT Results]

### Lock and Dam 26: 2-5

From the measured load transfer curves at an applied load corresponding to $\delta = 2.0''$, then $Q_{PT} = 59$ tons (ref 2). Also, at an embedded length of 59', then $Q_{RES}$ is approximately 35 tons (from Method Appendix 3-E) assuming the pile is ½ plugged.

Therefore, since

$$Q_{PT}^* = Q_{PT} + Q_{RES}$$
$$= (59 + 35)\text{ tons} \Rightarrow Q_{PT}^* = 94 \text{ tons}$$

For the zero plug case, then $A_{PT} = .149\ ft^2$ and

$$q_o^* = Q_{PT}^*/A_{PT} = 94 \text{ tons}/.149\ ft^2 : \underline{q_o^* = 631 \text{ tsf}}$$

With a $\underline{q_c = 228 \text{ tsf}}$ (from CPT results provided by Dr. Coyle), then:

$$X = q_o^*(\text{zero plug})/q_c = 631/228 : \boxed{X = 2.77}$$

### California -1A (Data for this pile provided by Dr Coyle)

From the measured load transfer curves at an applied load corresponding to $\delta = 2.0''$, then $Q_{PT} = 40$ tons. At an embedded length of 26 ft, assuming the tip is ½ plugged, then $Q_{RES} \doteq 7$ tons (from Appendix 3-E, HP 14 x 73)

Therefore, $Q_{PT}^* = Q_{PT} + Q_{RES} = (40 + 7)$ tons : $Q_{PT}^* = 47$ tons

For the zero plug case, then $A_{PT} = .192\ ft^2$ (HP 14 x 73) and

$$q_o^* = Q_{PT}^*/A_{PT} = 47 \text{ tons}/.192\ ft^2 : \underline{q_o^* = 244.8 \text{ tsf}}$$

From the CPT results, $\underline{q_c = 90.1 \text{ tsf}}$ (at the pile tip)

$$\therefore \quad X = q_o^*/q_c = 244.8/90.1 : \boxed{X = 2.72}$$

Copy available to DTIC does not permit fully legible reproduction



# APPENDIX 3-J
## [EXTRAPOLATION OF LOAD TRANSFER CURVES]

SAMPLE CALCULATIONS FOR ARKANSAS #6 (HP 14×73)

* ULTIMATE COMPRESSION CAPACITY ($Q_U$)
  FROM THE MEASURED LOAD-SETTLEMENT CURVE AT $\delta = 2.0''$, $Q_U = 194$ TONS (RE

* RESIDUAL LOAD ($Q_{RES}$)
  FROM APPENDIX 3-E, AT $D = 40$ FT AND ASSUMING THE PILE TIP TO BE PLUGGED, THEN $Q_{RES} = 16$ TONS ($A_{PT} = .765\ FT^2$, $q_{RES} = 21$ TSF)

* FOR $Q_{APP} = 175$ TONS (FROM MEASURED LOAD-TRANSFER CURVES, REF 9)
  - COMPUTE $Q_{RES}$: $\dfrac{Q_{RES}}{Q_{RES,MAX}} = \dfrac{Q_{APP}}{Q_U}$ ; $Q_{RES} = Q_{RES,MAX}\left(\dfrac{Q_{APP}}{Q_U}\right)$

    $Q_{RES} = (16\ \text{TONS})\left(\dfrac{175}{194}\right)$ ; $Q_{RES} = 14.4$ TONS

  - COMPUTE $\left(Q_S^*/Q_{PT}^*\right)$ AND $\left(Q_{APP}/Q_U\right)$

    $R_2 = \dfrac{Q_S^*}{Q_{PT}^*}$ : $Q_{PT} = 40.6$ TONS (FROM MEASURED LOAD TRANSFER CURVES, REF 9)

    SINCE $Q_{PT}^* = Q_{PT} + Q_{RES}$

    $= (40.6 + 14.4)$ TONS, $Q_{PT}^* = 55$ TONS

    SINCE $Q_S^* = Q_{APP} - Q_{PT}^* = (175 - 55)$ ; $Q_S^* = 120$ TONS

    $\therefore\ Q_S^*/Q_{PT}^* = 120/55$ ; $Q_S^*/Q_{PT}^* = 2.18$

    $R_1 = \dfrac{Q_{APP}}{Q_U}$ ; $Q_{APP}/Q_U = 175/194$ ; $Q_{APP}/Q_U = .902$

* FOR $Q_{APP} = 150$ TONS: (FROM MEASURED LOAD-TRANSFER CURVES, REF 9)
  - COMPUTE $Q_{RES}$ $\quad Q_{RES}/Q_{RES,MAX} = \left(Q_{APP}/Q_U\right)$ ; $Q_{RES} = Q_{RES,MAX}\left(Q_{APP}/Q_U\right)$

    $Q_{RES} = (16\ \text{TONS})\left(\dfrac{150}{194}\right)$ ; $Q_{RES} = 12.4$ TONS

Copy available to DTIC does not permit fully legible reproduction



• COMPUTE $\left(Q_s^*/Q_{PT}^*\right)$ AND $\left(Q_{APP}/Q_U\right)$

$R_2 = \left(Q_s^*/Q_{PT}^*\right)$; $Q_{PT} = 26$ TONS (FROM MEASURED LOAD-TRANSFER CURVES, REF 9)

SINCE $Q_{PT}^* = Q_{PT} + Q_{RES}$

$= (26 + 12.4)$ TONS; $Q_{PT}^* = 38.4$ TONS

SINCE $Q_s^* = Q_{APP} - Q_{PT}^*$

$= (150 - 38.4)$ TONS; $Q_s^* = 111.6$ TONS

$\therefore \left(Q_s^*/Q_{PT}^*\right) = \left(111.6/38.4\right)$; $Q_s^*/Q_{PT}^* = 2.91$

$R_1 = \left(Q_{APP}/Q_U\right)$; $Q_{APP}/Q_U = 150/194$; $Q_{APP}/Q_U = .773$

* FOR $Q_{APP} = 125$ TONS (FROM MEASURED LOAD TRANSFER CURVES, REF 9)

• COMPUTE $Q_{RES}$ $Q_{RES} = Q_{RES,MAX}\left(Q_{APP}/Q_U\right) = (16 \text{ TONS})\left(125/194\right)$; $Q_{RES} = 10.3$ TONS

• COMPUTE $\left(Q_s^*/Q_{PT}^*\right)$ AND $\left(Q_{APP}/Q_U\right)$

$R_2 = \left(Q_s^*/Q_{PT}^*\right)$; $Q_{PT} = 15.6$ TONS (FROM MEASURED LOAD-TRANSFER CURVES, REF 9)

SINCE $Q_{PT}^* = Q_{PT} + Q_{RES} = (15.6 + 10.3)$ TONS; $Q_{PT}^* = 25.9$ TONS

SINCE $Q_s^* = Q_{APP} - Q_{PT}^*$

$= (125 - 25.9)$ TONS; $Q_s^* = 99.1$ TONS

$\therefore \left(Q_s^*/Q_{PT}^*\right) = 99.1/25.9$; $Q_s^*/Q_{PT}^* = 3.83$

$R_1 = \left(Q_{APP}/Q_U\right)$; $Q_{APP}/Q_U = 125/194$; $Q_{APP}/Q_U = .644$

Copy available to DTIC does not permit fully legible reproduction



* TABLE OF RESULTS: $R_1 = Q_{APP}/Q_U$ ; $R_2 = Q_s^*/Q_{PT}^*$

| | Pile | $Q_U$ (TONS) | $Q_{RES,MAX}$ | $R_2$ | $R_1$ | $R_2$ | $R_1$ | $R_2$ | $R_1$ | $R_2$ | $R_1$ |
|---|---|---|---|---|---|---|---|---|---|---|---|
| (1) | ARK. #6 | 194 | 16 | 2.18 | .902 | 2.91 | .773 | 3.83 | .644 | | |
| (2) | ARK. #7 | 250 | 25 | 2.13 | .800 | 2.41 | .650 | 2.57 | .488 | | |
| (3) | ARK. #9 | 250 | 21 | 4.04 | .875 | 4.42 | .750 | 5.20 | .650 | | |
| (4) | L+DZ6:1-3 | 322 | 35 | .65 | 1.00 | .67 | .932 | .70 | .776 | .81 | .621 |
| | | | | .99 | .466 | .96 | .311 | | | | |
| (5) | L+DZ6:2-5 | 236.5 | 35 | 1.39 | .951 | 1.75 | .846 | 2.25 | .740 | 1.99 | .634 |
| | | | | 3.39 | .529 | 3.03 | .423 | | | | |
| (6) | CAL-1A | 83 | 7 | .77 | 1.00 | .87 | .904 | .98 | .843 | 1.03 | .783 |
| | | | | 1.21 | .723 | 1.32 | .662 | 1.45 | .602 | 1.92 | .492 |

* PLOT OF RESULTS: $R_1 = Q_{APP}/Q_U$

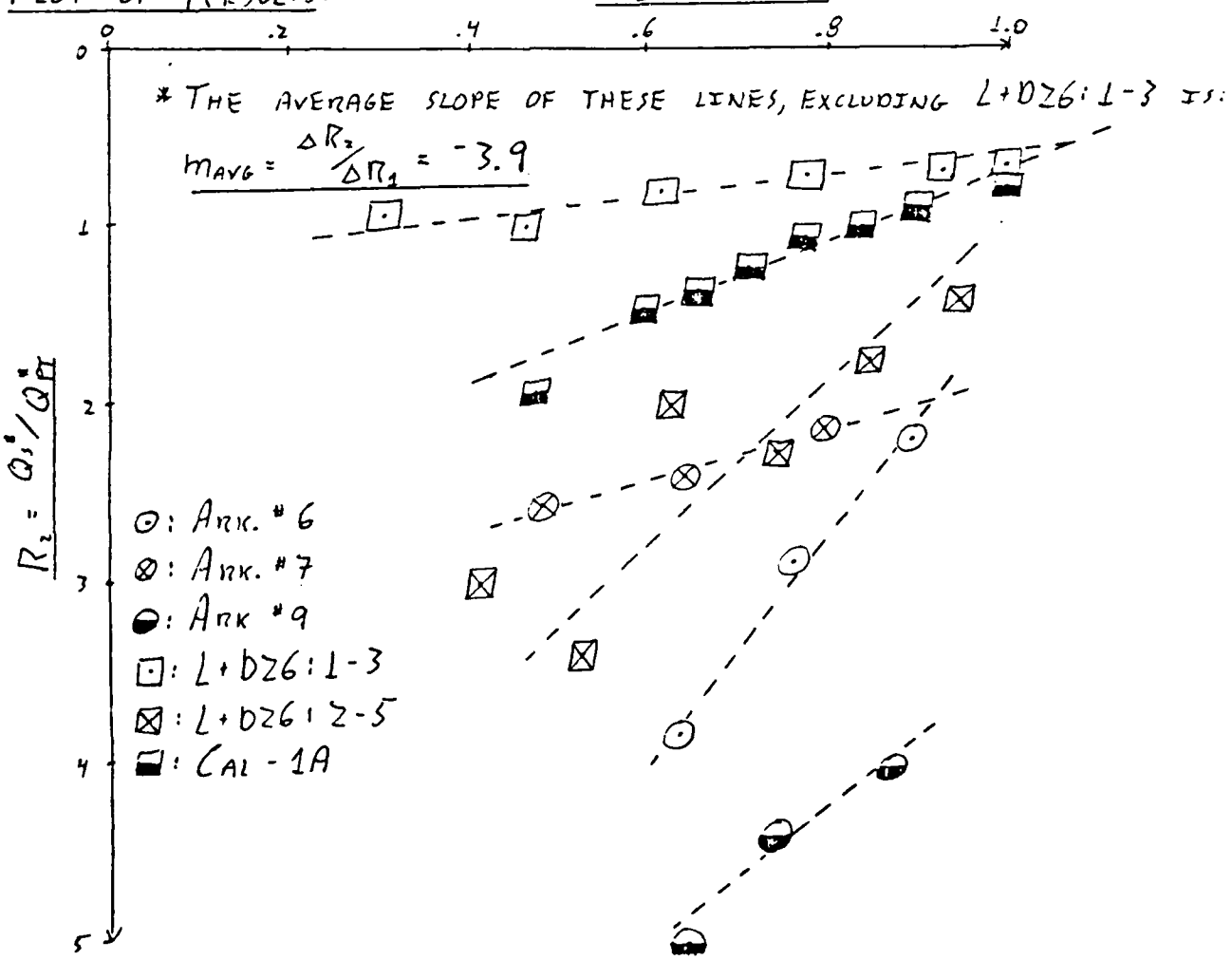

Copy available to DTIC does not permit fully legible reproduction



# APPENDIX 3-K
## [EXTRAPOLATION OF LOAD TRANSFER CURVES]

### ARKANSAS #7

- COMPUTE LOAD-TRANSFER CURVE AT $Q_{APP} = Q_U$

FROM THE LOAD-SETTLEMENT CURVE AT $\delta = 2.0''$ (REF 9), $Q_U = 250$ TONS.
FROM THE LOAD-SETTLEMENT CURVE IN TENSION AT $\delta = 1.2''$, $Q_{UT} = 65$ TON

USING $\lambda^* = Q_S^*/Q_{UT} = 1.8$, THEN, $Q_S^* = 1.8(65 \text{ TONS})$, $Q_S^* = 117$ TONS AT $R_1 = 1$

SINCE $Q_{PT}^* = Q_U - Q_S^*$,

$= (250 - 117)$ TONS, $Q_{PT}^* = 133$ TONS

### AT $Q_{APP} = .85 Q_U$:

WRITING AN EQUATION FOR $R_1$ VS $R_2$ (FROM 3-J-3), WITH $m = -3.$
YIELDS:

$R_2 = m R_1 + b$, OR, $b = R_2 - m R_1$ ; WITH $R_1 = Q_{APP}/Q_U$ ; $R_2 = Q$

$\therefore$ $b = R_2 + 3.9 R_1$, AT $R_1 = 1$, $R_2 = Q_S^*/Q_{PT}^* = 117/133$ ; $R_2 = .930$

$b = (.930) + 3.9(1)$, $b = 4.78$

$\therefore$ $R_2 = -3.9 R_1 + 4.78$

FOR $R_1 = .85$, THEN $R_2 = 1.465$, $\therefore$ (1) $Q_S^* = 1.465 Q_{PT}^*$

AND,

$Q_S^* = 126.3$ TONS (2) $Q_{APP} = .85 Q_U = 212.5 = Q_S^* + Q_{PT}^*$

$Q_{PT}^* = 86.2$ TONS

FOR $R_1 = .70$, THEN $R_2 = 2.05$, $\therefore$ (1) $Q_S^* = 2.05 Q_{PT}^*$

AND

$Q_S^* = 117.6$ TONS (2) $Q_{APP} = .70 Q_U = 175$ TONS $= Q_S^* + Q_{PT}^*$

$Q_{PT}^* = 57.4$ TONS

FOR $R_1 = .55$, THEN $R_2 = 2.635$, $\therefore$ (1) $Q_S^* = Q_{PT}^*(2.635)$

AND

$Q_S^* = 99.7$ TONS (2) $Q_{APP} = .55 Q_U = 137.5$ TON $= Q_S^* + Q_{PT}^*$

$Q_{PT}^* = 37.8$ TONS

APPENDIX 3-K

(3-K-

* TABULATION OF COMPUTED DATA

| PILE | $Q_u$ (TONS) | $Q_{UT}$ (TONS) | $R_1 = 1.0$ $Q_s^*$ | $R_1 = 1.0$ $Q_{PT}^*$ | $R_1 = .85$ $Q_s^*$ | $R_1 = .85$ $Q_{PT}^*$ | $R_1 = .70$ $Q_s^*$ | $R_1 = .70$ $Q_{PT}^*$ | $R_1 = .55$ $Q_s^*$ | $R_1 = .55$ $Q_{PT}^*$ |
|---|---|---|---|---|---|---|---|---|---|---|
| ARK. #7 | 250 | 65.0 | 117 | 133 | 126 | 86 | 117 | 57 | 100 | 38 |
| | | | | | | | | | | |
| L+D26:3IP-IIIS (METHOD 2) | 367 | 96.6 | 173 | 194 | 186 | 126 | 173 | 84 | 147 | 55 |
| L+D26:3IP-IIIS (METHOD 3) | 216 | 87.0 | 157 | 59 | 140 | 44 | 120 | 32 | 97 | 22 |
| L+D26: 1-3 | 322 | 64.4 | 116 | 206 | 146 | 128 | 120 | 105 | 124 | 53 |
| | | | | | | | | | | |
| CAN. 24-4 | 168.6 | 47.8 | 86 | 83 | 89 | 55 | 81 | 37 | 68 | 24 |
| | | | | | | | | | | |
| CAN. 24-5 | 88.8 | 33.7 | 61 | 28 | 55 | 20 | 48 | 14 | 39 | 10 |
| | | | | | | | | | | |
| CAN. 35-1 | 198.0 | 61.9 | 111 | 87 | 110 | 59 | 99 | 40 | 82 | 27 |
| | | | | | | | | | | |
| L+D26: 2-1 AND 2-5 | 236.5 | 108.4 | 195 | 41 | 169 | 32 | 142 | 24 | 113 | 17 |
| | | | | | | | | | | |
| L+D26: 2-4 AND 2-5 | 236.5 | 96.0 | 173 | 64 | 154 | 47 | 132 | 34 | 106 | 24 |
| | | | | | | | | | | |
| L+D6: K-8 | 387.5 | 145.8 | 262.4 | 125.1 | 240.0 | 89.4 | 207.8 | 63.5 | 169.2 | 43.9 |

## LOAD TRANSFER CURVES

1. ANK. #7 (FROM TABULATED DATA)

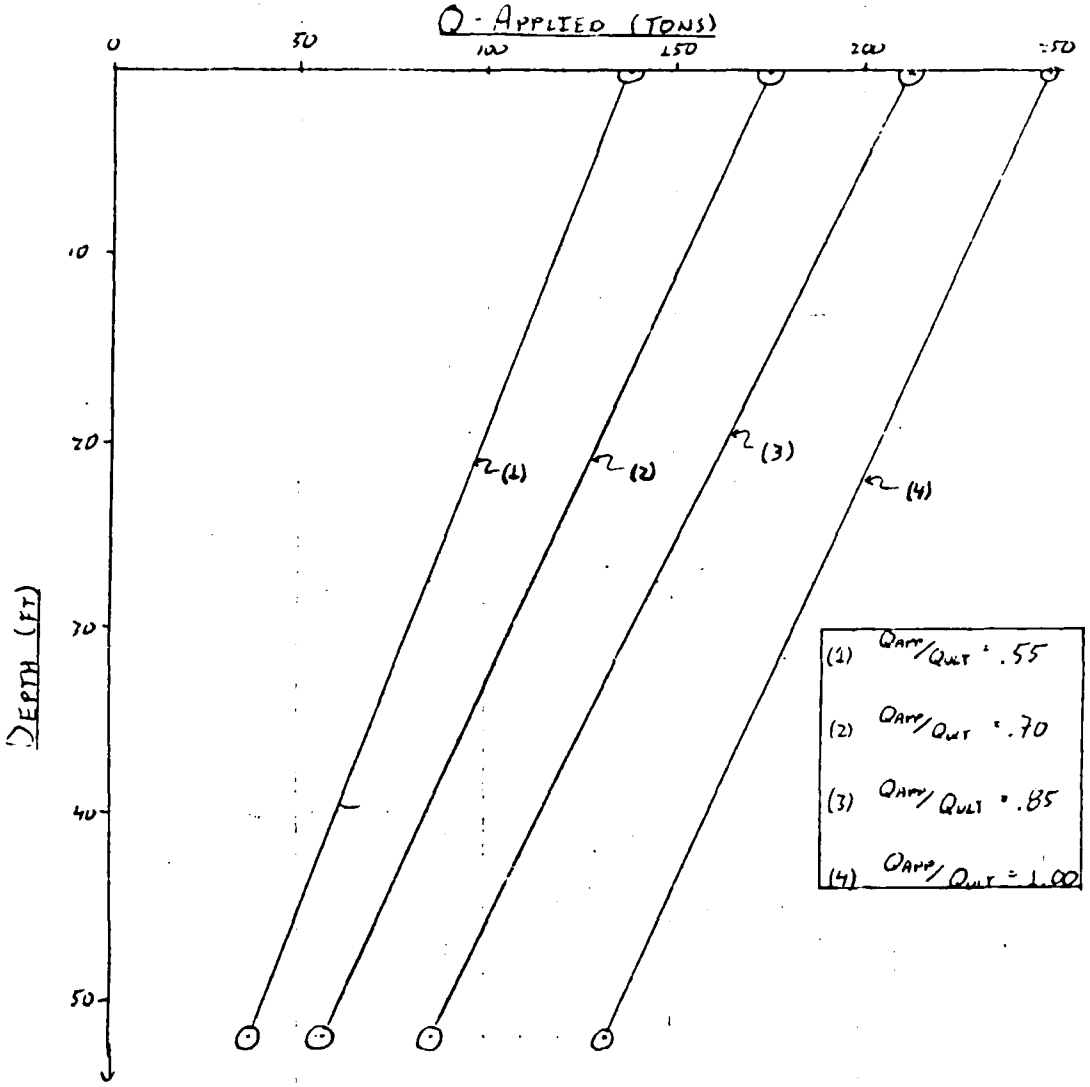

LOAD TRANSFER CURVES

D. L-V26-3IP-III S (METHOD 1) (FROM TABULATED DATA)

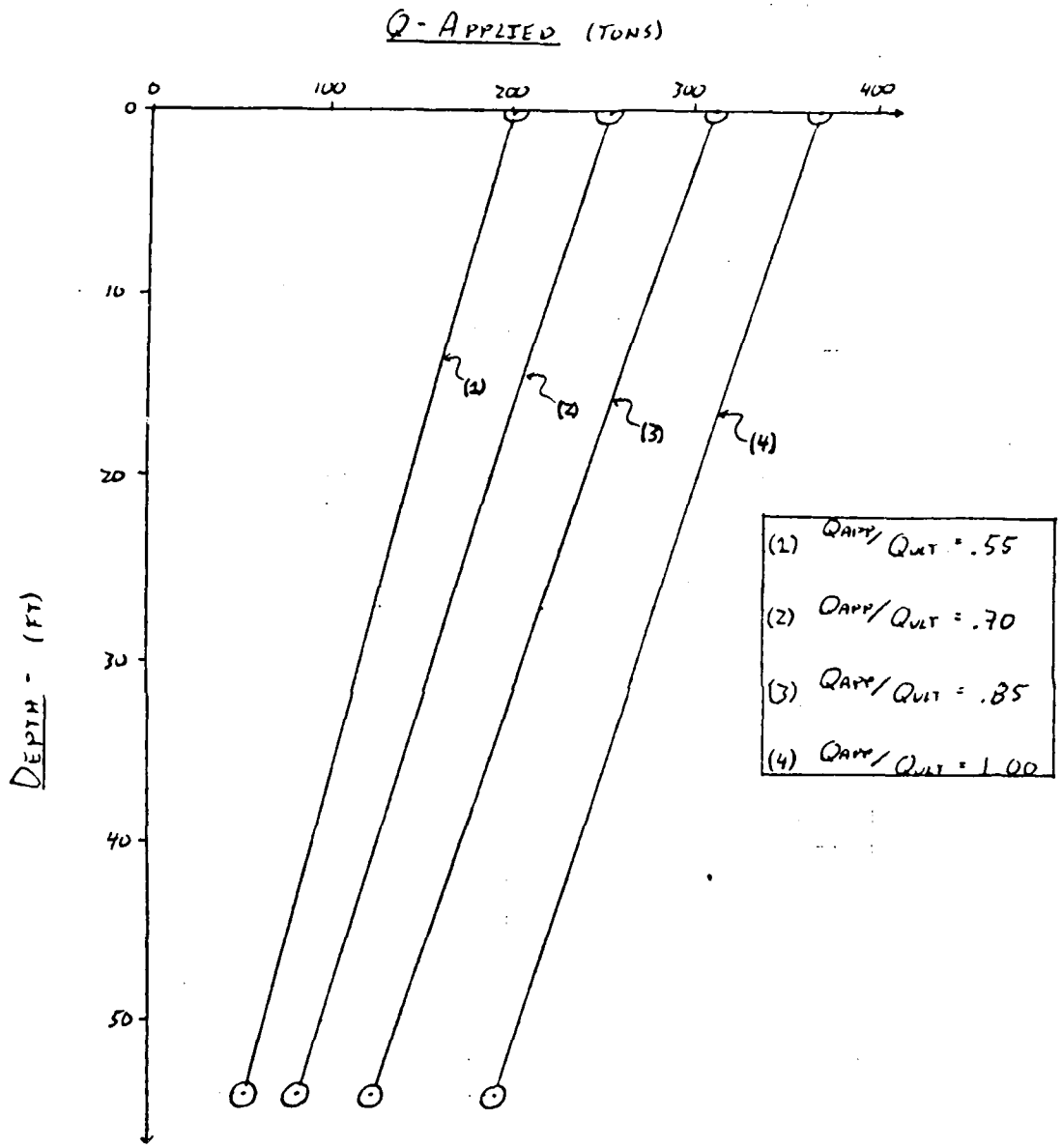

LOAD TRANSFER CURVES

E. L+D26: 3IP - III S (METHOD 2) (FROM TABULATED DATA)

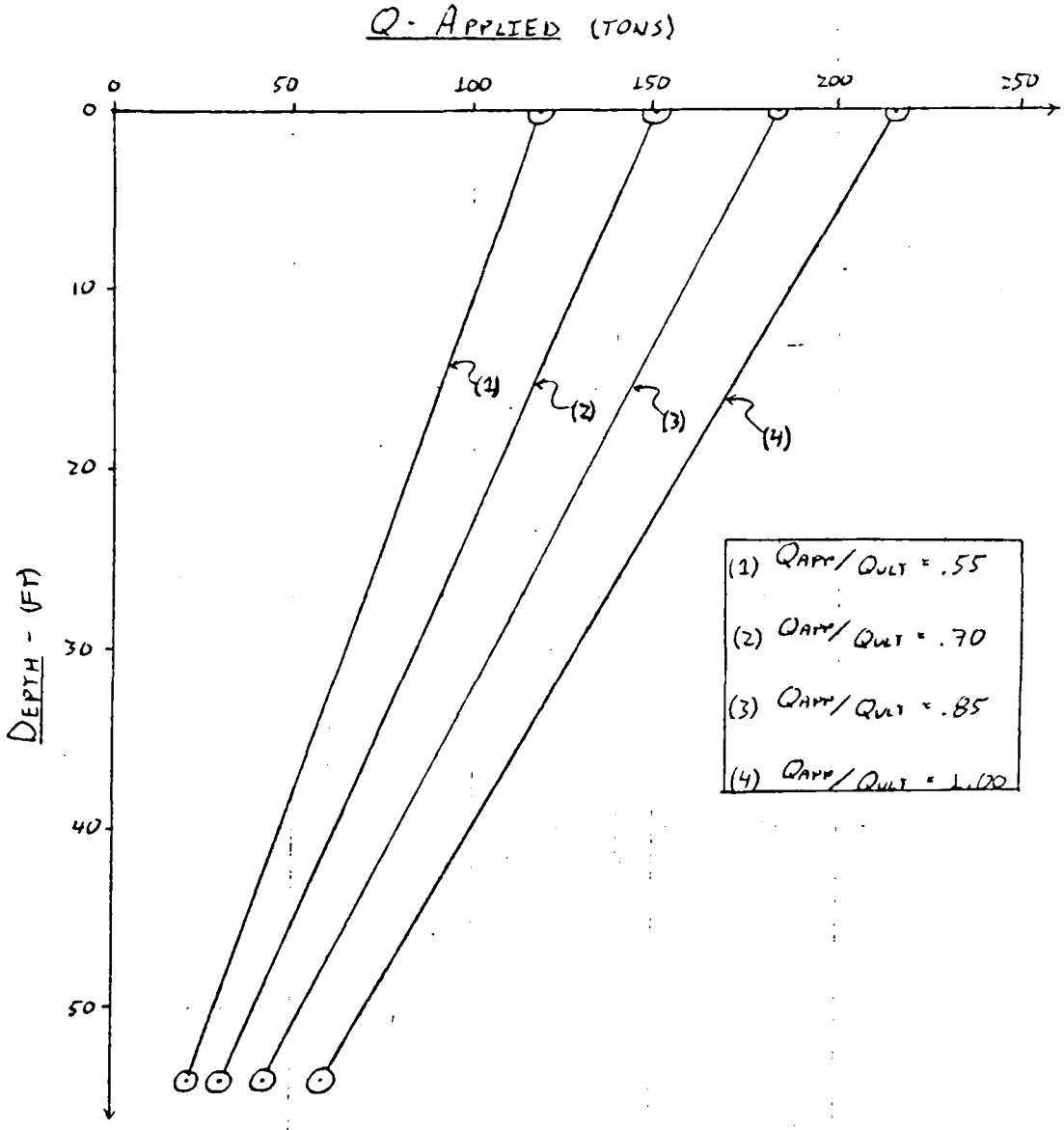

LOAD TRANSFER CURVES

F. L1D26:1-3 (FROM TABULATED DATA)

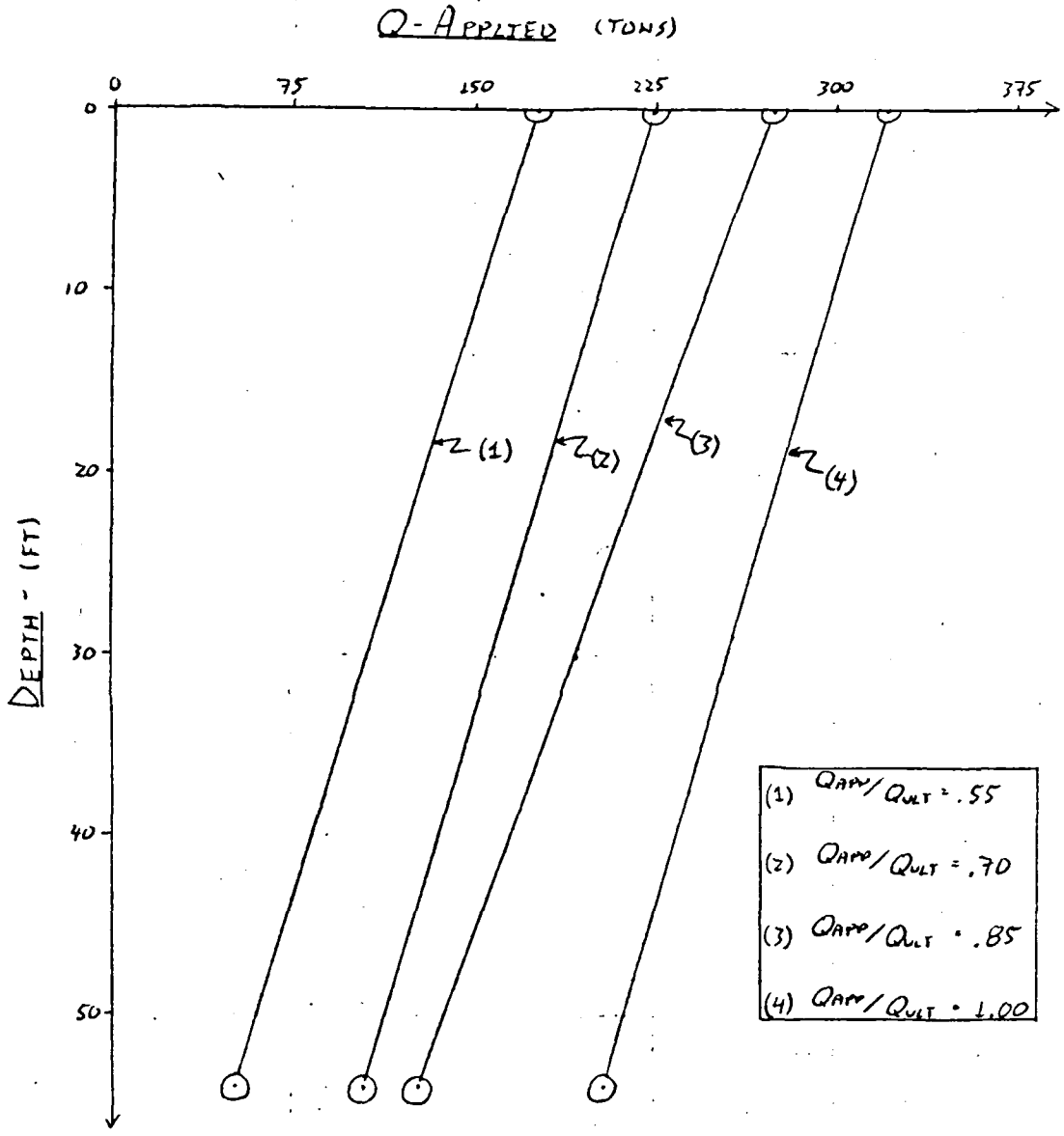

LOAD TRANSFER CURVES

G. CAN. 24-4 (FROM TABULATED DATA)

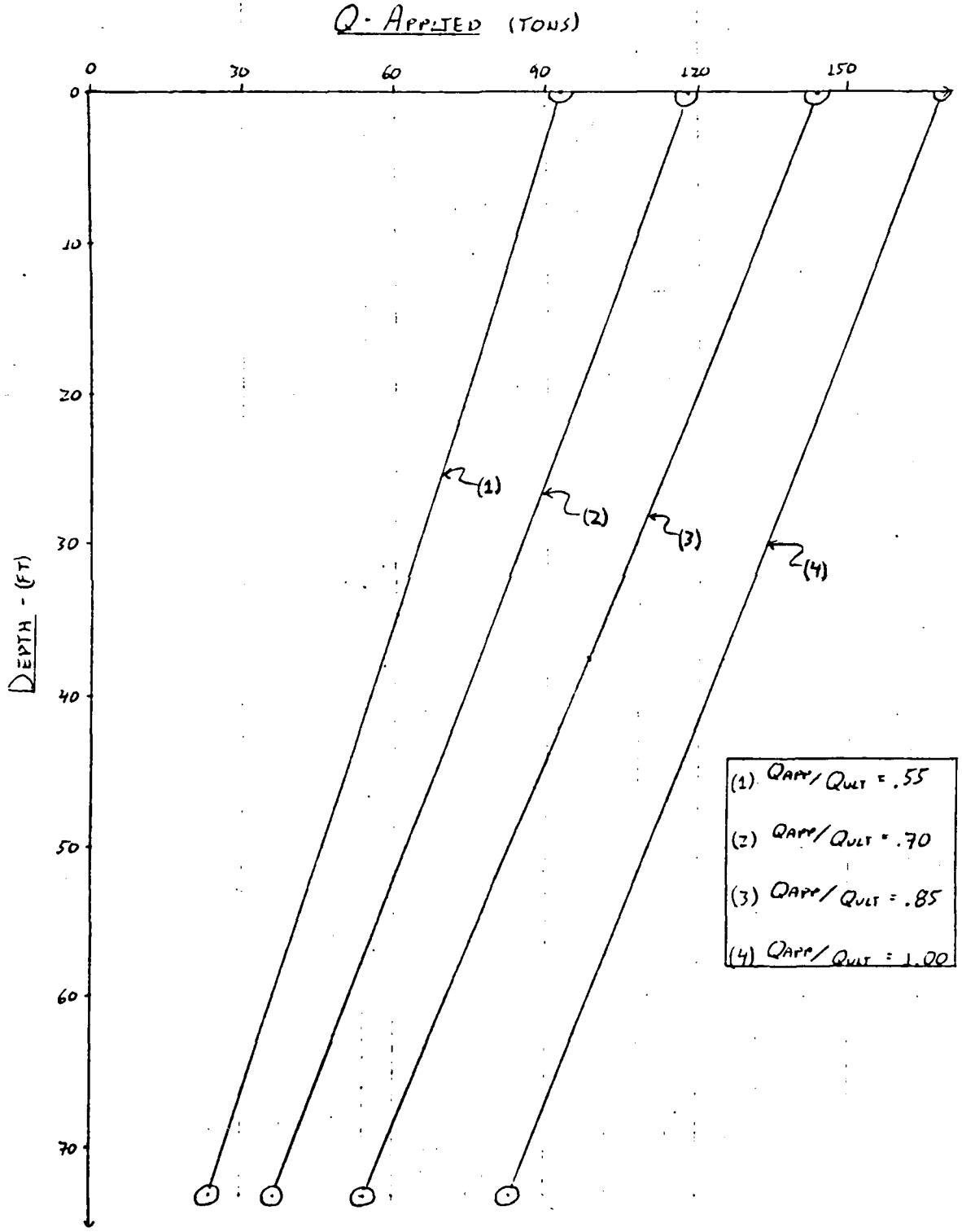

LOAD TRANSFER CURVES

H. CAN. 24-5 (FROM TABULATED DATA)

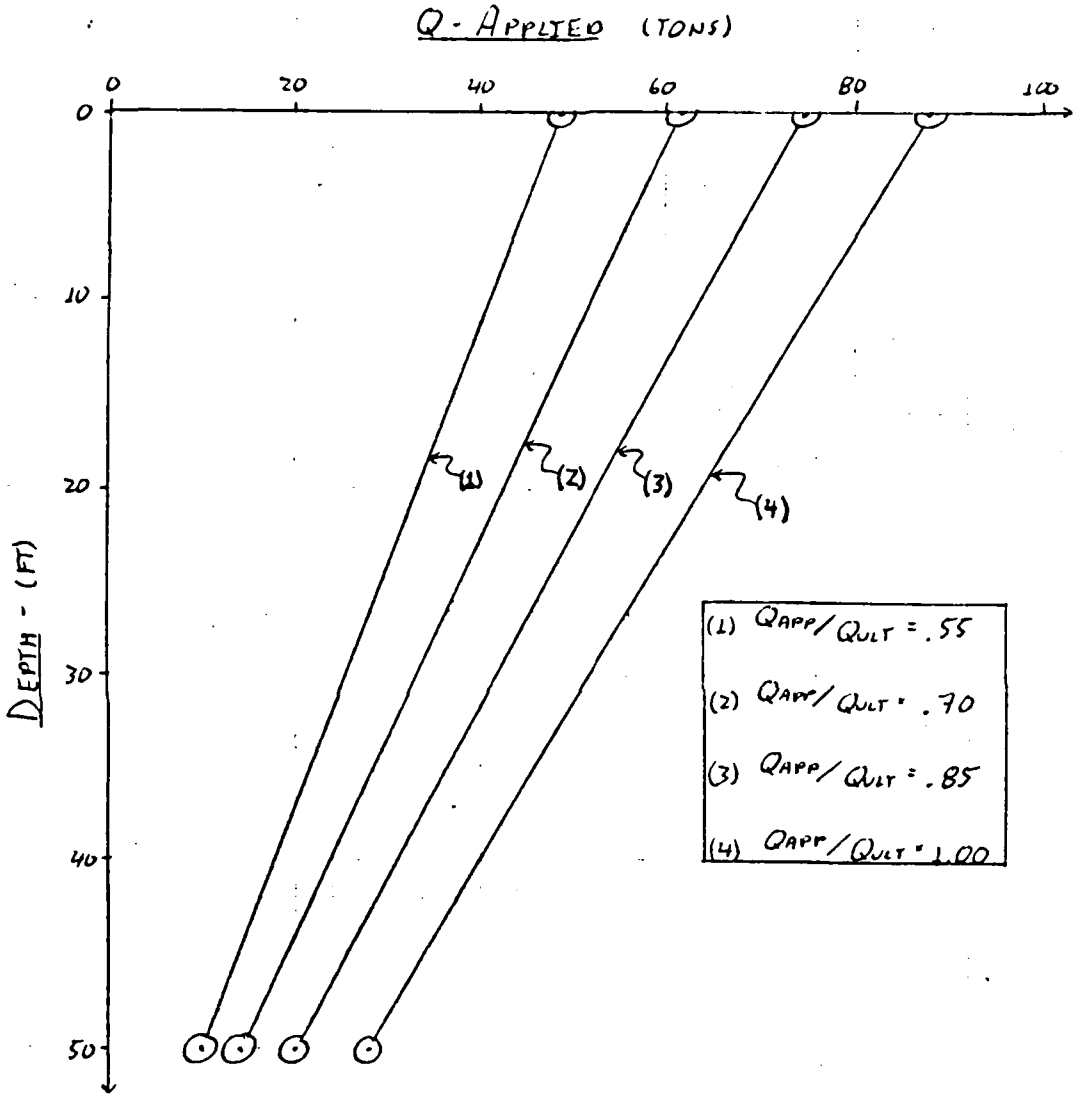

## LOAD TRANSFER CURVES

I. CAN. 35-1 (FROM TABULATED DATA)

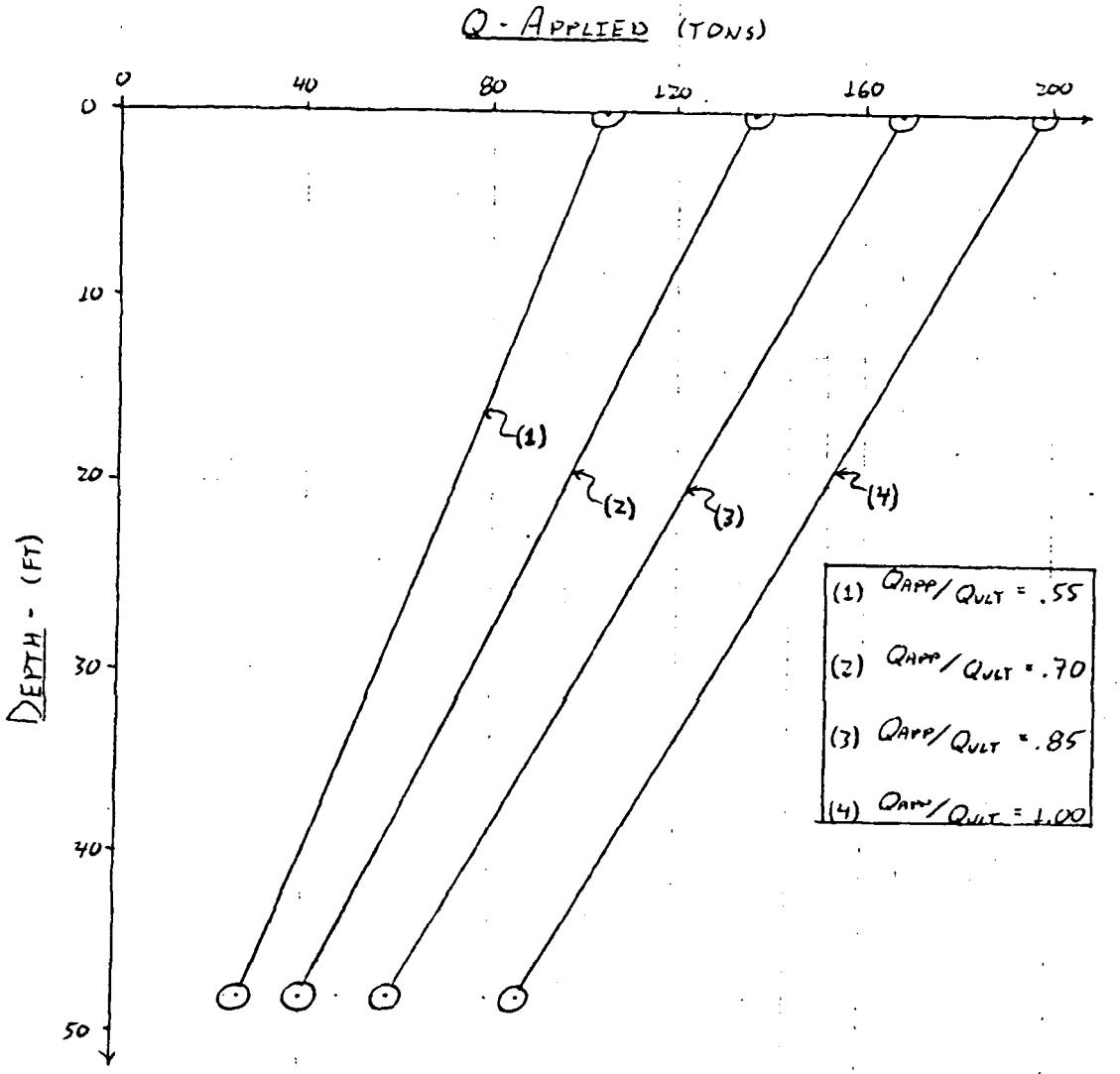

LOAD TRANSFER CURVES

J. L-D26: 2-1 AND 2-5 (FROM TABULATED DATA)

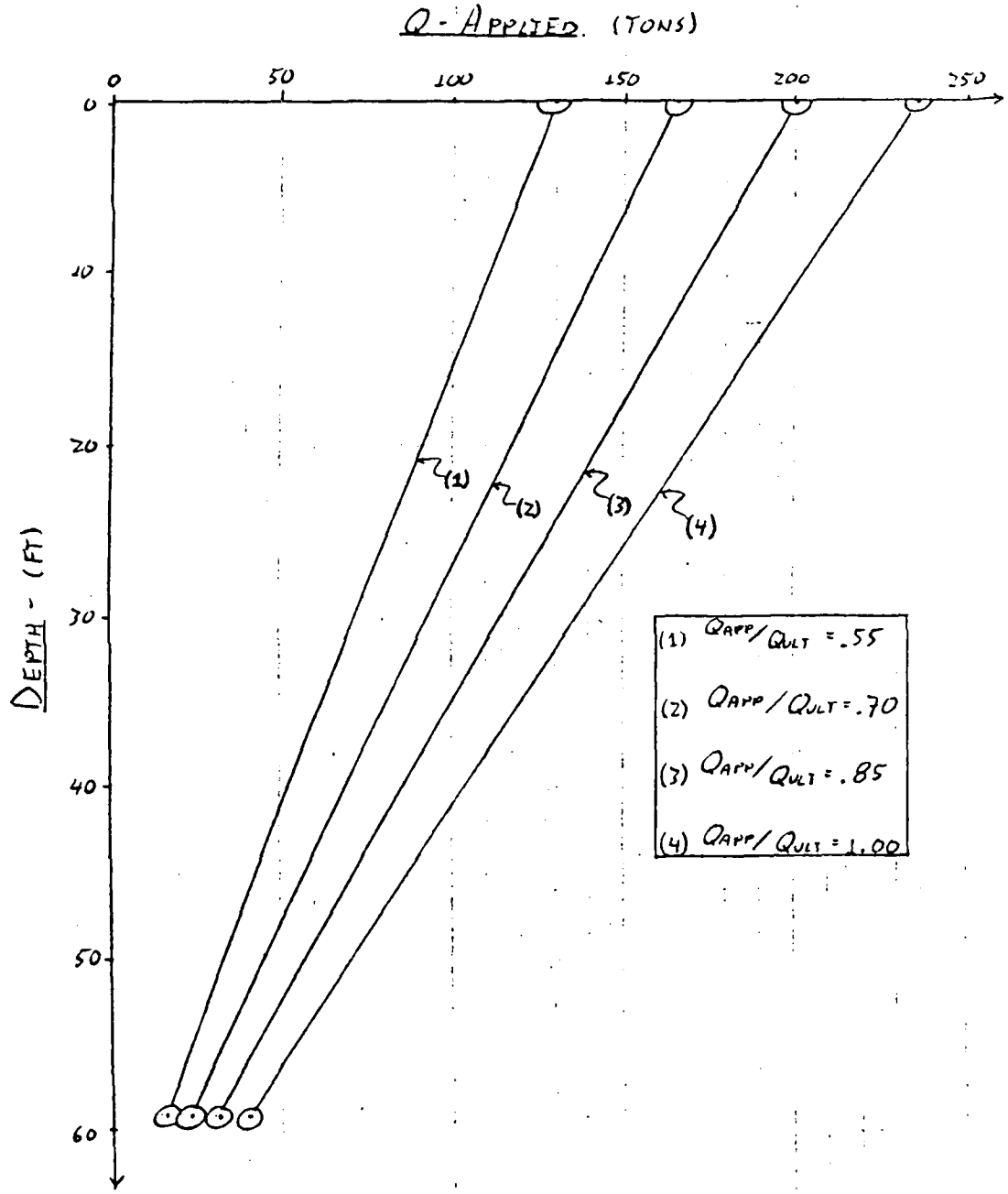

## LOAD TRANSFER CURVES

K. L+D26: 2-4 AND 2-5 (FROM THE TABULATED DATA)

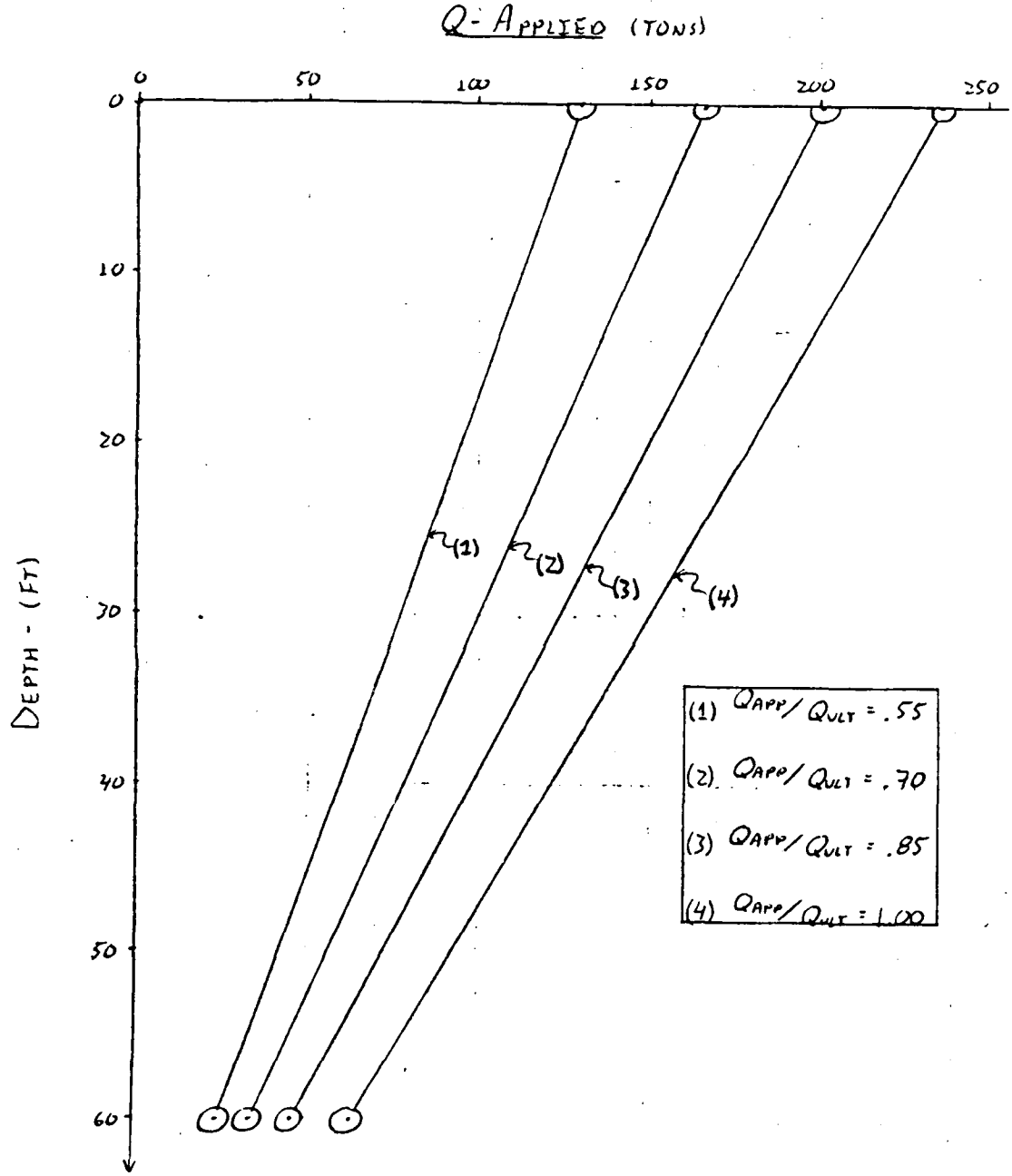

LOAD TRANSFER CURVES (L+D 6 : K-8)

6. LOAD TRANSFER CURVES

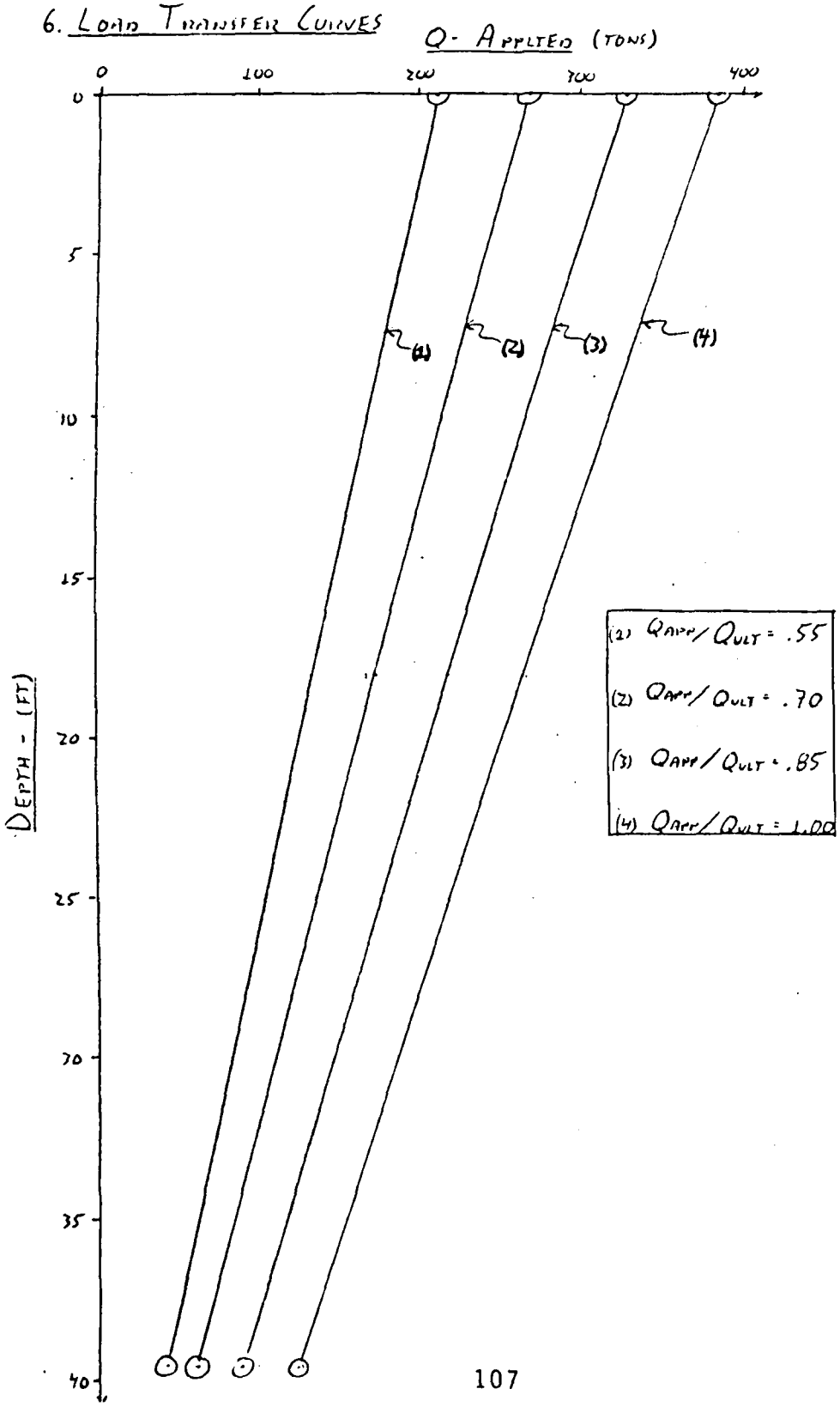

Copy available to DTIC does not permit fully legible reproduction

# APPENDIX 3-L

(3-L-1)

## [PILE MOVEMENTS AND UNIT RESISTANCES - INCLUDE EFFECTS OF ELASTIC DEFORMATION]

### ARKANSAS #7

* CALCULATE PILE MOVEMENTS

FROM THE GENERAL PILE DATA SHOWN IN REF 9:

$A = .179\ FT^2$ (INCLUDING CHANNEL IRON)

$E = 29 \times 10^6$ psi (FOR STEEL)

$L = 55$ FT (TOTAL PILE LENGHT)

- FOR $Q_{APP} = 250$ TONS (REFERRING TO GRAPH ON pg 3-K-3)
  - AT $D = 55'/2$, THEN $Q_1 = 187$ TONS, $\therefore P_{AVG} = \frac{(Q_{APP} + Q_1)}{2} = \frac{(250 + 187)\ TON}{2}$

    $P_{AVG} = 218.5$ TONS

    $\therefore Y_m = \frac{P_{AVG}(L/2)}{AE} = \frac{(218.5\ TONS)(L/2)}{AE}$ ; $Y_m = .194$ IN (AT PILE MIDPOINT)

    $\therefore Z_m = \delta - Y_m$ , WHERE $\delta = 1.85''$ (LOAD-SETTLEMENT CURVE AT $Q_{APP} = 250$ TONS, REF 9)

    $= (1.85 - .194)$ IN

    $Z_m = 1.66$ IN

  - AT $D = 55'$, THEN $Q_{PT}^* = 133$ TONS, $\therefore P_{AVG} = \frac{(\overset{Q_1}{187} + \overset{Q_{PT}^*}{133})\ TONS}{2}$ , $P_{AVG} = 160$ TONS

    $\therefore Y_T = \frac{P_{AVG}(L/2)}{AE} = \frac{(160\ TONS)(L/2)}{AE}$ ; $Y_T = .142$ IN (AT PILE TIP)

    $\therefore Z_T = Z_m - Y_T = (1.66 - .142)$ IN ; $Z_T = 1.52$ IN

Copy available to DTIC does not permit fully legible reproduction



- FOR $Q_{APP} = 212.5$ TONS (REFER TO GRAPH ON PG 3-K-3)
  - AT $D = \frac{L}{2}$: THEN $Q_L = 146$ TONS (AT PILE MIDPOINT)

    $\therefore P_{AVG} = \frac{(Q_{APP} + Q_L)}{2} = \frac{(212.5 + 146)}{2}$ TONS ; $P_{AVG} = 179.3$ TONS

    $\therefore Y_m = \frac{P_{AVG}(\frac{L}{2})}{AE} = \frac{(179.3 \text{ TONS})\frac{L}{2}}{AE}$ ; $Y_m = .159$ IN (AT PILE MIDPOINT)

    $\therefore Z_m = \delta - Y_m$, WHERE $\delta = 1.10$ IN (FROM LOAD-SETTLEMENT CURVE AT $Q_{APP} = 212.5$ TONS, REF 9)

    $= (1.10 - .159)$ IN

    $Z_m = .94$ IN

  - AT $D = L$: THEN $Q_{PT}^* = 86.2$ TONS (AT PILE TIP)

    $\therefore P_{AVG} = \frac{(Q_L + Q_{PT}^*)}{2} = \frac{(146 + 86.2)}{2}$ TONS ; $P_{AVG} = 116.1$ TONS

    $\therefore Y_m = \frac{P_{AVG}(\frac{L}{2})}{AE} = \frac{(116.1 \text{ TON})\frac{L}{2}}{AE}$ ; $Y_m = .103$ IN (AT PILE TIP)

    $\therefore Z_T = Z_m - Y_T = (.94 - .103)$ IN, $Z_T = .84$ IN

- FOR $Q_{APP} = 175$ TONS (REFER TO GRAPH ON PG 3-K-3)
  - AT $D = \frac{L}{2}$: THEN $Q_L = 113$ TONS (AT MIDPOINT)

    $\therefore P_{AVG} = \frac{(Q_{APP} + Q_L)}{2} = \frac{(175 + 113)}{2}$ TONS ; $P_{AVG} = 144$ TONS

    $\therefore Y_m = \frac{P_{AVG}(\frac{L}{2})}{AE} = \frac{(144)(\frac{L}{2})}{AE}$ ; $Y_m = .128$ IN (AT MIDPOINT)

    $\therefore Z_m = \delta - Y_m$, $\delta = .860$ IN (REF 9), $Z_m = (.860 - .128)$ IN, $Z_m = .73$ IN
  - AT $D = L$: THEN $Q_{PT}^* = 57.4$ TONS (AT PILE TIP)

    $\therefore P_{AVG} = \frac{(Q_L + Q_{PT}^*)}{2} = \frac{(113 + 57.4)}{2}$ TONS ; $P_{AVG} = 85.2$ TONS

    $\therefore Y_T = \frac{P_{AVG}(\frac{L}{2})}{AE} = \frac{(85.2 \text{ TONS})(\frac{L}{2})}{AE}$ ; $Y_T = .076$ IN (AT PILE TIP)

    $\therefore Z_T = Z_m - Y_T = (.73 - .076)$ IN ; $Z_T = .65$ IN

## * CALCULATION OF UNIT RESISTANCES ($q_o^*$ AND $f_s^*$)

USING $q_o^* = Q_{PT}^* / A_{PT}$ AND $f_s^* = Q_s^* / A_s$

WHERE $A_{PT} = .28\ FT^2$ AND $A_s = 390\ FT^2$ (ASSUME PILE IS UNPLUGGED)

- **AT $Q_{APP} = 250$ TONS**

FROM THE LOAD-TRANSFER CURVES (pg 3-K-3):

$Q_s^* = 117$ TONS AND $Q_{PT}^* = 133$ TONS, ∴

$f_s^* = Q_s^* / A_s = 117\ TONS / 390\ FT^2$ : $f_s^* = .30$ TSF

$q_o^* = Q_{PT}^* / A_{PT} = 133\ TONS / .28\ FT^2$ : $q_o^* = 475$ TSF

- **AT $Q_{APP} = 212.5$ TONS**

FROM THE LOAD TRANSFER CURVES (pg 3-K-3):

$Q_s^* = 126.3$ TONS AND $Q_{PT}^* = 86.2$ TONS, ∴

$f_s^* = Q_s^* / A_s = 126.3\ TONS / 390\ FT^2$ : $f_s^* = .32$ TSF

$q_o^* = Q_{PT}^* / A_{PT} = 86.2\ TONS / .28\ FT^2$ : $q_o^* = 308$ TSF

- **AT $Q_{APP} = 175$ TONS**

FROM THE LOAD-TRANSFER CURVES (pg 3-K-3):

$Q_s^* = 117.6$ TONS AND $Q_{PT}^* = 57.4$ TONS, ∴

$f_s^* = Q_s^* / A_s = 117.6\ TONS / 390\ FT^2$ : $f_s^* = .30$ TSF

$q_o^* = Q_{PT}^* / A_{PT} = 57.4\ TONS / .28\ FT^2$ : $q_o^* = 205$ TSF

| Pile | $Q_{ULT}$ (a) (tons) | $Q_{APP} = Q_{ULT}$ | | | | $Q_{APP} = .85\,Q_{ULT}$ | | | | $Q_{APP} = .70\,Q_{ULT}$ | | | | $Q_{APP} = .55\,Q_{ULT}$ | | | |
|---|---|---|---|---|---|---|---|---|---|---|---|---|---|---|---|---|---|
| | | $Z_m$ (1) | $f_i$ (2) | $Z_r$ (1) | $q_o$ (2) | $Z_m$ | $f_i$ | $Z_r$ | $q_o$ | $Z_m$ | $f_i$ | $Z_r$ | $q_o$ | $Z_m$ | $f_i$ | $Z_r$ | $q_o$ |
| (1) Anc. # 7 | 250 | 1.66 | 0.30 | 1.52 | 475 | 0.94 | 0.32 | 0.84 | 308 | 0.73 | 0.30 | 0.65 | 265 | 0.66 | 0.26 | 0.61 | 135 |
| (2) L+D26: 3IP-III S: (Method 2) | 367 | 1.72 | 0.43 | 1.51 | 691 | 1.38 | .46 | 1.23 | 449 | 1.04 | 0.43 | 0.93 | 299 | 0.70 | 0.36 | 0.62 | 198 |
| (3) L+D26: 3IP-III S: (Method 3) | 216 | 1.85 | 0.39 | 1.77 | 212 | 0.75 | 0.35 | 0.68 | 155 | 0.39 | 0.30 | 0.34 | 113 | 0.19 | 0.24 | 0.15 | 79 |
| (4) L+D26: 1-3 | 322 | 1.72 | 0.29 | 1.50 | 845 | 0.75 | 0.36 | 0.60 | 523 | 0.27 | 0.30 | 0.14 | 430 | (b) | 0.31 | (b) | 219 |
| (5) Can. 24-4 | 169 | 1.71 | 0.21 | 1.50 | 765 | 0.65 | 0.21 | 0.50 | 506 | 0.36 | 0.19 | 0.25 | 341 | 0.18 | 0.16 | 0.10 | 226 |
| (6) Can. 24-5 | 89 | 1.90 | 0.21 | 1.84 | 260 | 0.59 | 0.19 | 0.45 | 187 | 0.23 | 0.16 | 0.19 | 133 | 0.08 | 0.13 | 0.05 | 92 |
| (7) Can. 35-1 | 198 | 1.84 | 0.40 | 1.73 | 574 | 0.49 | 0.39 | 0.41 | 388 | 0.28 | 0.35 | 0.22 | 266 | 0.17 | 0.29 | 0.13 | 178 |
| (8) L+D26: 2-1 and 2-5 | 237 | 1.87 | 0.44 | 1.81 | 170 | 0.37 | 0.38 | 0.32 | 131 | 0.09 | 0.32 | 0.05 | 99 | (b) | 0.26 | (b) | 71 |
| (9) L+D26: 2-4 and 2-5 | 237 | 1.87 | 0.39 | 1.80 | 261 | 0.37 | 0.35 | 0.31 | 192 | 0.09 | 0.30 | 0.04 | 139 | (b) | 0.24 | (b) | 93 |

NOTES: (1) ALL MOVEMENTS IN INCHES
(2) ALL UNIT RESISTANCES IN TONS PER SQUARE FOOT

REMARKS: (a) $Q_{ULT}$ BASED ON PILE MOVEMENT OF 2.0 INCHES IN COMPRESSION.

(b) AFTER INCLUDING THE EFFECTS OF ELASTIC PILE DEFORMATION, ZERO MOVEMENT WAS CALCULATED - EVEN THOUGHT THE CORRESPONDING RESISTANCES ARE RELATIVELY SIGNIFICANT.

## T-Z AND P-TOTLD CURVES FOR INDIVIDUAL PILES

### A. ARK. #7

1. T-$Z_m$ CURVE

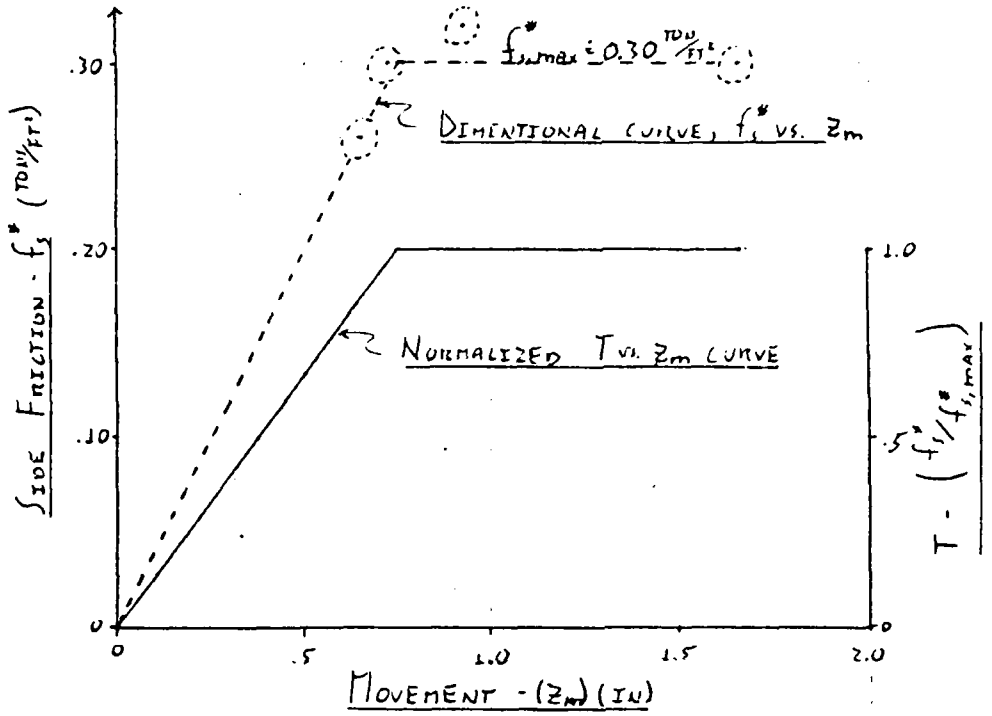


2. P-TOTLD CURVE

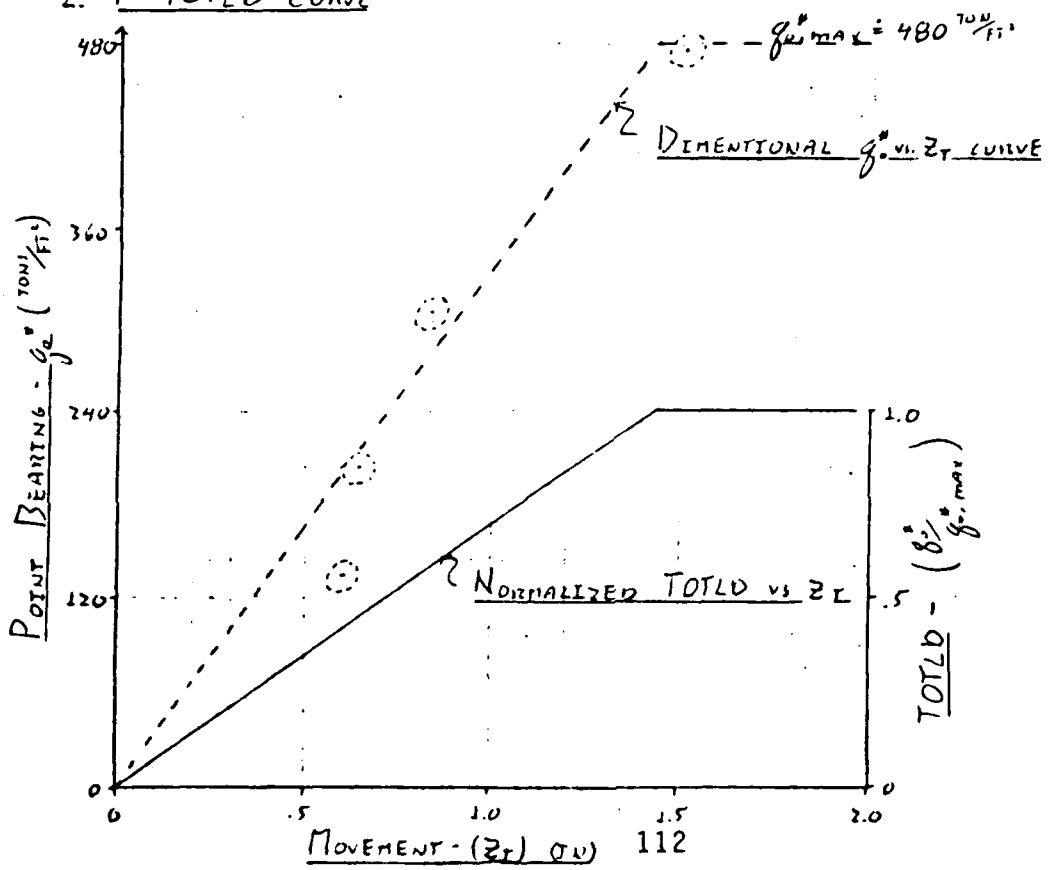

## T-Z AND P-TOTLD CURVES FOR INDIVIDUAL PILES

L-D26:JIP-IIIS (METHOD 1)

1. T-Z CURVE

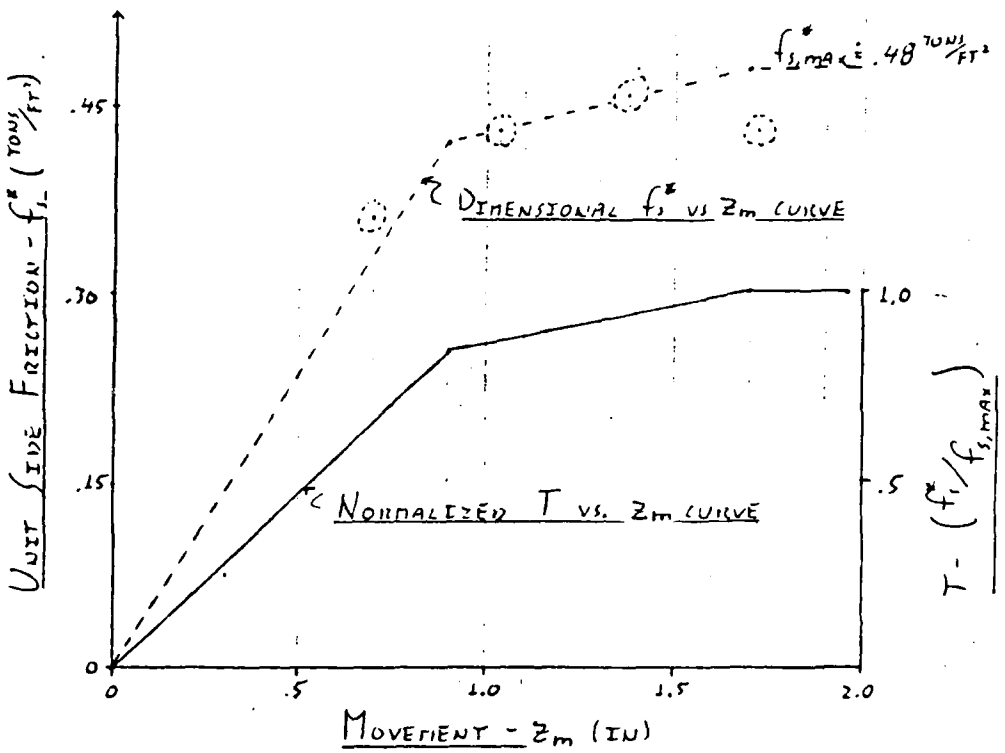


2. P-TOTLD CURVE

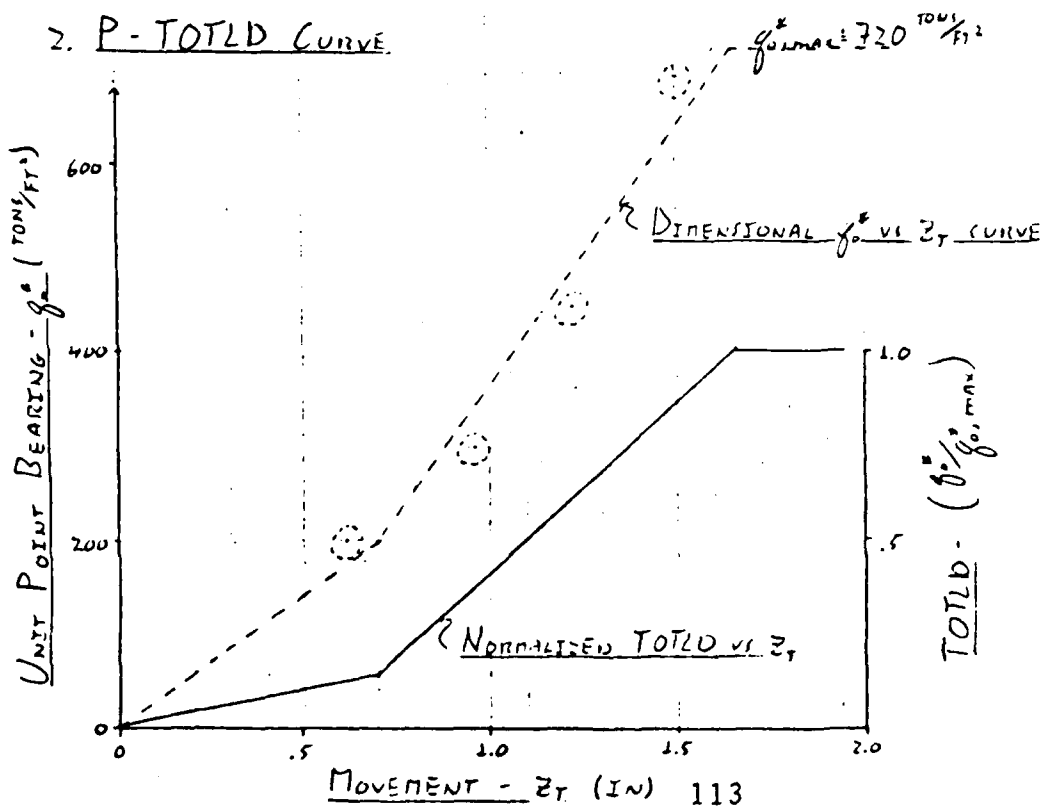

## T-Z AND P-TOTLD CURVES FOR INDIVIDUAL PILES

L+D26·JIP-III S (METHOD Z)

1. T-Z CURVE

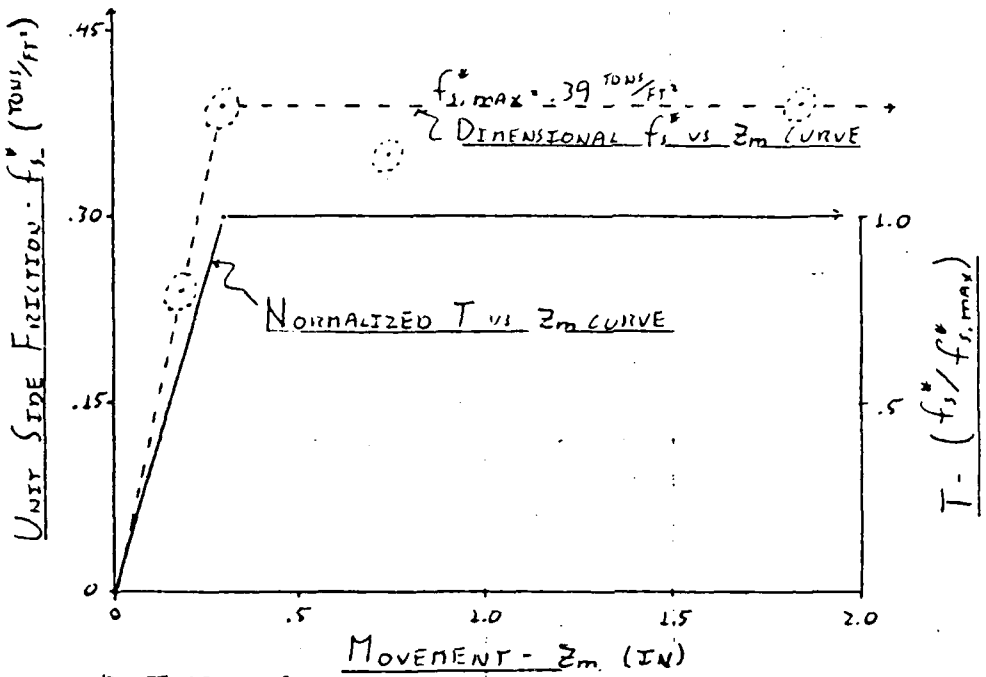


2. P-TOTLD CURVE

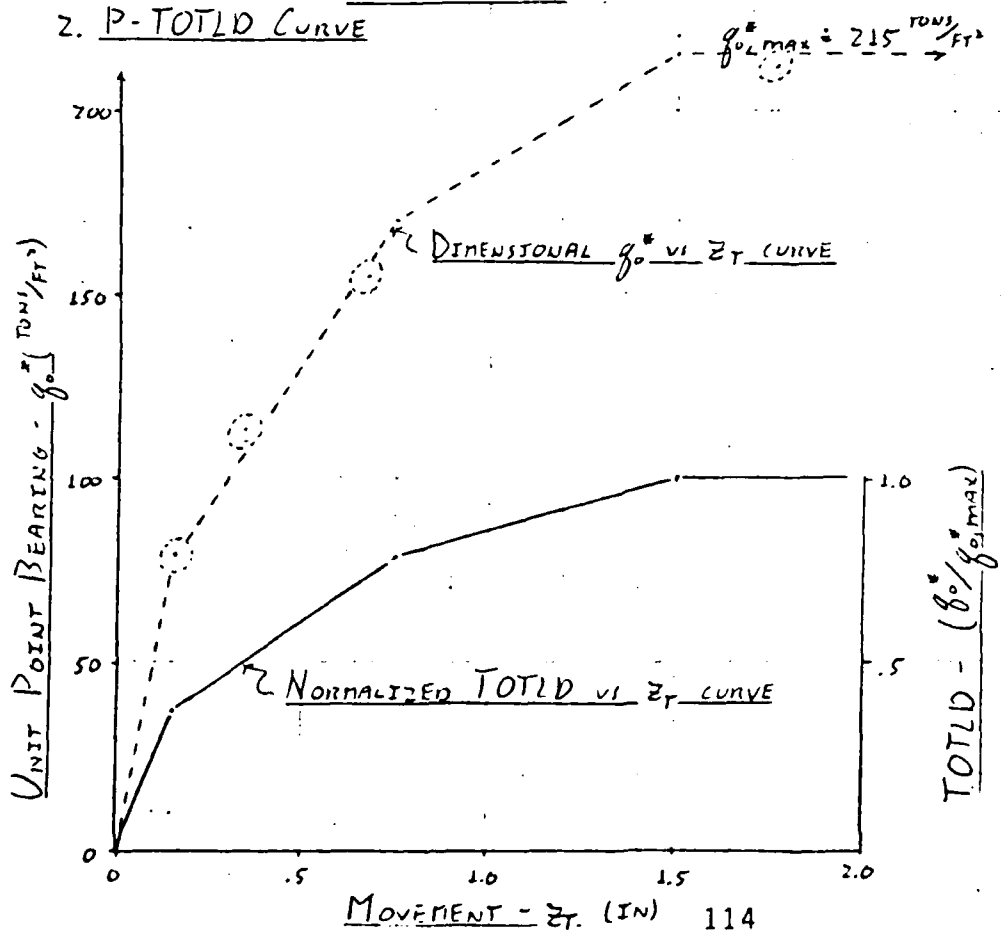

## IV T-Z AND P-TOTLD CURVES FOR INDIVIDUAL PILES

L·D26:1-3

### 1. T-Z CURVE

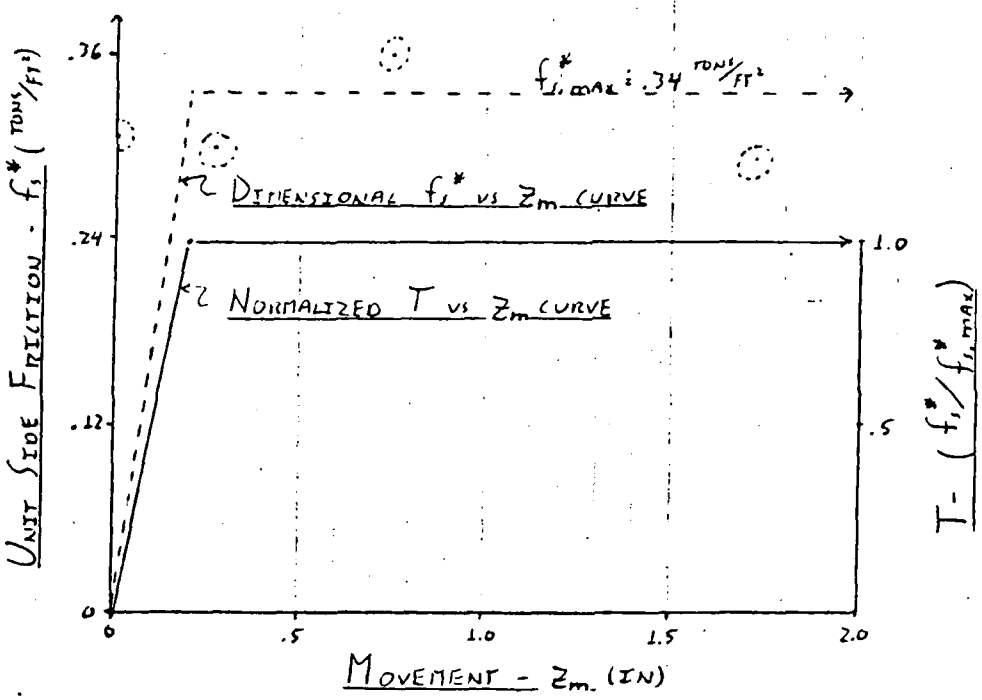


### 2. P-TOTLD CURVE

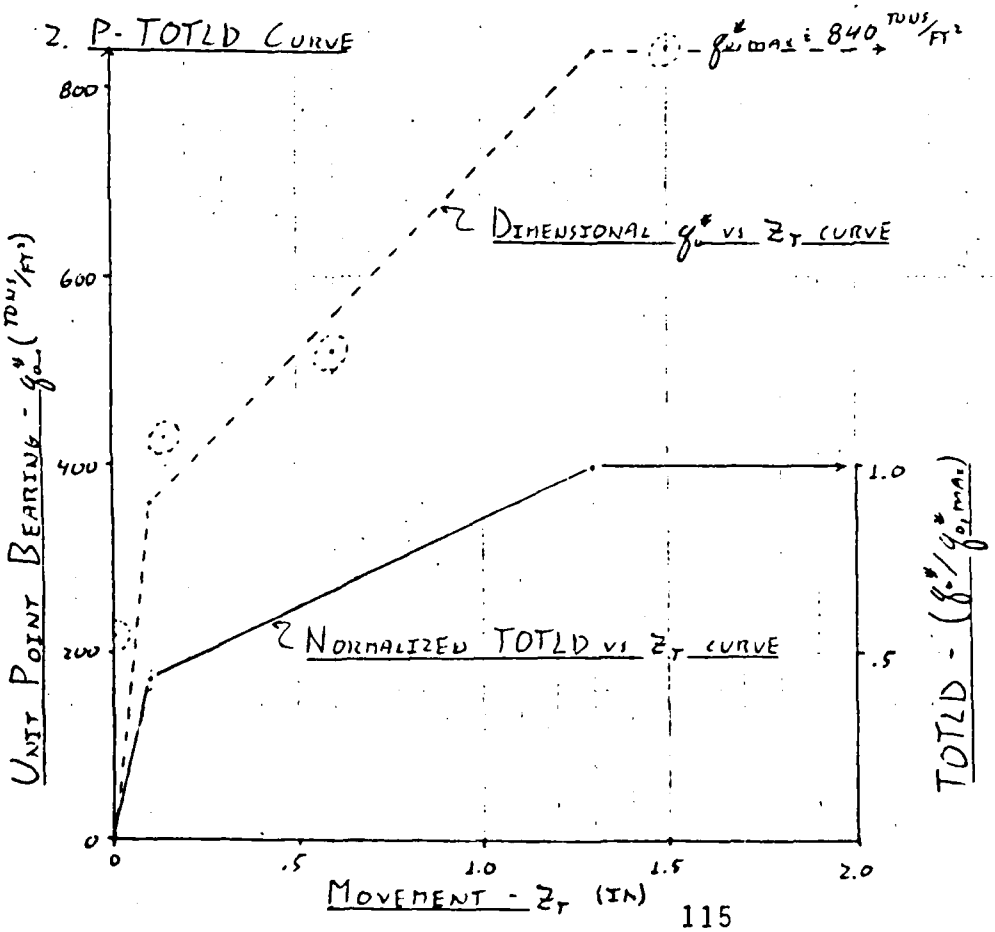

## T-Z AND P-TOTLD CURVES FOR INDIVIDUAL PILES

CAN. 24-4

1. T-Z CURVE

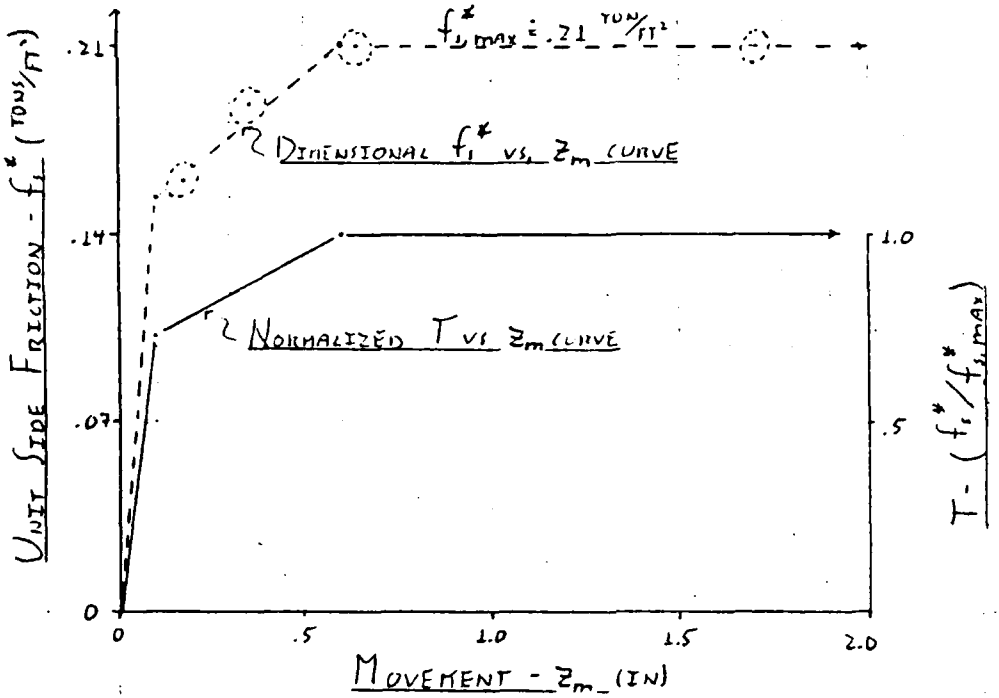


2. P-TOTLD CURVE

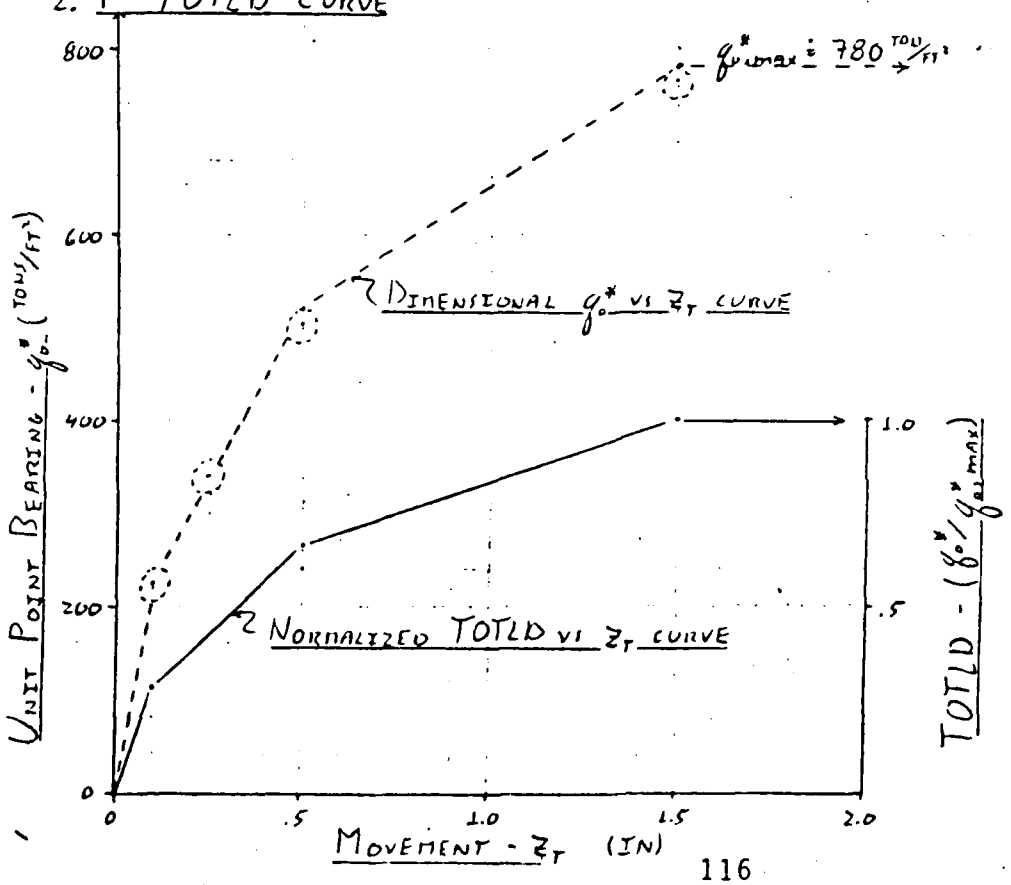

## T-Z AND P-TOTLD CURVES FOR INDIVIDUAL PILES

CAN. 24-5

1. T-Z CURVE

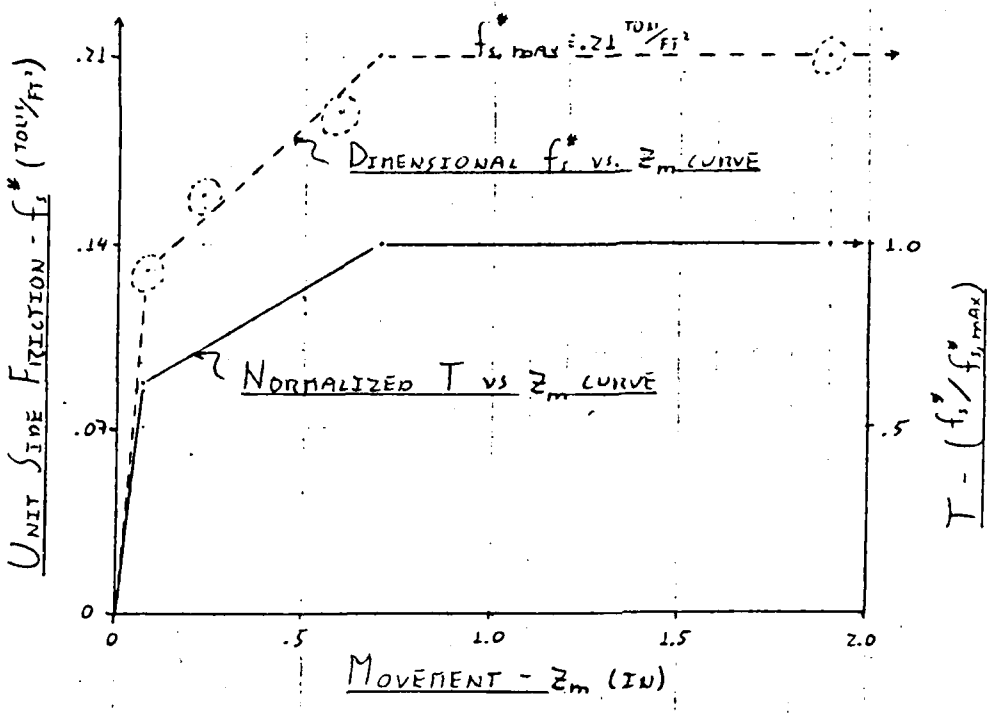


2. P-TOTLD CURVE

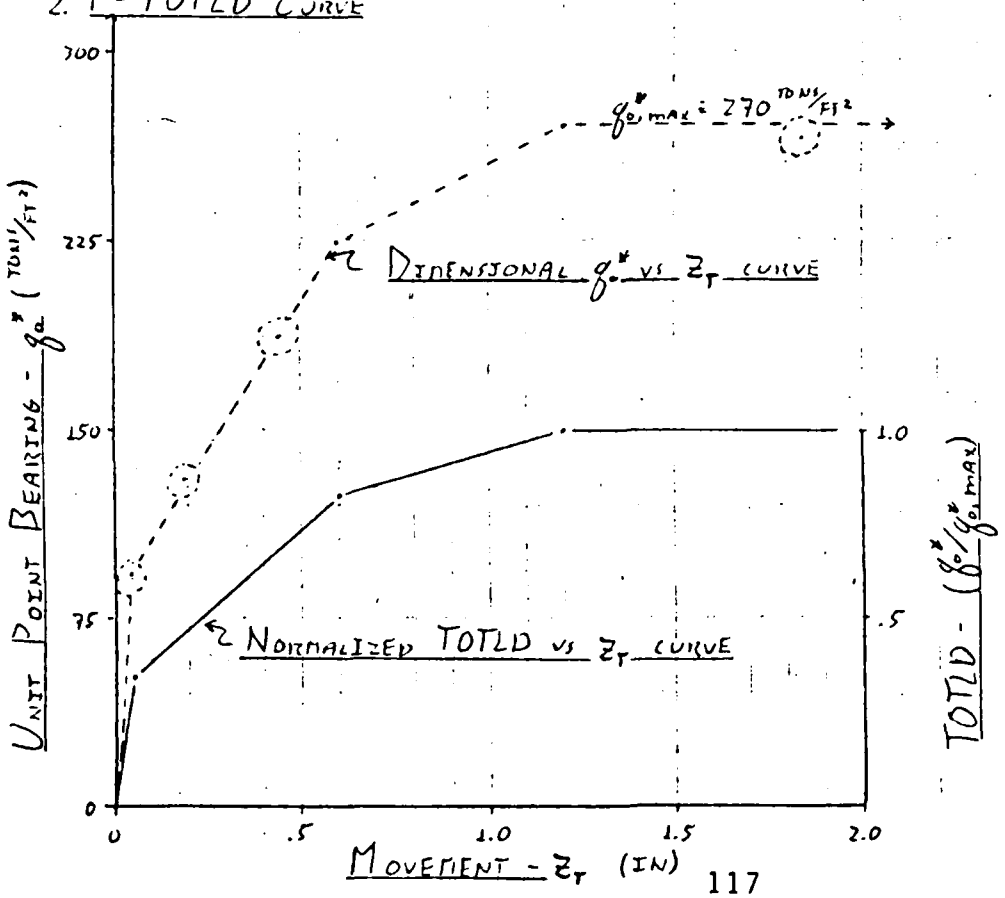

## T-Z AND P-TOTLD CURVES FOR INDIVIDUAL PILES

CAN. 35-1

1. T-Z CURVE

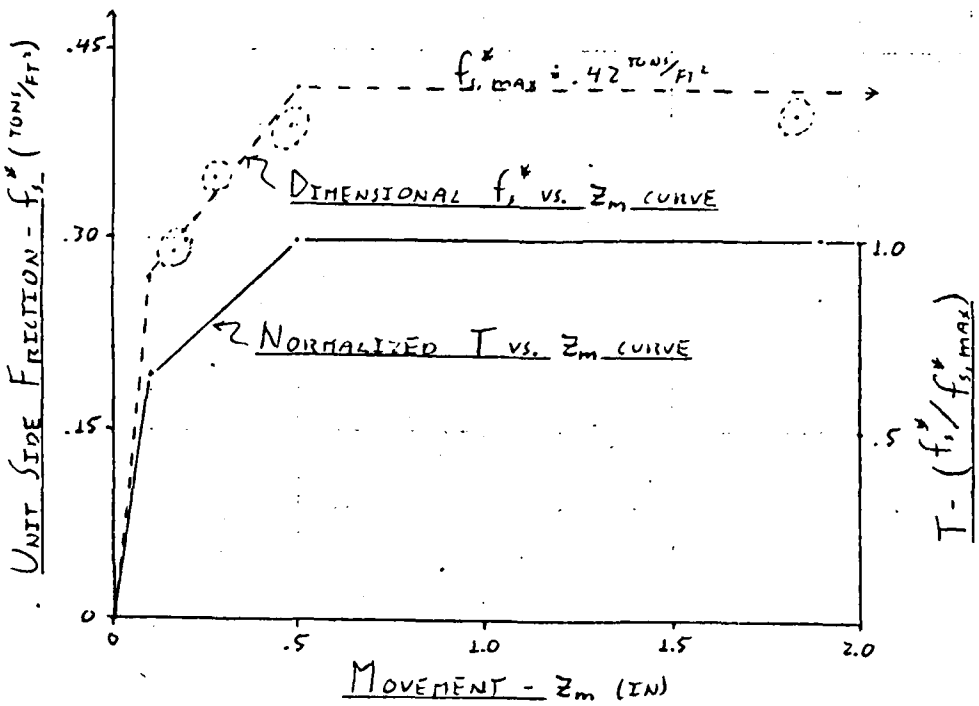


2. P-TOTLD CURVE

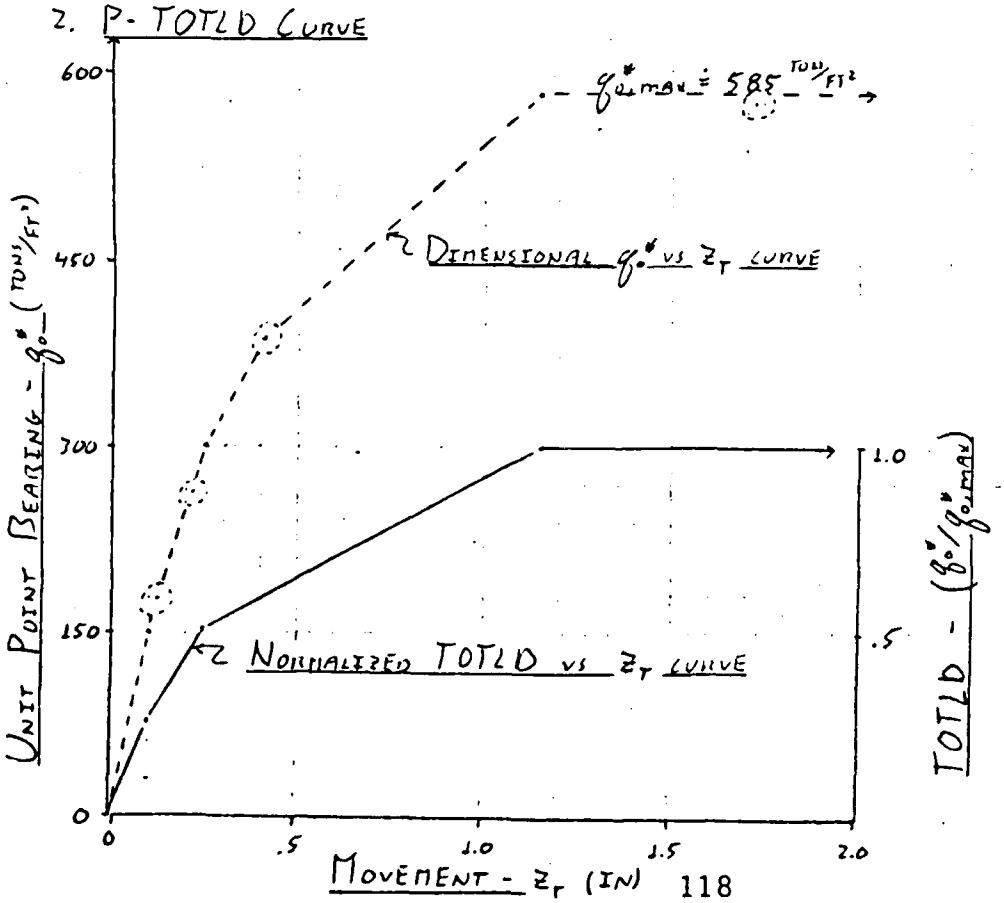

## T-Z AND P-TOTLD CURVES FOR INDIVIDUAL PILES

L+D26:Z-1 AND Z-5

1. T-Z CURVE

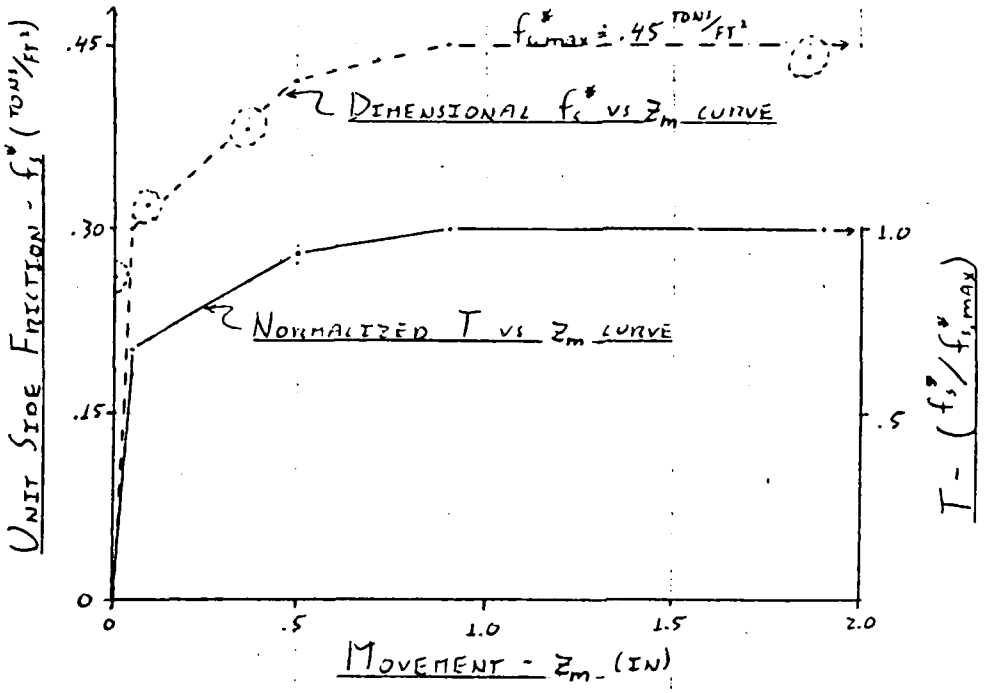


2. P-TOTLD CURVE

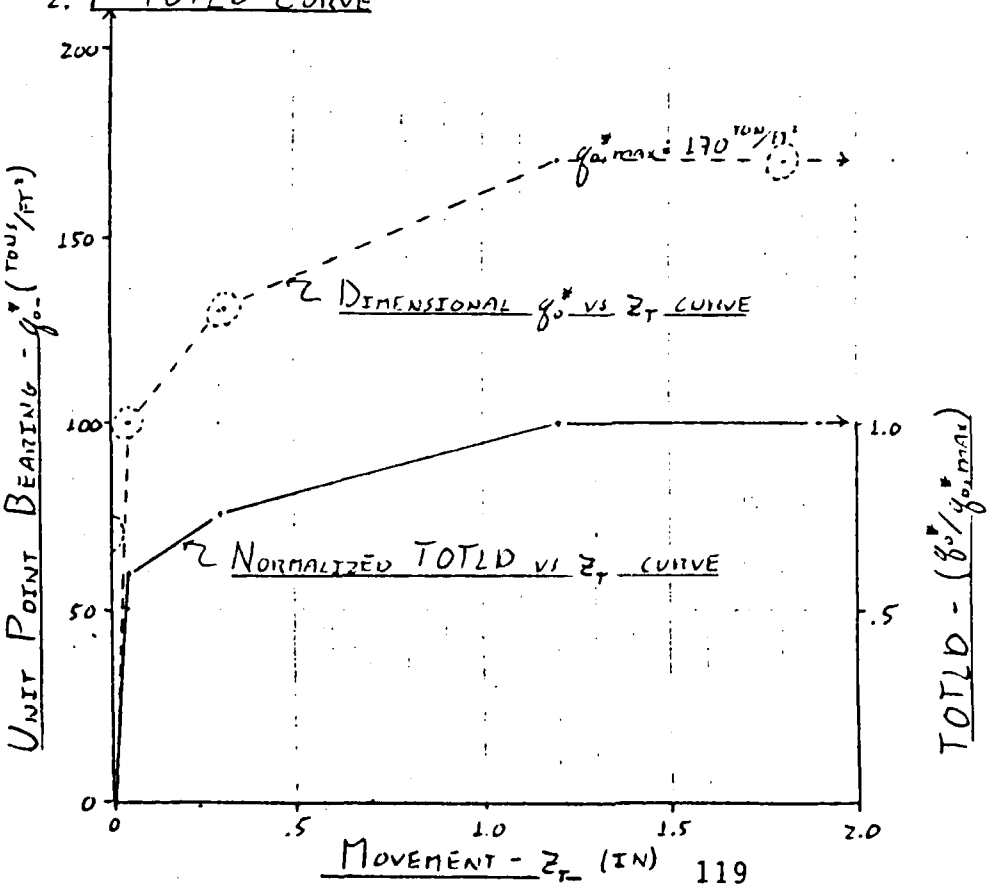

## T-Z AND P-TOTLD CURVES FOR INDIVIDUAL PILES

### L-D26-2-4 AND 2-5

1. T-Z CURVE

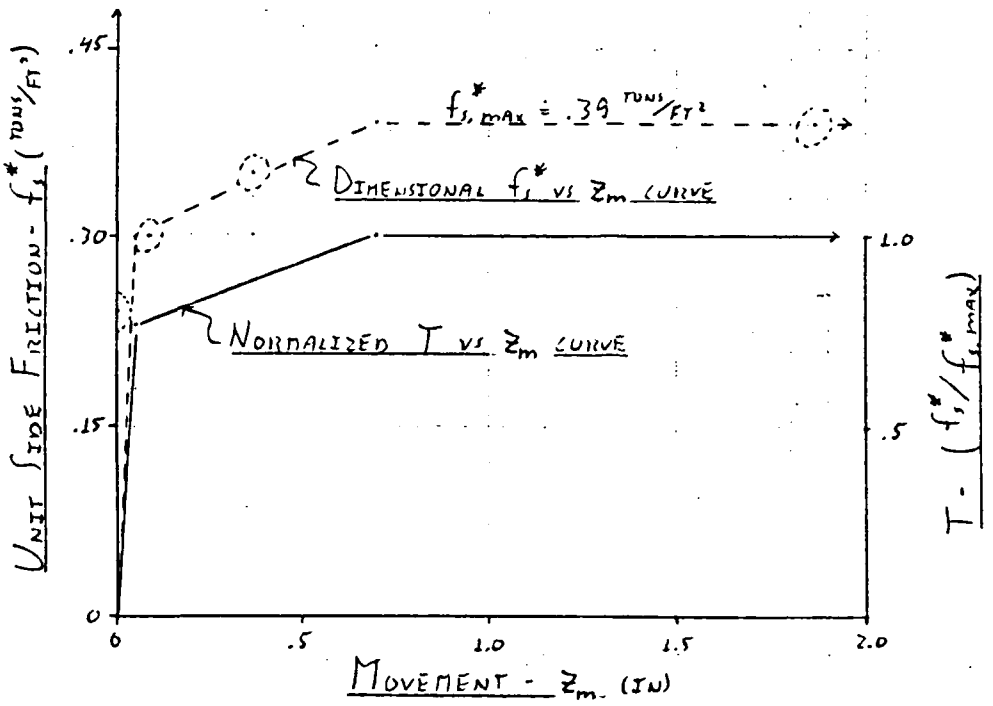


2. P-TOTLD CURVE

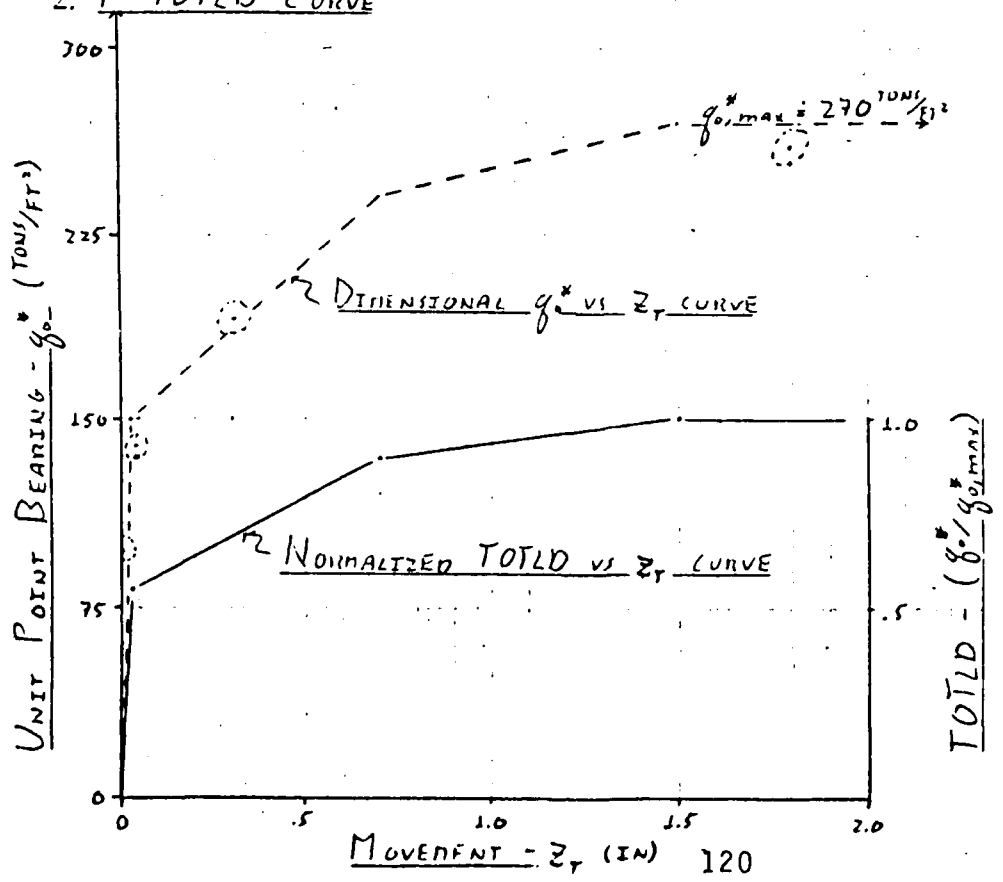

LOCK AND DAM 6: K-8

T-Z AND P-TOTLD CURVES

T-Z CURVE

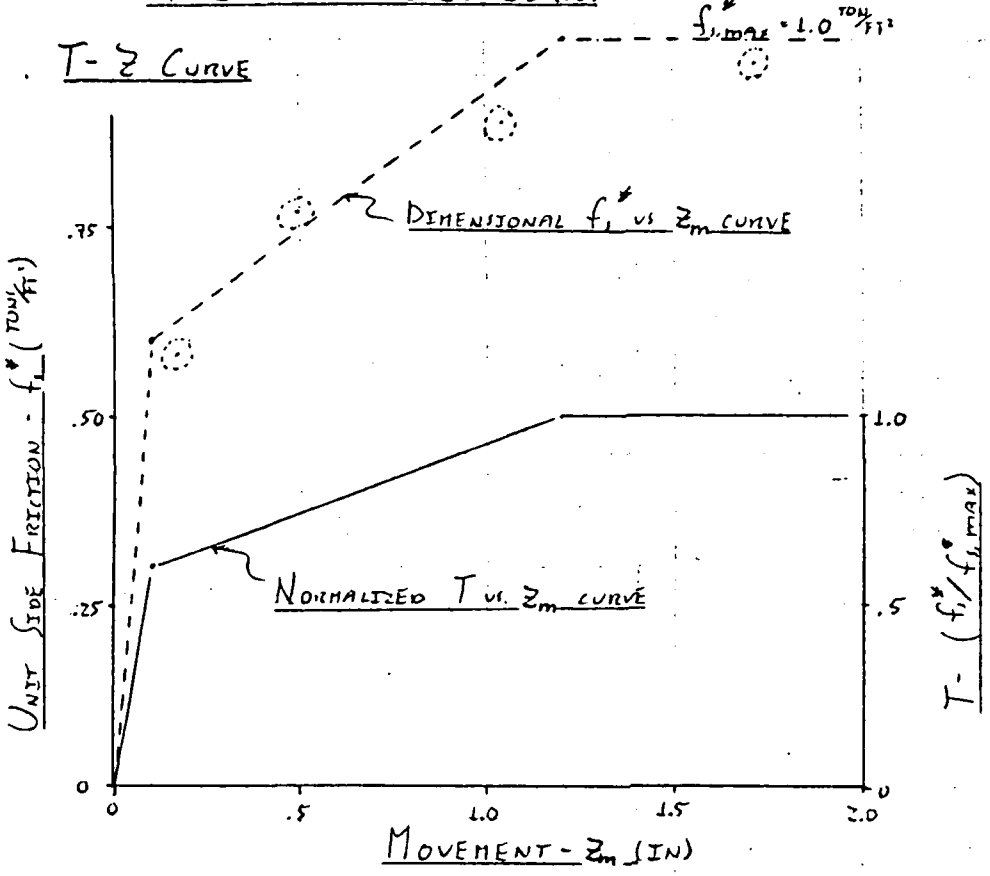


D. P-TOTLD CURVE

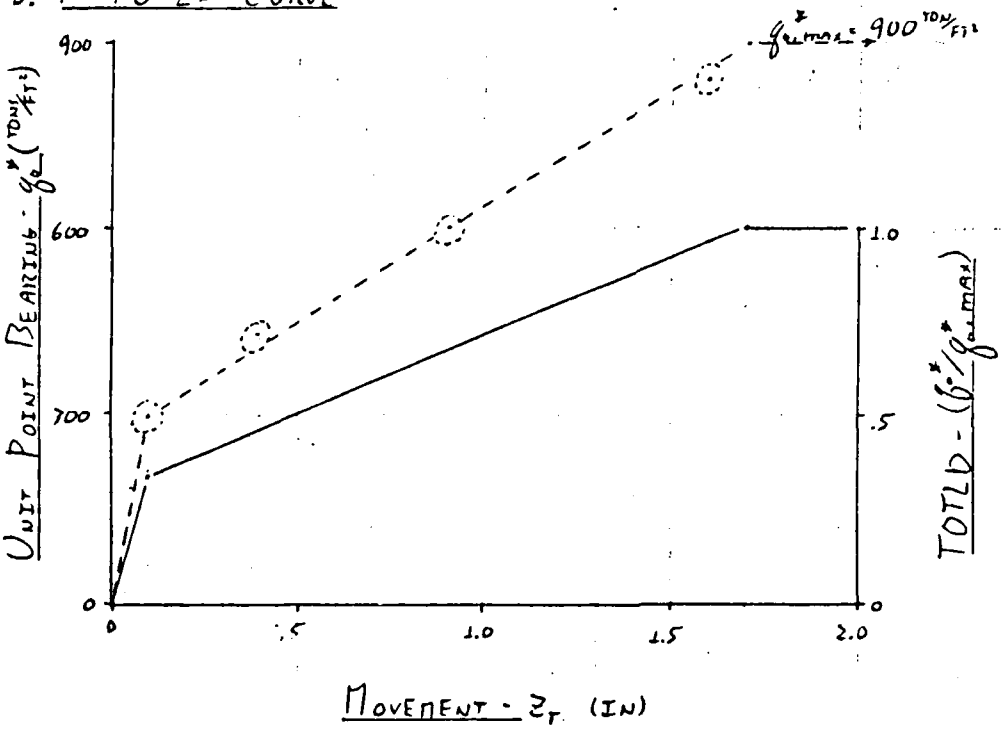

T-Z CURVE

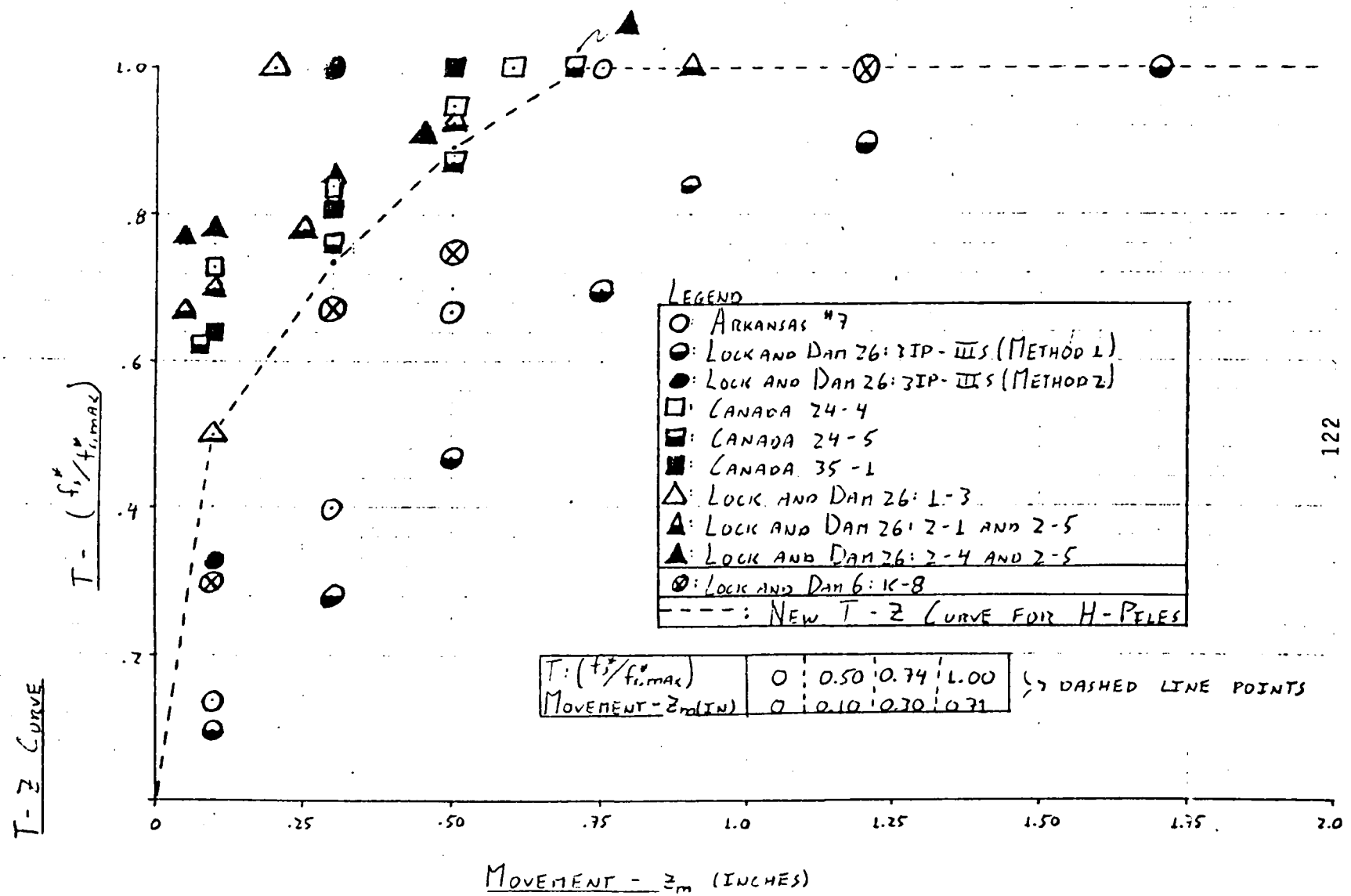
1.0
.8
.6
.4
.2
0
.25
.50
.75
1.0
1.25
1.50
1.75
2.0
T - ($f_s^*/f_{s,max}^*$)
MOVEMENT - $z_m$ (INCHES)
LEGEND
ARKANSAS #7
LOCK AND DAM 26: 3IP - IIIS (METHOD 1)
LOCK AND DAM 26: 3IP - IIIS (METHOD 2)
CANADA 24-4
CANADA 24-5
CANADA 35-1
LOCK AND DAM 26: 1-3
LOCK AND DAM 26: 2-1 AND 2-5
LOCK AND DAM 26: 2-4 AND 2-5
LOCK AND DAM 6: K-8
----: NEW T-Z CURVE FOR H-PILES
T: ($f_s^*/f_{s,max}^*$) 0 0.50 0.74 1.00
MOVEMENT - $z_m$(IN) 0 0.10 0.30 0.71
DASHED LINE POINTS

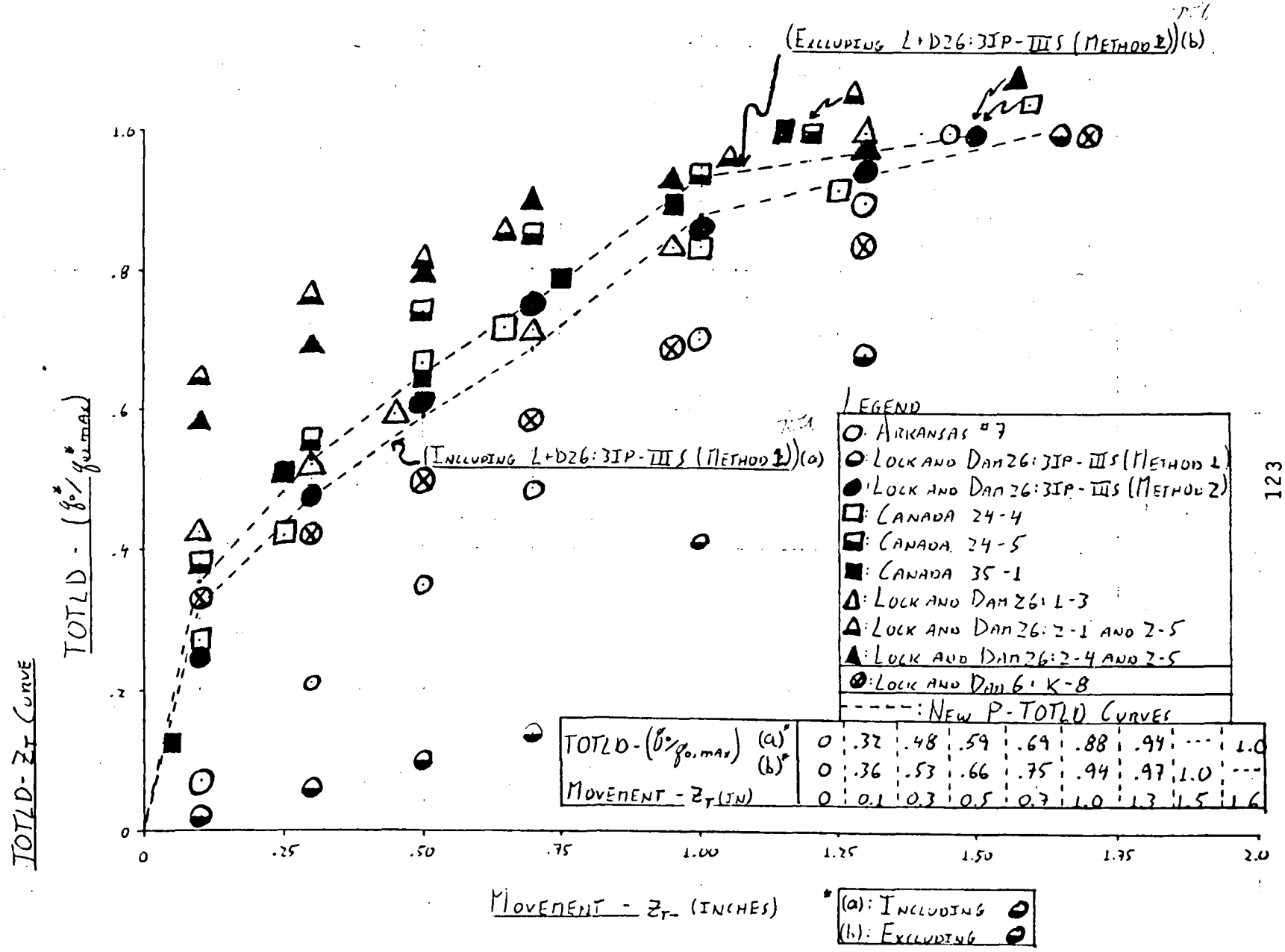


| | | | | | | | | | | |
|---|---|---|---|---|---|---|---|---|---|---|
| TOTLD - (δ*/δ*max) | (a)* | 0 | .32 | .48 | .59 | .69 | .88 | .94 | --- | 1.0 |
| | (b)* | 0 | .36 | .53 | .66 | .75 | .94 | .97 | 1.0 | --- |
| MOVEMENT - $Z_T$ (IN) | | 0 | 0.1 | 0.3 | 0.5 | 0.7 | 1.0 | 1.3 | 1.5 | 1.6 |

APPENDIX 3-O (3-O-1)

[INPUT DATA FOR APILE 1]

KANSAS CITY #4 (ALL PILE AND SOIL DATA FROM REF 11)

* T-Z CURVE INPUT

FROM THE T-Z CURVE ON pg 3-N-1, THE FOLLOWING T-Z CURVE IS INPUT ALONG THE ENTIRE EMBEDDED LENGTH:

| T (%) | Z (IN) |
|---|---|
| 0.00 | 0.00 |
| 0.50 | 0.10 |
| 0.74 | 0.30 |
| 1.00 | 0.71 |
| 1.00 | 3.00 |

* INPUT C-Y DATA

USING THE COYLE-CASTELLO CORRELATIONS, WITH:

$B = 1.145\ FT^2$ (HP 12X73, ASSUME FULLY PLUGGED)

$\phi_{SIDE} = 31°$ (USING $N_{AVG}$ FROM REF 11)

THEN:

| Z (FT) | $\frac{1}{2}(Z/B) = (Z/2.29)$ | $f_s$ (lb/FT²) |
|---|---|---|
| 0 | 0 | 0 |
| 5 | 2.2 | 100 |
| 10 | 4.4 | 180 |
| 15 | 6.6 | 240 |
| 20 | 8.7 | 300 |
| 25 | 10.9 | 360 |
| 30 | 13.1 | 400 |
| 35 | 15.3 | 440 |
| 40 | 17.5 | 480 |
| 45 | 19.7 | 500 |
| 50 | 21.9 | 520 |
| 55 | 23.1 | 550 |
| 60 | 25.3 | 570 |

* PILE STIFFNESS (AE) INPUT

- $E_{ST} = 29 \times 10^6$ psi
- $A_{PT} = A_{CROSS-SECTION} = .151\ FT^2$ (HP 12 × 74, ZERO PLUG)

$\therefore\ AE = (29 \times 10^6\ psi)(.151\ FT^2 \times 144)$ : $\underline{AE = 6.306 \times 10^9\ lb_f}$

* OUTSIDE PILE DIAMETER INPUT

UNDER THE FULLY PLUGGED CONDITION - FOR $f_s^*$ - ACHIEVED AT IN THIS REPORT, THEN FOR AN HP 12 × 74, $P = 3.855$ FT, WHERE $P$ IS THE PERIMETER OF THE STEEL AND SOIL OF A FULLY PLUGGED PILE.

SINCE,

$$P = \pi D_o, \quad D_o = \frac{P}{\pi} = \frac{3.855}{\pi}\ FT; \quad \underline{D_o = 1.227\ FT}$$

WHERE $D_o$ = THE DIAMETER OF A CIRCULAR PILE WITH A PERIMETER $P$.

* INPUT P-TOTLD CURVE

USING THE COYLE - CASTELLO CORRELATIONS AND ASSUMING THE PILE TO BE ½ PLUGGED WITH:

$$B = .867\ FT, \quad \left(\frac{D}{B}\right)_{PT} = \left(\frac{56}{.867}\right) = 64.5$$

EMBEDDED DEPTH

AND

$$\phi_{PT} = 32.5^\circ \text{ (FROM } N_{AVG} \cong 18, \pm 3 \text{ PILE DIAMETER FROM TIP, REF 11)}$$

THEN:

$q_{o,max} \cong 70$ TSF => FROM COYLE - CASTELLO, $q_o$ vs $\left(\frac{D}{B}\right)$ => $\phi_{PT} = 32.5^\circ$, $\left(\frac{D}{B}\right)_{PT} = 64.5$

SINCE $A_{PT} = .591\ FT^2$ (HP 12 × 74, ASSUMING ½ PLUGGED)

$\therefore\ Q_{P,max} = q_{o,max} \times A_{PT} = (70\ TSF)(.591\ FT^2)$ : $\underline{Q_{P,max} = 8.274 \times 10^4\ lb_f}$

USING THE TOTLD - $\Xi_T$ CURVE FROM APPENDIX 3-N AND $Q_{P,max}$:

| P (IN) | .01 | .03 | .05 | .10 | .20 | .30 | .50 | .70 | .90 | 1.2 | 1.5 | 1.8 |
|---|---|---|---|---|---|---|---|---|---|---|---|---|
| TOTLD ($lb_f$) | 2979 | 8936 | 14,890 | 29,790 | 36,410 | 43,850 | 54,610 | 62,060 | 72,810 | 79,430 | 82,740 | 82,740 |

# APPENDIX 3-0

(3-0-3)

## [INPUT DATA]

```
         6         6         6        10         8        14         2
01
.00000E 00.00000E 00
.60000E 00.20000E 00
.80000E 00.40000E 00
.95000E 00.80000E 00
.10000E+01.12000E+01
.10000E+01.30000E+01
02
.00000E 00.00000E 00
.60000E 00.20000E 00
.80000E 00.40000E 00
.95000E 00.80000E 00
.10000E+01.12000E+01
.10000E+01.30000E+01
03
.00000E 00.00000E 00
.60000E 00.20000E 00
.80000E 00.40000E 00
.95000E 00.80000E 00
.10000E+01.12000E+01
.10000E+01.30000E+01
 00000E 00.00000E 00
.12000E+03.50000E+01
.22000E+03.10000E+02
.32000E+03.15000E+02
.38000E+03.20000E+02
.44000E+03.25000E+02
.48000E+03.30000E+02
.54000E+03.40000E+02
.60000E+03.50000E+02
.66000E+03.60000E+02
.63060E+09.00000E 00
.63060E+09.56000E+02
.10000E-03.56000E+02.15350E+01
.10000E-01.16550E+04
.15000E-01.24820E+04
.30000E-01.49640E+04
.50000E-01.82740E+04
.10000E 00.16550E+05
.20000E 00.33100E+05
.30000E 00.49640E+05
.40000E 00.53160E+05
.50000E 00.56680E+05
.70000E 00.64120E+05
.90000E 00.71160E+05
.12000E+01.76120E+05
.15000E+01.78770E+05
.18000E+01.81094E+05
```

T-Z

T-Z

T-Z

C-Y CURVE

$E_{ST}$

P-TOTLD CURVE

KANSAS CITY #4

(1) CLASS T-Z

(2) CLASS P-TOTLD

(3) ASIDE OF ½ PLUGGED PILE.

# APPENDIX 3-0

(3-0-4)

## [INPUT DATA]

```
        5         5         5        10         8        14         2         1
1
.00000E 00.00000E 00
.50000E 00.10000E 00
74000E 00.30000E 00
10000E+01.71000E 00
.10000E+01.30000E+01
2
00000E 00.00000E 00
.50000E 00.10000E 00
74000E 00.30000E 00
10000E+01.71000E 00
.10000E+01.30000E+01
3
00000E 00.00000E 00
50000E 00.10000E 00
.7  00E 00.30000E 00
10000E+01.71000E 00
10000E+01.30000E+01
.00000E 00.00000E 00
30000E+02.50000E+01
14000E+03.10000E+02
.20000E+03.15000E+02
.24000E+03.20000E+02
28000E+03.25000E+02
32000E+03.30000E+02
.36000E+03.40000E+02
12000E+03.50000E+02
50000E+03.60000E+02
.62220E+09.00000E 00
62220E+09.56000E+02
.0000E-03.56000E+02.14420E+01
.10000E-01.37190E+04
.15000E-01.55780E+04
0000E-01.11160E+05
00000E-01.18590E+05
.10000E 00.37190E+05
0000E 00.45460E+05
0000E 00.54750E+05
40000E 00.61460E+05
50000E 00.68180E+05
000E 00.77480E+05
000E 00.90900E+05
12000E+01.99170E+05
5000E+01.10330E+06
8000E+01.10330E+06
```

T-Z

T-Z

T-Z

C-Y

$E_{sr}$

P-TOTLD

KANSAS CITY #8

(1) COMPUTED T-Z

(2) COMPUTED P-TOTLD

(3) ASSUME OF FULLY PLUGGED PILE.

# APPENDIX 3-0
## [INPUT DATA]

(3-0-5)

```
         6         6         6        10         8        14         2
01
.00000E 00.00000E 00
.60000E 00.20000E 00
.80000E 00.40000E 00   T-Z
.95000E 00.80000E 00
.10000E+01.12000E+01
.10000E+01.30000E+01
02
.00000E 00.00000E 00
.60000E 00.20000E 00
.80000E 00.40000E 00   T-Z
.95000E 00.80000E 00
.10000E+01.12000E+01
.10000E+01.30000E+01
03
.00000E 00.00000E 00
.60000E 00.20000E 00
.80000E 00.40000E 00   T-Z
.95000E 00.80000E 00
.10000E+01.12000E+01
.10000E+01.30000E+01
 00000E 00.00000E 00
.80000E+02.50000E+01
.16000E+03.10000E+02
.22000E+03.15000E+02
.28000E+03.20000E+02
.32000E+03.25000E+02   C-Y
.36000E+03.30000E+02
.42000E+03.40000E+02
.44000E+03.50000E+02
.48000E+03.60000E+02
.62220E+09.00000E 00   Est
.62220E+09.56000E+02
.10000E-03.56000E+02.18480E+01
.10000E-01.20700E+04
.15000E-01.31000E+04
.30000E-01.62000E+04
.50000E-01.10330E+05
.10000E 00.20660E+05
.20000E 00.41320E+05   P-TOTLD
.30000E 00.61980E+05
.40000E 00.66370E+05
.50000E 00.70760E+05
.70000E 00.80050E+05
.90000E 00.88840E+05
.12000E+01.95040E+05
.15000E+01.98340E+05
.18000E+01.10124E+06
```

KANSAS CITY #8

(1) CLASS T-Z
(2) CLASS P-TOTLD
(3) ASSUME OF ½ PLUGGED PILE.

APPENDIX 3-0

[OUTPUT DATA]

(3-0-6)

| | |
|---|---|
| 7.00000E-01 | 6.20600E+04 |
| ASSUMED TIP MOVEMENT IN | POINT BEARING LB |
| 9.00000E-01 | 7.28100E+04 |
| ASSUMED TIP MOVEMENT IN | POINT BEARING LB |
| 1.20000E+00 | 7.94300E+04 |
| ASSUMED TIP MOVEMENT IN | POINT BEARING LB |
| 1.50000E+00 | 8.27400E+04 |
| ASSUMED TIP MOVEMENT IN | POINT BEARING LB |
| 1.80000E+00 | 8.27400E+04 |

AXIALLY LOADED PILE, CONSTANT OD

| TOP LOAD LBS | TOP MOVEMENT INCHES |
|---|---|
| .74365E+04 | .15992E-01 |
| .11154E+05 | .23988E-01 |
| .22308E+05 | .47976E-01 |
| .37177E+05 | .79955E-01 |
| .69136E+05 | .15753E+00 |
| .84143E+05 | .26967E+00 |
| .10095E+06 | .38436E+00 |
| .11125E+06 | .49334E+00 |
| .12156E+06 | .60231E+00 |
| .13748E+06 | .81616E+00 |
| .14828E+06 | .10277E+01 |
| .15490E+06 | .13347E+01 |
| .15821E+06 | .16382E+01 |
| .15821E+06 | .19382E+01 |

KANSAS CITY #4

(1) COMPUTED T-Z

(2) COMPUTED P-TOTLD

(3) $A_{TIPE}$ OF FULLY PLUGGED PILE.